

# Design and Testing of an Advanced Eurofix Demodulator

Arthur  
Helwig

Delft University of Technology

Department of Electrical Engineering

Telecommunications and

Traffic Control Systems Group

## **Design and Testing of an Advanced Eurofix Demodulator**

Author: Arthur W.S. Helwig

Thesis Report

64 pages

November 1995

Professor: D. van Willigen  
Mentor: G.W.A. Offermans  
Code: A - 687  
Period: April - November 1995

Keywords: Eurofix  
Loran-C  
Linear cross-correlation demodulation  
Distortion detection

## **Preface**

This report concludes the research that I did on the development of a demodulation scheme for a Eurofix datalink receiver. The Eurofix project is part of the Beek program 'Integrated Navigation for Traffic and Transportation'. A lot of work still needs to be done before Eurofix will be up and running, but I hope that my research has helped in the process.

I would like to express my gratitude to professor van Willigen for the way he motivates people in his group, including me. I would also like to thank all the students of the P&N-group for always creating a pleasant atmosphere in the lab.

A special word of thanks goes out to Cor van der Knaap, for helping me out whenever the hardware needed adjustment. Finally, I would like to express my sincere gratitude to Gerard Offermans, for the way he assisted me along the way.

Arthur Helwig  
November 1995

## Summary

In the Eurofix system, DGPS corrections are transmitted using an already existing infrastructure: the Loran-C system. Primarily, this provides a cost-effective way to supply coverage for DGPS-corrections over a large area. Secondly, the use of the Loran-C navigation system in combination with normal GPS will yield a combined system with improved integrity and availability.

In this report, the capabilities of the Eurofix datalink are investigated. The goal is to optimize the datalink for speed and error-rate. Both 2-level and 3-level Eurofix coding are investigated.

The Eurofix datalink is a difficult one: there is a number of factors limiting the performance. The largest reduction in performance is caused by a phenomenon that is inherent to the way that Loran-C operates: Cross-rate. Secondly, atmospheric effects can overpower the normal Loran-C signal.

A method is devised to detect whether individual Loran-C pulses are distorted by Cross-rate or severe atmospheric conditions. Then, a demodulation scheme is presented that is capable of demodulating both 2- and 3-level Eurofix modulation.

A new method of testing is developed that allows normal (unmodulated) Loran-C signals to appear to the demodulator under test as if they were modulated. This method is very realistic.

The 2-level coding scheme gives a lower pulse error rate than the 3-level coding scheme. On the other hand, the transmitted Loran-C signals can be more balanced with 3-level than with 2-level modulation.

Distortion detecting certainly prevents the demodulator from making incorrect decisions. Since it is easier for an error-correcting code to deal with erasures than with errors, distortion detection will improve the performance of the Eurofix datalink.

The proposed demodulator works as expected. It is difficult, however, to develop a theoretical model that accounts for all effects to which the Eurofix datalink is subjected.

## Abbreviations

CRI	Cross-Rate Interference
CW	Continuous Wave
CWI	Continuous Wave Interference
DGPS	Differential GPS
I-Q	In phase and Quadrature
Loran	Long Range Navigation
LF	Low Frequency
GPS	Global Positioning System
PER	Pulse Error Rate
PDF	Probability Density Function
RTCM	Radio Technical Commission for Maritime Services
RTCM-SC	RTCM Special Committee
SNR	Signal-to-Noise Ratio

# Table of Contents

Preface .....	iii
Summary .....	iv
Abbreviations .....	v
1. Introduction .....	1
2. The Eurofix datalink .....	3
2.1 Loran-C .....	3
2.2 GPS .....	3
2.3 Using the Loran-C system for data transmission.....	4
2.3.1 Modulation of the Loran-C system .....	4
2.3.2 Pulse-position modulation - 2-level.....	4
2.3.3 Pulse-position modulation - 3-level.....	5
3. Performance of the Eurofix datalink.....	6
3.1 Signal-to-Noise ratio of the Loran-C pulse.....	6
3.2 Thermal noise.....	7
3.3 Atmospheric noise.....	7
3.4 Cross-rate interference.....	8
3.5 Continuous Wave Interference.....	9
4. Pulse distortion detection and reduction .....	10
4.1 Noise sources .....	10
4.1.1 Gaussian noise .....	10
4.1.2 Cross-rate & Lightning .....	10
4.2 Counteracting Cross-rate and Lightning - pulse distortion detection.....	11
4.2.1 Using the envelope of the received signal as a means to detect distortion.....	11

4.3 Changes in the envelope not caused by distortion.....	13
4.3.1 Differences between received and expected envelope caused by Eurofix modulation ...	14
4.3.2 Envelope detection of the signal - Quadrature sampling.....	15
4.3.3 Skywaves.....	16
4.3.4 Dynamics.....	18
4.3.5 Thermal noise and Gaussian atmospheric noise.....	19
4.3.6 Consequences for the distortion detection.....	19
4.4 The Reference Figure .....	20
4.5 Extending the distortion detection to erasure detection .....	21
4.6 Parameters of the pulse distortion-detecting and reducing algorithm .....	23
<b>5. The Demodulator.....</b>	<b>25</b>
5.1 Demodulator structures .....	25
5.1.1 Hard-limited single point demodulators.....	25
5.1.2 Linear single point demodulator.....	26
5.1.3 Hard-limited cross-correlation demodulator .....	26
5.1.4 Linear cross-correlation demodulator.....	27
5.2 Demodulation of Eurofix-modulated pulses using linear cross-correlation .....	27
5.3 A Linear cross-correlation demodulator .....	29
5.3.1 The Pulse Shifter .....	30
5.3.2 The reference figures.....	32
5.4 Thermal noise influence on the linear cross-correlation method .....	32
<b>6. Testing of the proposed demodulator .....</b>	<b>36</b>
6.1 The Transmission medium .....	36
6.2 Acquiring Time-shifted Loran-pulses .....	36
6.3 The Demodulator .....	39
6.4 The Test-setup .....	40
<b>7. Results.....</b>	<b>42</b>
7.1 The effect of the distortion detecting filter .....	44

7.2 Sylt - 2-level coding.....	46
7.3 Sylt - 3-level coding.....	47
7.4 Lessay - 2-level coding .....	48
7.5 Lessay - 3-level coding .....	49
7.6 Soustons - 2-level coding.....	50
7.7 Soustons - 3-level coding.....	51
7.8 Comparison between measurements and the theoretical analysis.....	52
<b>8. Conclusions and Recommendations .....</b>	<b>53</b>
8.1 Conclusions.....	53
8.2 Recommendations .....	54
<b>9. References.....</b>	<b>56</b>
<b>Appendix A - Overview of used software .....</b>	<b>57</b>
<b>Appendix B - Location, power and distances of Loran-C transmitters to the Delft University of Technology .....</b>	<b>58</b>

## 1. Introduction

At the time of this writing, GPS is dominating the world as the leading navigation system. Apparently, the accuracy of the system and the global coverage it provides, combined with easy-to-use, cheap receivers is appealing to a lot of people and organizations. The GPS certainly has raised the people's interest in the world of radionavigation.

The accuracy of GPS by itself, though, is not terribly high: its  $2\sigma$ -accuracy is limited to about 100 m. For example, this is not accurate enough for ships that want to do harbour-approaches. Furthermore, at the moment many questions are being raised about the integrity of the GPS system.

Eurofix can be used to overcome both problems: the normal Loran-C system can be used as a backup to the GPS system, thereby improving the integrity of the combined system. In addition to this, by modulating the Loran-C signal, DGPS data and integrity information can be transmitted.

This thesis concentrates on how to design different modules of a Eurofix demodulator such that, given the limitations, the maximum performance is achieved. The following effects are dealt with:

- The Eurofix datalink is mostly disturbed by atmospheric noise and Cross-rate interference. To counteract these effects, special algorithms are designed to deal with just these sources of interference.
- The shape of the Loran-C signals can change substantially - especially during the night - by skywave influences. Although this effect is generally regarded as undesirable, a demodulator is developed that uses the received signal - including possible skywaves - to the maximum extent.

After a brief introduction to the Eurofix system and its components in Chapter 2, the sources of interference for the Eurofix datalink are discussed in Chapter 3.

In Chapter 4, a method is introduced that is able to detect which part of the received signal is distorted by Cross-rate or lightning.

Chapter 5 describes a demodulator capable of demodulating multi-level Eurofix modulation.



## Introduction

---

In Chapter 6, a method is described for real-time testing of the Eurofix datalink. The results of these tests are presented in Chapter 7.

Finally, in Chapter 8 conclusions are drawn from the tests regarding the performance of the newly introduced concepts.



## 2. The Eurofix datalink

This chapter will give a short introduction to the Eurofix datalink.

The reader is assumed to have knowledge of radionavigation principles, and of existing radionavigation systems. This chapter only describes the basic properties of the Eurofix datalink - more detailed information on Eurofix and its components can be obtained from the references.

### 2.1 Loran-C

The Loran-C system is a two-dimensional terrestrial radio navigation system, meaning that the transmitters are located on the surface of the earth, and that the user does not get height information. Loran-C operates at a low frequency, i.e. 100 kHz. These low-frequency signals can be received at distances up to 1500 km from the transmitter.

Loran-C transmitters transmit pulses with a carrier frequency of 100 kHz. Each Loran-C transmitter transmits 8 consecutive pulses, all separated 1 ms. Such a group of 8 Loran-C pulses is called a Loran-*burst*. The Loran-C transmitter repeats this burst with a certain repetition time, called the Group Repetition Interval (GRI). The GRI is used as one of the means by which the receiver can identify the origin of the pulses it is receiving. GRI's range from 40.00 ms to 100.00 ms. By requirement, a GRI is always a multiple of 10  $\mu$ s.

The coverage of Loran-C includes the entire United States, Japan, Saudi-Arabia, Northern Europe and, although not yet fully operational, Western Europe.

The 2d-rms accuracy of Loran is 450 m at the border of the coverage area of Loran-C. In general, though, its accuracy is much better.

More information about Loran-C can be found in [1].

### 2.2 GPS

The Global Positioning System (GPS) is fully operational since July 1995. It makes use of 24 satellites orbiting the globe.

The horizontal  $2\sigma$  (95%) accuracy of normal GPS is specified to be 100 m.

The accuracy of GPS can greatly be improved by providing the user with correction information for each satellite, the so-called Differential GPS (DGPS) data. A more in-depth discussion about contents of this DGPS data can be found in [2].

## 2.3 Using the Loran-C system for data transmission

By modulating the pulses broadcast by a Loran-C transmitter, the Loran-C system can be used to transmit data. Modulating the Loran-C pulses, however, will inevitably lead to a decreased signal-to-noise ratio (SNR) for the existing Loran-C receivers. The modulation needs to be chosen such that this loss of performance does not cause the existing receivers to fail the requirements on Loran-C navigation specified by the RTCM SC-70 [3].

### 2.3.1 Modulation of the Loran-C system

One of the possible types of modulation of the Loran-C pulses is pulse-position modulation. By applying a little variation to the time of transmission of normal Loran-pulses, data can be broadcast. The first 2 pulses of each burst, however, can not be modulated, as they are used to indicate malfunction of the Loran-C system (blinking). Therefore, only 6 out of 8 pulses can be modulated.

### 2.3.2 Pulse-position modulation - 2-level

The Eurofix datalink as described in [4] proposes 2-level pulse-position modulation for the Loran-C pulses. The modulation index  $\mu$  is proposed to be  $1 \mu\text{s}$  (10% of the cycle time of the 100 kHz signal). This means that the time of transmission of each Loran-C pulse is either advanced by  $1 \mu\text{s}$  (an *early* pulse) or delayed by  $1 \mu\text{s}$  (a *late* pulse). To ensure proper functioning of existing Loran-C receivers, however, the number of advanced pulses must equal the number of late pulses on average - the transmitted pattern must be *balanced*. This puts restrictions on the number of possible early/late combinations that can be used to encode the data with. Balanced and nearly-balanced coding schemes are investigated in [5].

The value of  $1 \mu\text{s}$  for the modulation index is subject to further investigation. It is a compromise between the degradation of the normal Loran-C system and the admissible Pulse Error Rate of the Eurofix datalink.

### 2.3.3 Pulse-position modulation - 3-level

Rather than transmitting only early and late pulses, it is also possible to increase the number of levels of the time-shift for each Loran-C pulse. With a 3-level modulation scheme, for instance, each Loran-C pulse can either be transmitted  $1 \mu\text{s}$  early (an early pulse),  $1 \mu\text{s}$  late (a late pulse), or on time (a prompt pulse).

Using the same number of Loran-pulses, more data can be sent with 3-level coding than with 2-level coding. Furthermore, there are more balanced early/prompt/late patterns than balanced early/late patterns, making it feasible to develop a coding scheme that is balanced for each burst. With 3-level coding and 6 pulses to be modulated, there are  $3^6=729$  (9.5 bit) possible combinations, 141 (7.1 bit) of which are balanced. With 2-level coding, there are  $2^6=64$  (6 bit) combinations, of which only 20 (4.3 bit) are balanced. So, if an integer number of bits per pattern is assumed, upgrading from 2-level to 3-level coding yields a 9/6 (50%) increase in transmission speed. If balanced codes are considered, the increase of the transmission speed is 7/4 (75%). More information about 2- and 3-level coding schemes can be found in [6].

Increasing the number of levels of the time-shift, however, will inevitably lead to an increased probability of demodulating a pulse incorrectly, and hence an increased Pulse Error Rate (PER). It is anticipated, however, that the majority of pulses that are incorrectly demodulated will be distorted in such a way that the pulse can not correctly be demodulated at all - no matter how small the number of possible levels.

In this report, 3-level coding as well as 2-level coding is investigated. The time-shifts that are used for the 2-level coding are  $-1 \mu\text{s}$  (early) and  $+1 \mu\text{s}$  (late). For the 3-level coding, time-shifts of  $-1 \mu\text{s}$  (early),  $0 \mu\text{s}$  (prompt) and  $+1 \mu\text{s}$  (late) are used.

### 3. Performance of the Eurofix datalink

In this chapter, the possible sources of interference on the Loran-C signal are investigated. First, the meaning of the term Signal-to-Noise ratio for the Loran-C pulse will be discussed.

#### 3.1 Signal-to-Noise ratio of the Loran-C pulse

Since the Loran-C pulse is not a continuous wave (CW) signal, standard formulas for calculating its received signal power do not apply.

The RTCM SC-70 [3] defines the signal-to-noise ratio of the Loran-C pulse as the signal-to-noise ratio of a single CW carrier having the same amplitude as the Loran-pulse at the so-called ‘standard sample-point’ (25  $\mu\text{s}$ ).

This is illustrated in the following figure:

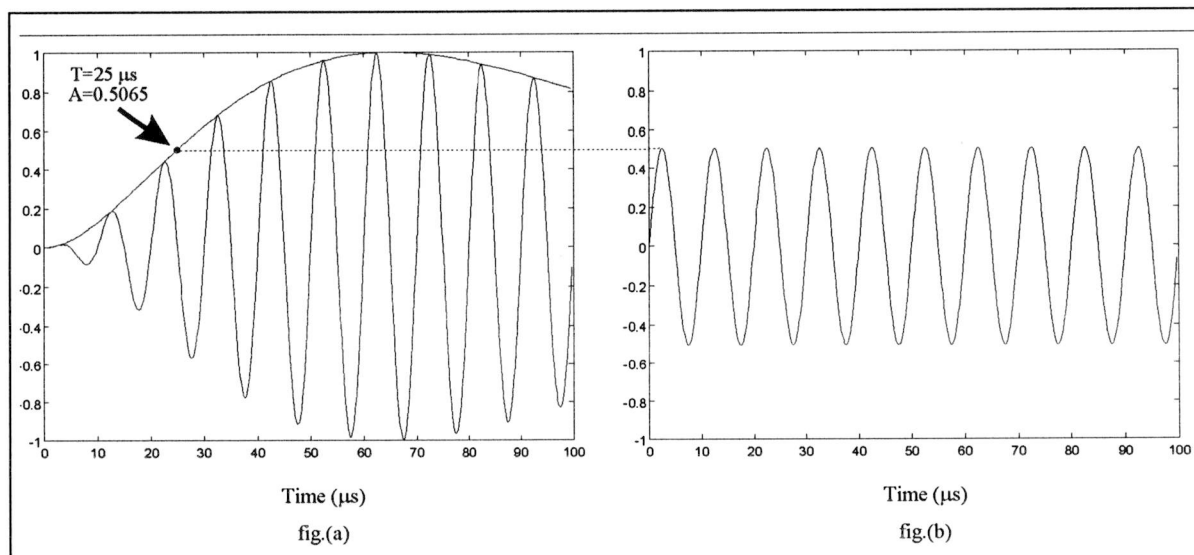


Figure 3.1: (a) Amplitude of the Loran-C pulse at  $T=25 \mu\text{s}$ , and (b) sinusoidal wave with the same amplitude

If the maximum envelope of the Loran-C pulse is normalized to 1, the envelope at  $T=25 \mu\text{s}$  is 0.5065. Furthermore, the averaged normalized power contained in a general sinusoidal waveform  $A \cdot \sin(\omega \cdot t)$  is equal to  $\frac{1}{2}A^2$ .

This yields the following formula for the power of a Loran-C pulse:

$$P_{Signal} = \frac{(0.5065 \cdot A_{max})^2}{2} \approx 0.1283 \cdot A_{max}^2 \quad \text{Formula 3.1}$$

where  $A_{max}$  is the maximum value of the envelope of the Loran-C pulse.

The power contained in bandpass-filtered Gaussian noise is:

$$P_{noise} = N_0 B = \sigma^2 \quad \text{Formula 3.2}$$

with  $N_0$  the normalized spectral density,  $B$  the bandwidth and  $\sigma^2$  the variance of the noise.

### 3.2 Thermal noise

As is the case with any real-life radio-signal, thermal noise will be present on the Loran-C signal. This thermal noise is assumed to be Gaussian, with variance  $\sigma^2$ . In the coverage area of a Loran-C transmitter the SNR of the received signal is at least -10 dB [7]. Normal Loran-C receivers can integrate the received signal for a certain period of time to get a better SNR. With the Eurofix datalink, however, this is not possible since each received pulse carries data which must be demodulated. The minimum SNR that yields an acceptable Pulse Error Rate (PER) for the Eurofix datalink is subject to further investigation.

### 3.3 Atmospheric noise

Atmospheric noise is caused by electrostatic discharges in the atmosphere. These discharges can have tremendous power compared with the received Loran-C signals. Lightning is a form of atmospheric noise.

If the power of the electrostatic discharge is weak, it can be treated as weak Cross-rate. If it is weaker, it can probably be treated as thermal noise. If the power is large, however, it will be impossible to demodulate the Loran-C pulse without a high error-probability.

The effect of thermal noise is negligible compared to atmospheric noise - very weak electrostatic discharges will still easily overpower the thermal noise. Unfortunately, though, the effect of the electrostatic discharges is hard to model. Therefore, in the remainder of this report, weak atmospheric noise will be considered to be Gaussian.

### 3.4 Cross-rate interference

Probably the most important source of interference will be Cross-rate interference: due to the fact that all Loran-C stations share the same frequency, some of the pulses from a Loran-C station transmitting at one GRI will be received at the same time as pulses from another Loran-C station transmitting at another GRI. Since the receiver can not distinguish between the 2 pulses, the probability of incorrect demodulation of the received signal will be high.

The effect of Cross-rate is illustrated in figure 3.2.

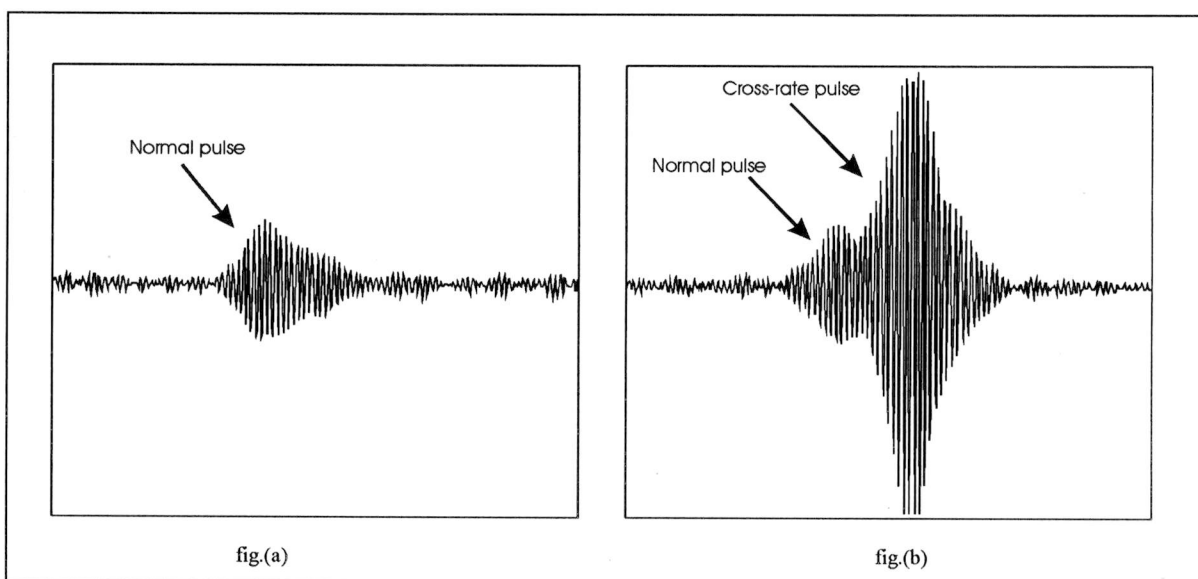


Figure 3.2: Example of the effect of Cross-rate.

Figure (a) is the undistorted signal received from the Soustons transmitter.

In (b), the last part of the pulse is clearly hit by Cross-rate from another (stronger) transmitter.

If the power of the interfering signal is relatively small, its effect will be negligible. If it is relatively large, the probability of correctly demodulating the signal will be low, but the fact that the received pulse is hit by another signal is easy to acknowledge.

Cross-rate has its worst influence if the power of the interfering signal is comparable to the power of the desired signal; that is, when the power is too large to have a negligible influence, and too small to be recognized as an interfering signal.



### **3.5 Continuous Wave Interference**

Interference caused by radio transmitters operating at frequencies close to the Loran-C band (90-110 kHz) is called continuous wave interference (CWI). However, as described in [5], CWI can successfully be suppressed by notch-filters in addition to the standard Loran-C bandfilter. In the remainder of this report, the effects of CWI are assumed to be sufficiently suppressed by such filters to be negligible.

## 4. Pulse distortion detection and reduction

In this chapter, a method is proposed to detect whether (and if so, which part of) a particular Loran-C pulse is distorted by Cross-rate or lightning. Then, this method is extended to reducing the effect of the distortion on the received Loran-C pulse.

### 4.1 Noise sources

As discussed in the previous Chapter, the received signal from a particular Loran-C transmitter can be distorted by the following sources:

- Gaussian noise (thermal noise and weak atmospheric noise)
- Cross-rate
- Strong atmospheric noise (Lightning)
- Continuous Wave Interference

In this report, only Gaussian noise, Cross-rate and lightning will be discussed further.

#### 4.1.1 Gaussian noise

Thermal noise and weak atmospheric noise are assumed to be Gaussian, which means that the probability density function (PDF) of the noise has a normal distribution, a mean value of 0 and a standard deviation of  $\sigma$ , where  $\sigma^2$  equals the power of the noise signal. One of the means to reduce the effects of Gaussian noise is to average the desired signal over a certain period of time. Because the desired signal is averaged coherently, and the noise signal is averaged incoherently, this effectively leads to an increase of the signal-to-noise ratio (SNR).

#### 4.1.2 Cross-rate & Lightning

Both Cross-rate and lightning differ significantly from Gaussian noise, in the respect that Gaussian noise is always present. Cross-rate and lightning, however, tend to distort only individual pulses. This means that one can expect at least a reasonable number of pulses that is not affected in any way by Cross-rate or lightning. This type of interference is quite rare in normal communication channels. Counteracting it, therefore, requires a special approach.

## 4.2 Counteracting Cross-rate and Lightning - pulse distortion detection

Even *if* a pulse has been hit by Cross-rate, it is usually hit only partially: in general, the interfering signal will not be lengthy enough to distort the entire desired pulse. (In some cases, Cross-rate *will* hit the entire pulse. This can happen if the start of the interfering pulse arrives at the receiver at the exact moment the desired pulse arrives, or, more likely, when the interfering pulse is longer than the desired pulse due to skywaves). The performance of a demodulator may be increased by being able to identify which part of the pulse is still undistorted. The part of the pulse that is apparently hit by some sort of interference can then be processed keeping in mind that that part of the received signal possibly differs significantly from how it was transmitted by the Loran-transmitter.

If a Loran-pulse is hit by another Loran-pulse (as is the case when Cross-rate occurs), or when a Loran-pulse is distorted by an electromagnetic pulse caused by lightning, the interfering signal is generally received with an amplitude that differs from the pulses originating from the transmitter that is being tracked (i.e., the desired signal). When this amplitude is much lower than the amplitude of the desired pulse, its disturbing effect will be negligible. We will therefore focus on the case where the interfering signal has a larger amplitude than the desired pulse.

### 4.2.1 Using the envelope of the received signal as a means to detect distortion

If, at any particular point in time, the amplitude of the received signal differs significantly from the amplitude that can be expected given the shape of the pulses as they were received 'in the past', that part of the pulse must have been hit either by Cross-rate or by lightning.

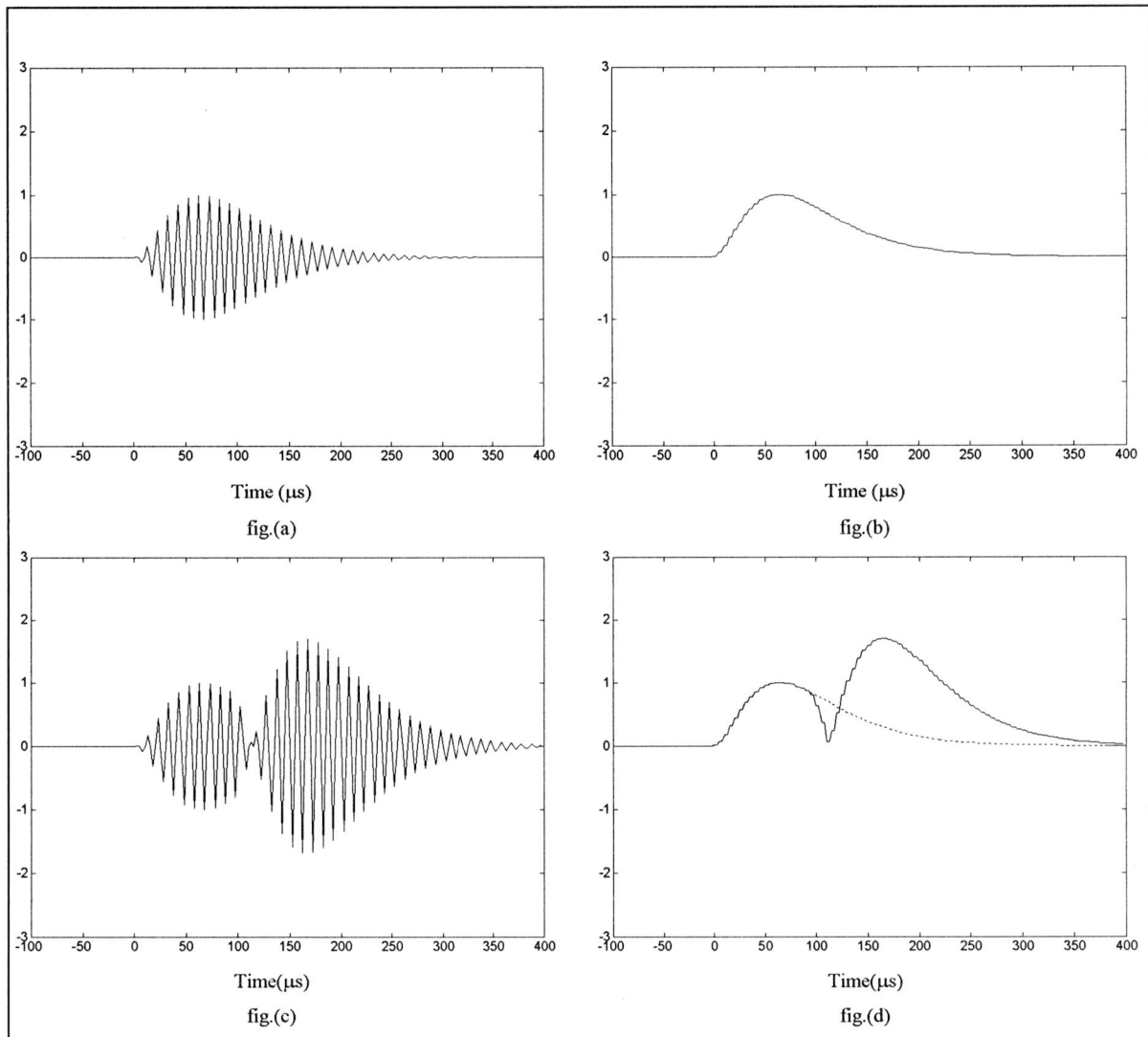


Figure 4.1:

- (a) A 'normal' Loran-pulse,
- (b) Envelope of the 'normal' Loran-pulse,
- (c) A Loran-pulse hit by Cross-rate. The Cross-rate signal is +6dB, and interferes from  $t=95 \mu\text{s}$ ,
- (d) Envelope of the Loran-pulse hit by Cross-rate, compared with figure (b) (dashed).

Figure 4.1 illustrates this by merging a 'normal' pulse with Cross-rate signal which is 6 dB stronger and interferes from  $t=95 \mu\text{s}$ . In 4.1(d), the difference between the envelopes of the desired pulse and the distorted pulse can clearly be seen.

By comparing the envelope of the expected pulse with the envelope of the received signal, the part of the signal which is distorted can be identified. To avoid that part of the signal having influence on the demodulator, the signal is suppressed (i.e., all samples are made 0) when the envelope differs 'significantly' from the expected envelope.

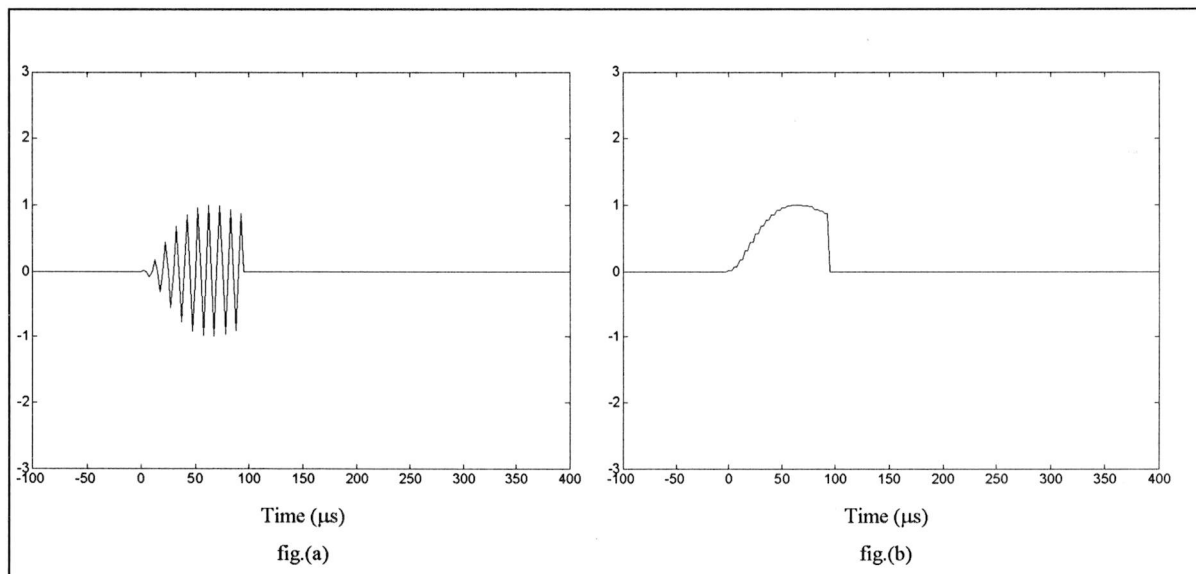


Figure 4.2: The modified pulse after distortion detection (a), with the resulting envelope (b).

By ‘nulling’ the signal at those points where distortion is suspected, the remaining pulse shape has a high probability of being undistorted. This proves to give a large reduction of errors in the demodulator, because the demodulator can now use only the samples at those points where the signal is (supposed to be) undistorted.

### 4.3 Changes in the envelope not caused by distortion

It was stated in the previous section that the sample values of the received signal were nulled when the envelope differed ‘significantly’ from the expected envelope. This term will now be defined more strictly.

There are certain predictable effects that cause a change in the envelope of the signal. The effects causing the changes investigated in this report are:

- Changes in the expected envelope caused by Eurofix modulation
- Accuracy of the envelope-detecting algorithm
- Changes in envelope caused by skywaves
- Changes in envelope caused by the dynamics of the receiver.

Of course, changes in envelope caused by these effects should not result in any modifications by the distortion-detecting algorithm.

After investigating each of these sources, the term ‘significantly’ can be given a numerical value.

#### 4.3.1 Differences between received and expected envelope caused by Eurofix modulation

If the received Loran-pulse is Eurofix-modulated, its envelope will have a certain time-shift compared to the non-modulated pulse. When the envelopes are compared without taking this time-shift into account, the envelopes appear to differ:

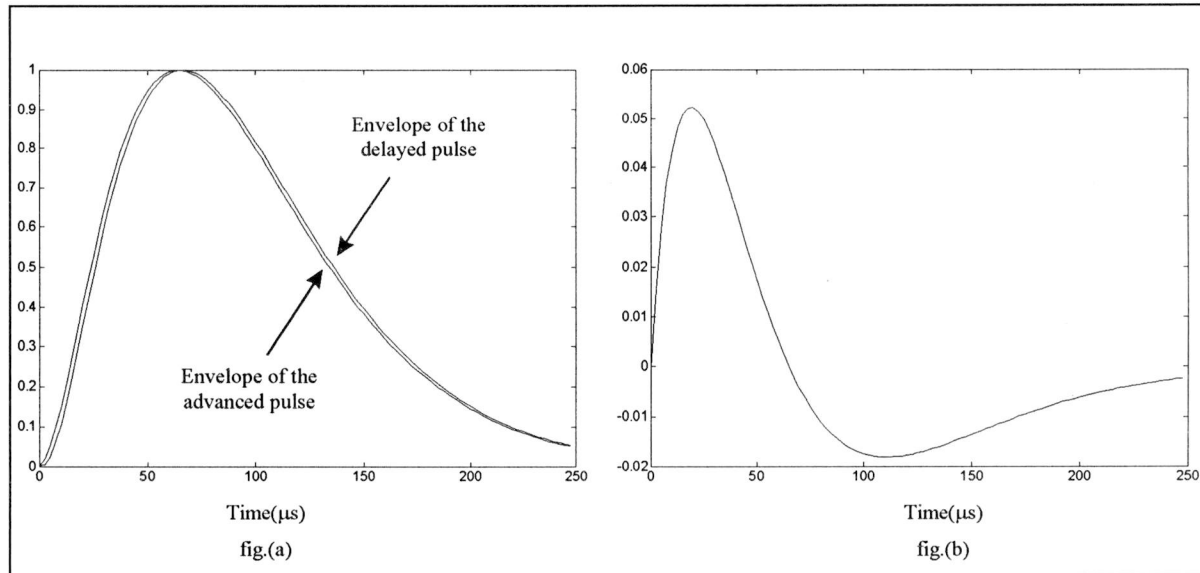


Figure 4.3: (a) Envelopes of an ‘early’ pulse and of a ‘late’ pulse, and (b) the difference between the two envelopes.

From figure 4.3 it can be seen that the maximum difference between the two envelopes caused by Eurofix modulation is 0.052 (or 5.2%), at  $t=20 \mu\text{s}$ .

A difference of 5.2% between the received envelope and the expected envelope can thus be caused by Eurofix modulation.

### 4.3.2 Envelope detection of the signal - Quadrature sampling

When the received signal is sampled taking both an in-phase and a quadrature sample at a rate higher than the Nyquist-frequency (so called Quadrature sampling), the envelope of the signal can be acquired by using the formula:

$$E_k = \sqrt{i_k^2 + q_k^2} \quad \text{Formula 4.1}$$

where

$E_k$  = the envelope at the  $k$ 'th samplepoint

$i_k$  = the  $k$ 'th in-phase sample

$q_k$  = the  $k$ 'th quadrature sample

Note that although  $i_k$  and  $q_k$  ideally should be taken at the same moment in time, this is generally not feasible. In most practical applications when A/D converters are used, only one sample can be taken at any moment in time (since taking more samples at the same moment in time requires multiple A/D converters, and hence increased cost). This is circumvented by rather than taking 2 samples at the same moment in time at the Nyquist rate, 1 sample is taken at twice the Nyquist rate. So, in reality:

$i_k$  =  $s_{2k}$

$q_k$  =  $s_{2k+1}$

$s$  = a vector of samples taken at 2 times the Nyquist-frequency.

If (as is the case with Loran-pulses) the envelope of the signal is not constant, the envelope of the signal is changed between the moment  $i_k$  was taken and the moment  $q_k$  was taken. This introduces an error on this method of envelope detection.

The carrier frequency of the Loran-pulse is 100 kHz. The Nyquist rate is therefore 200 kHz, and the single A/D converter has to have a sample frequency of 400 kHz. This means that a sample has to be taken every 2.5  $\mu$ s.

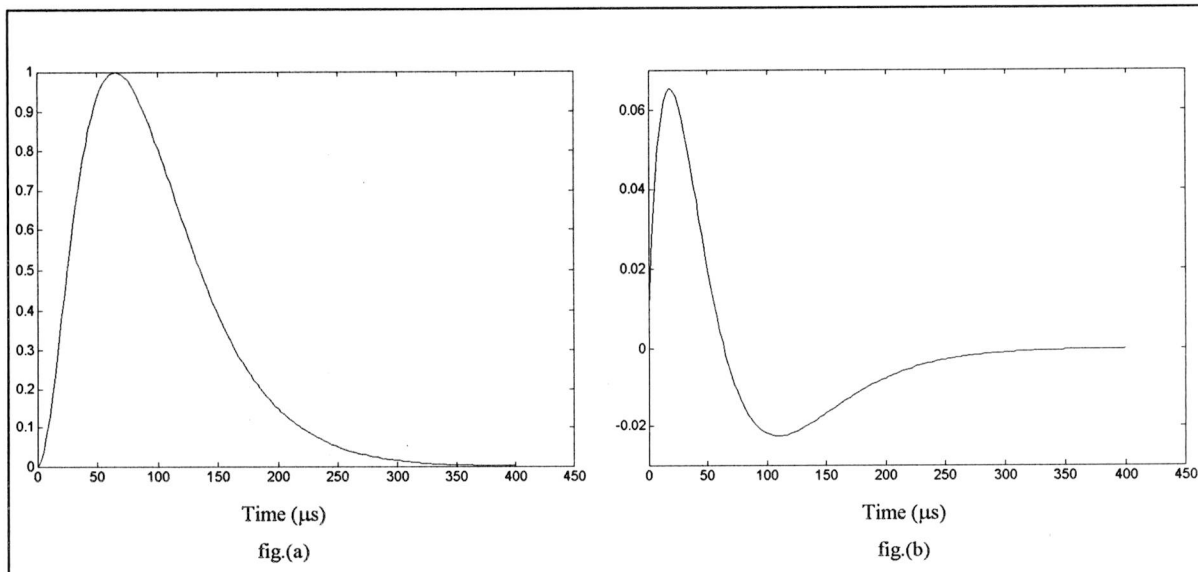


Figure 4.4: (a) Envelope of the Loran-C pulse (sampled at 400 kHz), (b) its derivative

From figure 4.4(b), it can be seen that the maximum difference in amplitude between 2 consecutive samples is 0.065 (or 6.5%), and that this occurs at  $t=17.5 \mu\text{s}$ .

This means that in the worst case the envelope detected by this method can be off 6.5%. The method is, however, accurate within 0.5% for 90% of the duration of the Loran-pulse.

The error could be suppressed by time-shifting both the in-phase and the quadrature set of samples by using an interpolating filter. More information on Quadrature sampling can be found in [8].

A difference of 6.5% between the received envelope and the expected envelope can thus be caused by the method by which the envelope of the received signal is determined.

### 4.3.3 Skywaves

Another reason for changes of the envelope of the received pulse are changes in the ionosphere. These changes cause the skywaves that are always received in combination with the groundwave-signal of the Loran-pulse to change. Since the received pulse consists of the addition of both the groundwave and skywaves, the envelope of the received pulse also changes.

Unfortunately, little is known about the way in which the ionosphere changes. The ionosphere is affected by sunlight and other atmospheric conditions - all of which are hard to model. Furthermore, the resulting effect of a changing atmosphere on skywave propagation is equally hard to model.

To get some idea of changes in the received pulse shape over time due to changing skywaves, data of 'live' Loran-C signals was collected, and the pulse shape was monitored from GRI to GRI over a long period of time. It was noted that during daytime, the received pulse shape remained fairly constant - even for signals originating from distant transmitters at about 1,000 km (and therefore are influenced quite severely by skywaves).

During the night, however, the received pulse shape can change relatively fast. It was noted that, in the worst cases, in a few minutes the pulse shape could change completely. This is especially true for those cases where the received signal consisted mainly of skywaves (i.e., when the transmitter was far away). In these cases where the groundwave signal could easily be recognized in the received signal, it was noted that that portion of the signal hardly changed.

The effect of skywaves can be seen from the following figure:

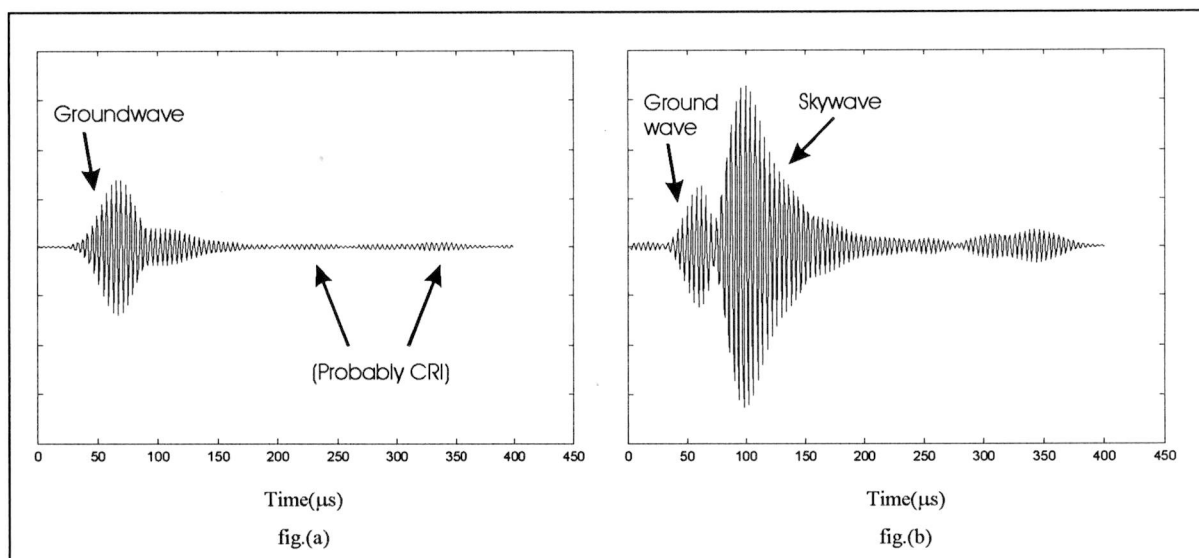


Figure 4.5: Effect of skywaves.

Fig. (a) represents the signal as it is received from Soustons at 12.00 pm (noon).

Fig. (b) is the signal from the same transmitter received at 1.00 am. The effect of the skywave can clearly be seen.

For calculation of the percentual change in the envelope between GRI's, it is assumed (based on the measurements mentioned above) that in the worst case, in 3 minutes less than 10% of the original envelope remains. If the time between two GRI's is assumed to be 100 ms, then the percentual change in envelope between two GRI's is:

$$1 - \frac{180s}{100ms\sqrt{0.1}} \approx 1 - 0.9987 \approx 0.13\%$$

This is negligible compared to changes in the envelope between GRI's caused by other factors.

#### 4.3.4 Dynamics

When the receiver moves geographically, the received signal strength (and thus the received envelope) will vary. However, these changes are quite small over time, compared to changes in the envelope due to other reasons, as the following example will illustrate:

Suppose that the receiver is moving at about 100 km/h (or 27 m/s). Suppose further that the distance from the receiver to the transmitter is 1 km (1000 m). If the receiver moves another 1000 m away from the transmitter, the received power will be one quarter of what it was before, since the received power decreases quadratically with distance. The envelope will then be 0.5 times the original envelope. It will take the receiver  $1000/27 \approx 37$  seconds to cover this distance.

The speed of 100 km/h and the distance of 1000 m can safely be used as limits as to the maximum speed of the receiver and the minimum distance between the receiver and the transmitter. A more typical distance between receiver and transmitter would be 100 km.

The time between 2 Loran-bursts is typically in the order of 100 ms. This time is very short compared with the time of 37 seconds calculated above. The percentual change in envelope between 2 bursts is:

$$1 - \frac{37s}{100ms\sqrt{0.5}} \approx 1 - 0.9981 \approx 0.19\%$$

This is negligible compared to changes in the envelope between GRI's caused by other factors.

Other dynamic effects (for example, when driving in a city) can probably also cause large changes in the amplitude of the received signal. These effects remain to be investigated - if the changes in envelope

caused by dynamics become unacceptably large (i.e., larger than the changes caused by skywaves), then the received pulse probably needs to be scaled to achieve a maximum fit with the reference envelope.

#### 4.3.5 Thermal noise and Gaussian atmospheric noise

The received pulse will also contain a certain amount of random noise. This will also cause a change in the envelope. Contrary to the previous causes, however, the amount of random noise that is received does not change with the received Loran-C signal strength or the momentary envelope of the Loran-pulse. Its influence is therefore measured as a fixed value; rather than a percentage of the expected envelope.

#### 4.3.6 Consequences for the distortion detection

From the previous paragraphs it can be concluded that the largest changes in envelope that are not caused by distortion, are caused by:

- the error in the method of envelope-detection (6.5%), and
- the change in the expected envelope caused by the Eurofix-modulation (5.2%)

These two errors are independent from each other - the errors can add up. So, the error that is made in the worst case is  $(1.065 \cdot 1.052 - 1) = 0.12$ , or about 12%. This is the allowed percentual change in the tolerance band, called  $T_{\text{perc}}$ .

The envelope of a received pulse must therefore differ at least 12% from the expected envelope before it can safely be concluded that the pulse in fact is hit by Cross-rate or lightning.

The pulse needs only to be adjusted (i.e., nulled) at those points where the influence of the distortion is severe. If the pulse is hit by, for instance, very weak Cross-rate, an adjustment of the pulse is not necessary. Therefore, the tolerance band can be extended so that a larger difference is still tolerated.

Furthermore, to accommodate for a certain amount of random noise the tolerance band must be extended by a fixed value. This is the allowed fixed change in the tolerance band, called  $T_{\text{fixed}}$ .

An example of the resulting expected envelope, including its tolerance band, is given in the following figure:

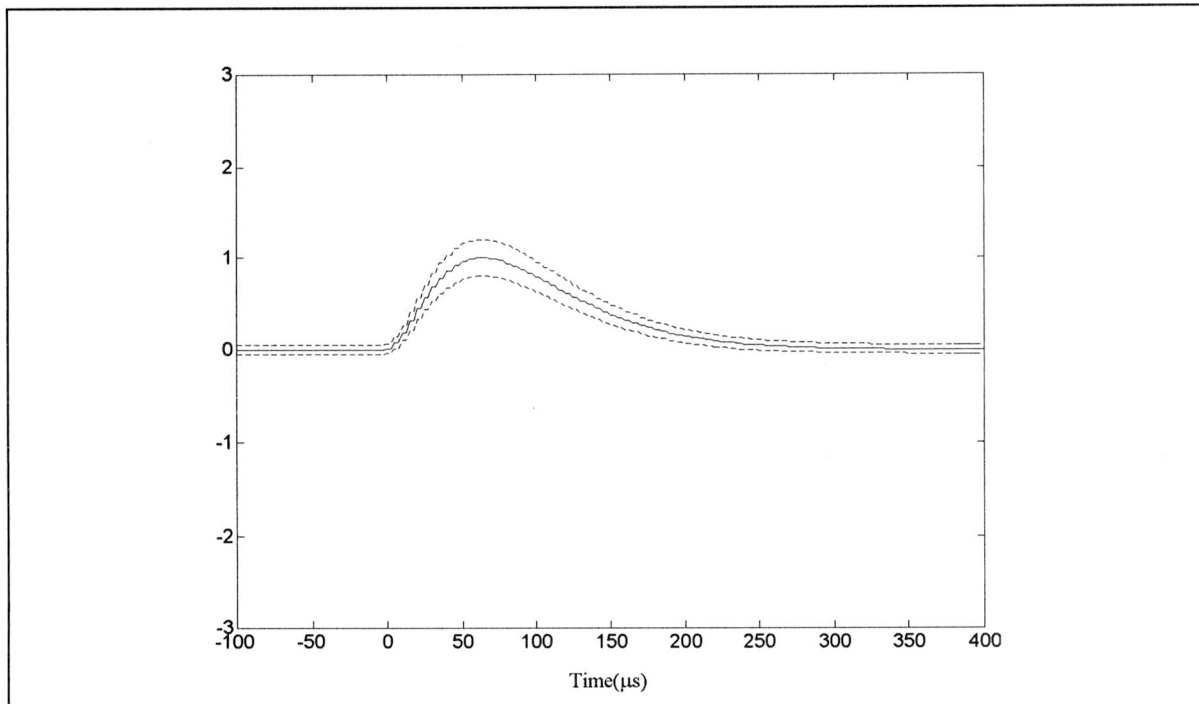


Figure 4.6: The expected envelope, with a tolerance band (the area enclosed between the dashed lines)

At all points where the envelope of the received pulse does not lie within the area enclosed by the two dashed lines, the samples are nulled (as described in section 4.2.1).

#### 4.4 The Reference Figure

The receiver will have to 'know' the shape of the pulse it can expect. For this purpose, a reference figure that contains the expected envelope is kept in the memory of the receiver. Pulse shapes that differ significantly from this reference figure are assumed to be distorted.

As described in the previous sections, there are influences that can cause the expected envelope to change slowly. This is the case when:

- skywaves occur, or
- the receiver moves geographically.

The differences will not vary much between successive pulses, but the expected envelope will slowly drift over time. Of course, signals that differ slightly from the expected signal must not be interpreted by the receiver as signals distorted by interference.

The reference figure will therefore have to be continually adjusted over time to make sure that it keeps resembling the momentary pulse shape if it is received without interference. The reference figure is chosen to be a moving average over the received envelope shapes.

In formula form:

$$R_k = q_{hold} \cdot R_{k-1} + (1 - q_{hold}) \cdot X_k \quad \text{Formula 4.2}$$

where:

- $R_k$  = the reference figure
- $X_k$  = the envelope of the received signal, averaged over 1 GRI (8 pulses)
- $q_{hold}$  = a parameter that controls how fast changes in the received signal are incorporated in the reference figure

If we state that all pulses that were received more than  $n$  GRI's ago must have an influence less than 0.1% on the reference figure, the parameter  $q_{hold}$  can be calculated as follows:

$$q_{hold} = \sqrt[n]{0.001},$$

which can be calculated by

$$q_{hold} = e^{\frac{\ln(0.001)}{n}} \quad \text{Formula 4.3}$$

*Example:*

Suppose we are listening to GRI 8940, and we want all pulses that occurred more than 1 minute ago to have an influence of less than 0.1% on the reference figure.

In 1 minute (60 seconds),  $60 \cdot (1/8940e-5) = 671$  GRI's occur.

$q_{hold}$  is then calculated by  $q_{hold} = e^{\frac{\ln(0.001)}{671}} = 0.9898$ .

#### 4.5 Extending the distortion detection to erasure detection

After detecting which parts of the received pulse are being affected by Cross-rate or lightning, it is not difficult to determine a measure to indicate whether the received pulse still has a fair chance of being decoded correctly. If it is determined that the chance of incorrect decoding the pulse is large, it is better

to accept this fact and not even attempt decoding. The symbol can then be marked as an ‘erasure’.

Erasures are easier to correct by error-correcting codes than errors.

The power of the part of the signal that is not distorted (and therefore has not been ‘nulled’ by the distortion detecting algorithm) can be used as a measure for erasure-detection. If this amount of power becomes small compared to the total amount of power of a complete Loran-pulse, the received pulse is badly damaged and demodulation can only be done with an increased probability of making a wrong decision.

In other words:

If  $P_{\text{received signal}} < E_{\text{thresh}} \cdot P_{\text{reference figure}}$ , then the received pulse is marked as an erasure. The factor  $E_{\text{thresh}}$  is called the Erasure threshold factor. It is a compromise between the number of erasures and the number of errors. If it is chosen too low, then the erasure rate will go down, at the cost of the pulse error rate going up. If it is chosen too high, the pulse error rate will be lower, but the erasure rate will go up.

If the distance to the transmitter is small (i.e., the received signal power is high), then the factor  $E_{\text{thresh}}$  can be relatively low, because even if only a small portion of the received pulse is undistorted, this undistorted portion will still carry enough information to decode the pulse correctly. If the received signal power is smaller, then  $E_{\text{thresh}}$  will have to be chosen higher, since random noise will have a larger influence on the undistorted portion of the pulse, which leads to an increased probability of incorrect demodulation of the pulse.  $E_{\text{thresh}}$  should therefore be dependent on the SNR of the received signal.

The erasure threshold factor can be used to balance the amount of erasures received, and the number of received pulse errors. The higher the factor, the less pulse errors will be received, but many pulses will be marked as an erasure. If the factor is lowered, the erasure rate goes down, but the pulse error rate will go up.

Since the (modified) envelope of the received signal is already available, the power of the undistorted part of the signal can easily be calculated by squaring the envelope and integrating it over the length of the entire pulse.

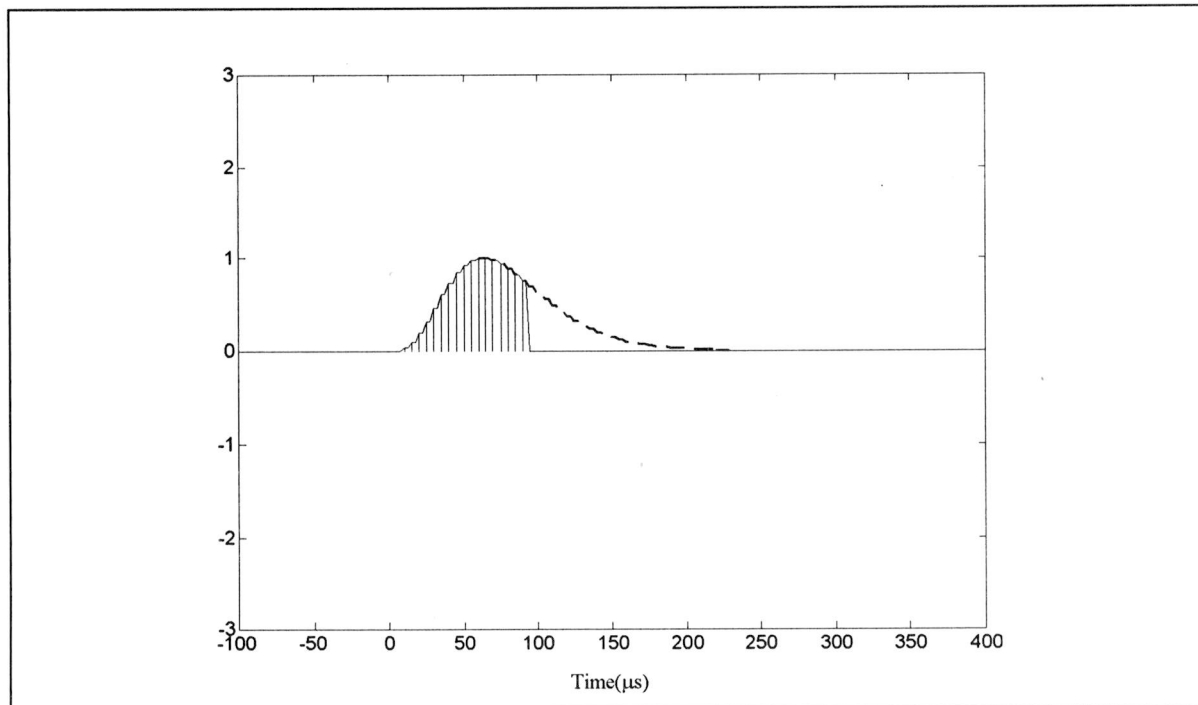


Figure 4.7: Power of the undistorted part of the received signal (dashed area)

From figure 4.7 the amount of power contained in the undistorted part of the received signal from figure 4.1(c) can be seen as the dashed area.

#### 4.6 Parameters of the pulse distortion-detecting and reducing algorithm

A number of parameters were presented with the introduction of the pulse distortion-detecting and reducing algorithm. All relevant parameters, and their influences, are described below:

- The width of the tolerance band, composed of:

$T_{perc}$ : the allowed percentual change in the expected envelope. This factor must be chosen such that all changes in the expected envelope caused by non-distorting phenomena (like Eurofix modulation and the error in the envelope detection) all have an impact on the received envelope that is less than  $T_{perc}$  times the expected envelope. If this factor is chosen too low, pulses will be marked as being hit by Cross-rate when they are not. If it is chosen too high, pulses distorted by Cross-rate or severe atmospheric noise will not be detected as such.

$T_{fixed}$ : the allowed random change in the envelope. This factor allows a certain amount of random signals (such as thermal noise, weak atmospheric noise and weak Cross-rate) to be present on the received signal. If this factor is chosen too low, the tolerance band will be very small on the points when the expected envelope is small in amplitude. This means

that all changes in the envelope at those points (for instance, by a skywave building up over time) will be marked as distorted, which is undesirable. If the factor is chosen too high, pulses that are distorted by Cross-rate or atmospheric conditions will pass unnoticed.

- $q_{\text{hold}}$ : the expected envelope hold factor. This factor controls how fast changes in the received envelope are incorporated in the reference (expected) envelope. The lower  $q_{\text{hold}}$ , the faster the reference envelope follows changes in the received envelope. This factor should be low enough to follow the fastest changes in the received envelope caused by skywaves and dynamics, but high enough not to allow envelope-changes caused by Cross-rate or lightning to have any impact on the stored reference envelope.
- $E_{\text{thresh}}$ : the erasure threshold factor. This factor determines how much of the power of a Loran-pulse must remain undistorted before an erasure is declared. This factor balances the erasure rate and the pulse error rate - if  $E_{\text{thresh}}$  is lowered, the pulse error rate will go up and the erasure rate will go down - if  $E_{\text{thresh}}$  is increased, the opposite happens.  $E_{\text{thresh}}$  should be inversely proportional to the mean SNR, as explained in section 4.5.

## 5. The Demodulator

In this chapter, a demodulator for the Eurofix datalink is developed. First, the possible demodulator structures are discussed.

### 5.1 Demodulator structures

There is a number of possible Loran-C receiver structures that can decode Eurofix modulation:

- Single point receivers
  - Hard-limited single point receivers
  - Linear single point receivers
- Cross-correlation receivers
  - Hard-limited cross-correlation receivers
  - Linear cross-correlation receivers

All these receiver structures are described more extensively in [9]. For completeness, a short description of each demodulator type is given here:

#### 5.1.1 Hard-limited single point demodulators

A hard-limited single point demodulator takes only one sample of each Loran-C pulse, and uses only the sign (positive or negative) of this sample. The sample is taken at a point in the Loran-pulse where no skywaves are assumed to be present. If the transmitted signal was early, the sign will be negative - if it was late, the sign will be positive. If the transmitted code was balanced, then on average the number of positive samples and negative samples must be zero. This provides a tracking mechanism for the Loran-C receiver, since if the average is not equal to zero, the sample-moment must be adjusted. More information about tracking can be found in [5].

This demodulator is appealing because of its simplicity - its implementation is very simple, and the hardware needed is very cheap. It is, however, quite susceptible to noise, because a certain amount of noise on the sample point results directly in increased probability of incorrect decoding of the pulse.

This technique can be used to demodulate Eurofix 2-level coding, but is unusable for demodulation of 3- or more level coding schemes, because only 1 bit of information per Loran-C pulse is acquired.



### 5.1.2 Linear single point demodulator

This type of demodulator also takes only one sample per Loran-C pulse, but it acquires more information than the hard-limited case because it uses the value of the sample rather than just the sign of the sample. This demodulator structure is still quite simple, and thus cheap.

This demodulator structure is capable of decoding 3- or more level Eurofix coding, since the value of the sample provides a measure on how much the transmitted pulse was advanced or delayed. However, a 'moving average' set of reference values (1 per level) is needed to determine the level of shifting of the transmitted Loran-pulse, because influences other than Eurofix-modulation (for instance, the signal strength) will affect the value of the sample that is taken.

For exactly the same reason as was given for the hard-limited case, this demodulator is also quite susceptible to noise.

### 5.1.3 Hard-limited cross-correlation demodulator

This type of demodulator takes a large number of samples per Loran-C pulse, and cross-correlates the signs of this set of samples with a stored reference set. Then, the demodulator cross-correlates the same signs of the received set of samples with a time-shifted version of the stored reference set. The demodulator repeats this process for each possible level of modulation. The time-shift of the received signal is then determined by the time-shift of the reference set that yields the highest correlation.

Cross-correlation demodulators use much more information per pulse than single-point demodulators do. Theoretically, since on average the (Gaussian) noise that is always present at each sample taken is zero, the more samples per Loran-C pulse are taken, the more the noise influence is reduced considered over all of the samples taken.

Practically, however, a band filter will have to be used in the receiver. The filter causes the noise influence on consecutive samples to be correlated to a certain extent. This puts an upper limit to the number of samples that can be taken, above which further reduction in noise influence is negligible.



### 5.1.4 Linear cross-correlation demodulator

This type of demodulator uses the same concept as the hard-limited cross-correlation demodulator, but instead of only using the signs of the sample values, the sample values itself are being used for the received pulse and the reference figures. This way, the information that is contained in the amplitude of the received signal is also taken into account, yielding a higher performance.

This demodulator structure has the highest complexity of all types of demodulators presented here. Its performance, however, will be better than that of the other demodulator structures. This demodulator acquires the largest amount of information about the signal compared with the other demodulators.

In the light of the continuing increase in speed and decrease in cost of computing hardware, the complexity of this demodulator will not have a large impact on its price - costwise, it will probably be competitive with the simpler types of demodulators presented. Therefore, this type of demodulator is the most promising of the types presented here.

### 5.2 Demodulation of Eurofix-modulated pulses using linear cross-correlation

The demodulator calculates the correlation value of the incoming pulse with stored reference figures; one for each level of shift. The reference figure that yields the highest correlation value with the incoming pulse is assumed to have the same timeshift as the received pulse.

The following figure is a graph of the 3 autocorrelation functions of an early, a prompt and a delayed pulse.

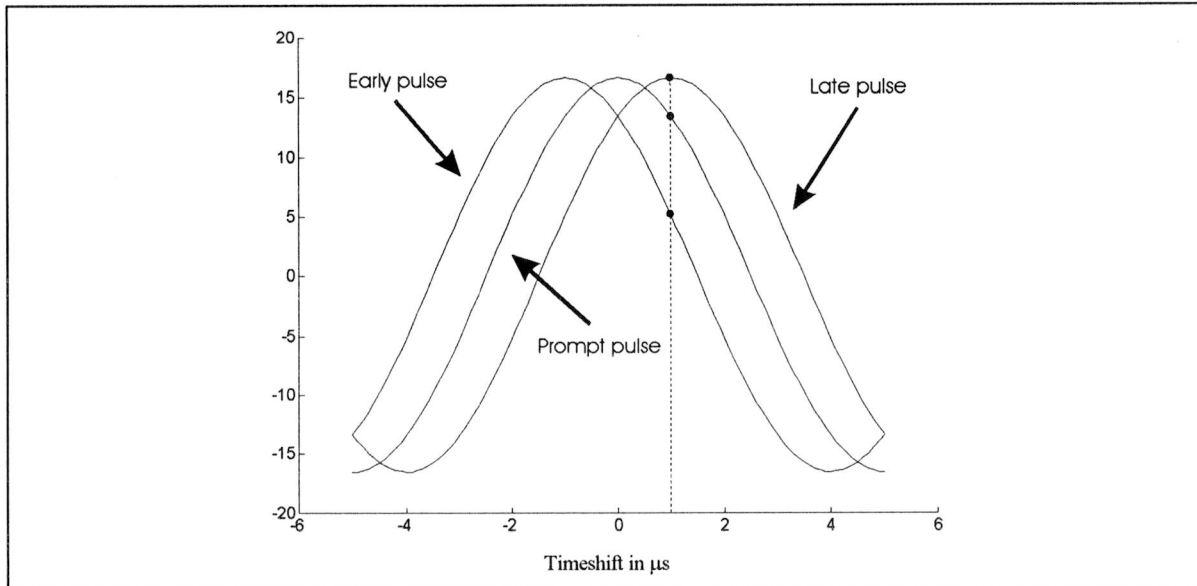


Figure 5.1: Cross-correlation values: correlation function of a normalized early, a prompt and a delayed pulse with a time-shifted Loran-C pulse - all sampled at 400 kHz

As an example, a Loran-C pulse with a time-shift of 1  $\mu\text{s}$  is represented as a dashed line. The correlation values between the Loran-C pulse and the 3 reference figures are represented as black dots. Since the correlation value with the 'late' pulse is highest, the pulse will be decoded as a 'late' pulse.

For our purposes, the most interesting values that can be seen from this figure are the correlation values at the points of intersection between all possible levels of shifting of the pulses. The difference between these values is a measure of the selectivity of the demodulator. These are summarized in the following table:

shift	-1 $\mu\text{s}$ (early)	0 $\mu\text{s}$ (prompt)	1 $\mu\text{s}$ (late)
-1 $\mu\text{s}$ (early)	16.635 (1.000)	13.456 (0.809)	5.137 (0.309)
0 $\mu\text{s}$ (prompt)	13.456 (0.809)	16.635 (1.000)	13.456 (0.809)
1 $\mu\text{s}$ (late)	5.137 (0.309)	13.456 (0.809)	16.635 (1.000)

Table 5.1: Correlation values and factors of normalized Loran-C pulses (sampled at 400 kHz) with different levels of shifting. The correlation factors are bracketed.

It can be seen from the table that the correlation between an early and a prompt pulse yields a much higher value than the correlation between an early and a late pulse. Since the correlation value is the only criterion used to classify a received pulse as an early, a prompt or a late pulse, we can expect to

find that the probability that an early pulse will be decoded as a prompt pulse is much higher than the probability that the same pulse is decoded as a late pulse.

This table illustrates a well-known principle in telecommunications: the greater the alphabet of symbols that can be transmitted over any telecommunications channel, the higher the possibility that an error is made in the demodulation of a given symbol, and hence an increased Symbol Error Rate (SER). The question whether the increase in speed outweighs the increased SER is subject to investigation.

### 5.3 A Linear cross-correlation demodulator

The concept of the linear cross-correlation demodulator is given in the following figure. 3-level Eurofix coding is assumed.

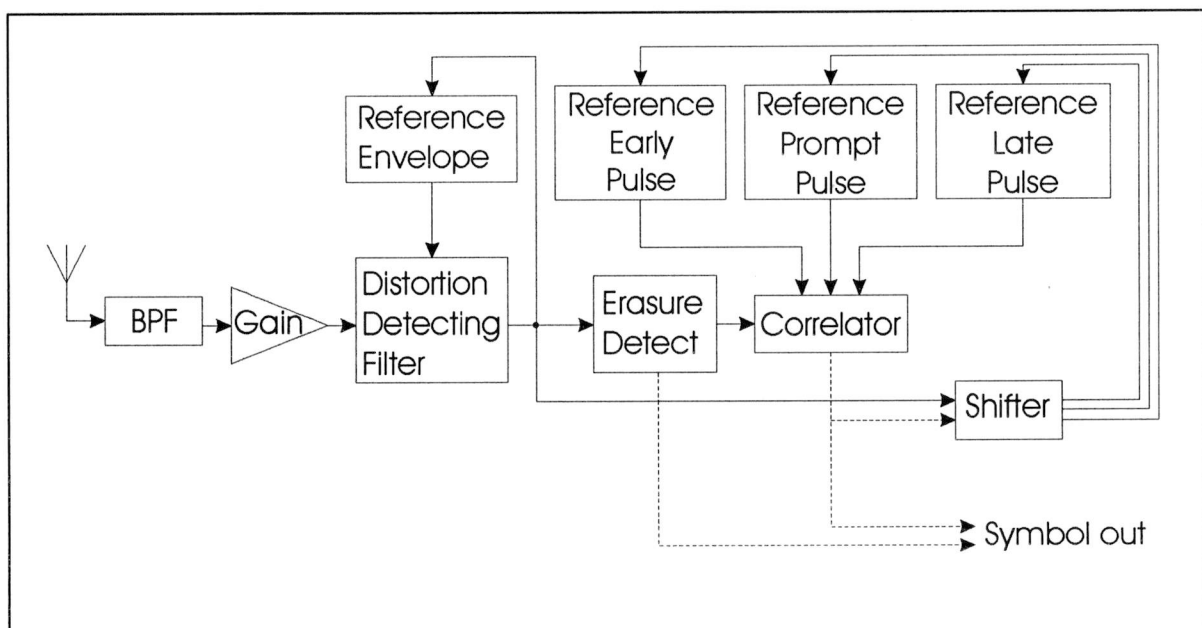


Figure 5.2: The demodulator structure. The solid lines display the signal path; the dashed lines display the control path

The Loran-C signal is received by the antenna, and fed through a band-pass filter to filter out all frequencies outside the Loran-C band (90-110 kHz). The signal is then fed through the distortion-detecting filter that was introduced in Chapter 5. If the filter did not detect the received pulse as being an erasure, the filtered signal is correlated with 3 reference figures. The correlator decides which of the 3 reference figures yields the highest correlation with the received (filtered) signal, and outputs the result.

The shifter takes the received (filtered) pulse, and calculates from this data 3 new sets of data: 1) one that matches the pulse had it been transmitted early, 2) one set had it been transmitted prompt and 3) one had it been transmitted late.

The symbol output can be either a valid symbol, or an erasure. This data can further be processed by a decoder that can extract messages from the data, correcting errors and erasures from the demodulator with an error-correcting protocol.

Two of the components used in this demodulator structure will be discussed a bit more in-depth in the following paragraphs. These are:

- The pulse shifter, and
- The reference figures

### 5.3.1 The Pulse Shifter

The pulse shifter is used to calculate ‘shifted versions’ of a particular set of data. For instance, if the received set of data is the sampled version of a prompt pulse, and represented by:

$$p_i = S_i * T_{\text{sample}} \tag{Formula 5.1}$$

where:

$p$  is the set of sample values of the prompt pulse,

$S_T$  is the received signal sampled at time  $T$ , and

$1/T_{\text{sample}}$  is the sampling frequency (assumed to be 400 kHz),

then the shifter should calculate:

$$e_i = S_i * T_{\text{sample}} + 1 \mu\text{s} \tag{Formula 5.2}$$

$$l_i = S_i * T_{\text{sample}} - 1 \mu\text{s} \tag{Formula 5.3}$$

where:

$e_i$  is the set of sample values of the early pulse,

$l_i$  is the set of sample values of the late pulse,

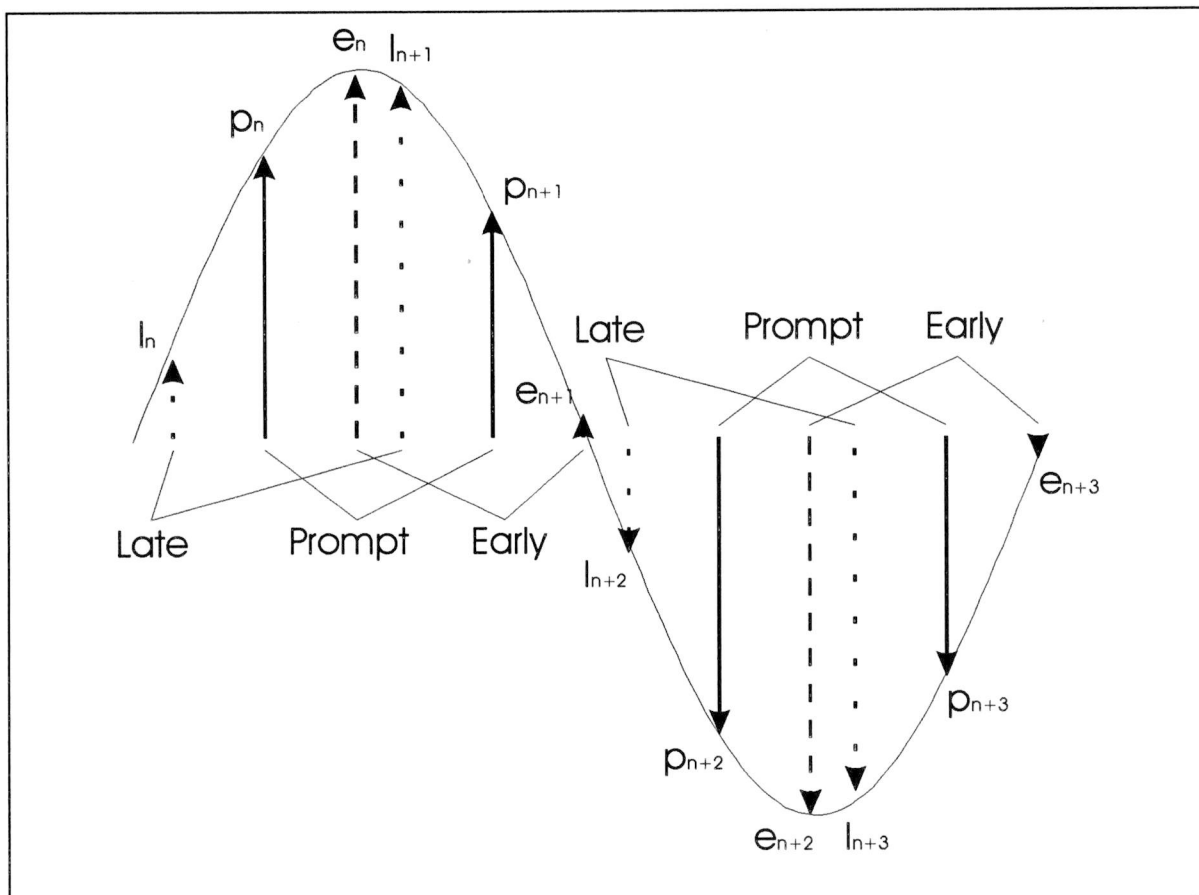


Figure 5.3: Graphical representation of the function the Shifter performs: given the Prompt samples, the shifter calculates the Late and the Early sample values.

In other words, the shifter should interpolate the values of the received signal at those points in time where the real samples would have been taken when the signal was early or late.

Given the fact that the samples are taken at twice the Nyquist frequency, this is theoretically possible, since all information about the signal is contained in the samples.

Its practical implementation, however, is not trivial: theoretically, to calculate any interpolated samplepoint, all other sample points need to be included in the calculation, making this a very lengthy process.

By cleverly giving weight factors to the samplepoints, however, it is possible to design a filter for shifting Loran-pulses that uses only 6 coefficients [10]. The difference between an advanced pulse that has been calculated by shifting a prompt pulse and a normal advanced pulse is smaller than  $1.5e-4$ .

### 5.3.2 The reference figures

The reference figures that are used to store the representations of an early, a prompt and a late Loran-C pulse bear a great similarity to the reference figure used for the distortion detecting, as described in section 5.4. This means that the update rate of the reference figures should be slow enough to minimize the influence of non-consistent disturbances, but fast enough to follow consistent changes in the shape of the Loran-C pulse due to skywaves.

### 5.4 Thermal noise influence on the linear cross-correlation method

To find the probability of the linear cross-correlation method of making an incorrect decision due to thermal (Gaussian) noise, the result of this Gaussian noise on the received signal is investigated first.

The probability of an incorrect decision using the linear cross-correlation method can be expressed as a function of the signal-to-noise ratio of the received signal.

A sampled version of the Loran-C signal is expressed as:

$$x_i = \left(\frac{t}{t_p}\right)^2 \cdot \exp\left(2 - \frac{2t}{t_p}\right) \cdot \sin\left(2\pi \cdot t \cdot 100 \cdot 10^3\right), \quad \text{Formula 5.4}$$

with  $t=i \cdot 2.5 \mu\text{s}$ ,  $t_p=65 \mu\text{s}$  and  $i=0..399$ .

The samples of the received signal are represented by the vector  $y_i$ . The corresponding values of the reference figure are denoted as  $x_i$ . The correlation  $C$  is then calculated by:

$$C = \sum_i x_i \cdot y_i \quad \text{Formula 5.5}$$

We can assume a certain amount of Gaussian distributed noise on each of the samples  $y_i$ , denoted by  $e_i$ . Each element of  $e_i$  is a normally distributed random value with  $m=0$  and variance  $\sigma^2$ . So:

$$y_i = x_i + e_i \quad \text{Formula 5.6}$$

Equation 5.5 now becomes:

$$\begin{aligned}
 C &= \sum_i x_i \cdot (x_i + e_i) \\
 &= \sum_i x_i^2 + \sum_i x_i \cdot e_i
 \end{aligned}
 \tag{Formula 5.7}$$

The value of the first right-hand term in this equation can be found in table 5.1, and is equal to 16.635.

We want to calculate the probability that a pulse is demodulated incorrectly. Mathematically:

$$P\left(\sum_i x_i^B \cdot y_i > \sum_i x_i^A \cdot y_i\right)
 \tag{Formula 5.8}$$

where  $x^A$  and  $x^B$  represent two different reference figures. With equation 5.6, this can be rewritten as:

$$\begin{aligned}
 &P\left(\sum_i x_i^B(x_i^A + e_i) > \sum_i x_i^A(x_i^A + e_i)\right) = \\
 &P\left(\sum_i x_i^B x_i^A + \sum_i x_i^B e_i > \sum_i (x_i^A)^2 + \sum_i x_i^A e_i\right) = \\
 &P\left(\sum_i e_i(x_i^B - x_i^A) > \sum_i x_i^A(x_i^A - x_i^B)\right)
 \end{aligned}
 \tag{Formula 5.9}$$

In this formula,  $x^A$  and  $x^B$  are known. The problem, however, lies in the elements of  $e_i$ ; because the thermal noise is bandpass filtered, these noise samples will not be statistically independent.

Instead, all samples  $e_i$  are dependent on a new random variable and all previous values of  $e_i$ .

$$e_i = r(0)Z_i + r(1)Z_{i-1} + r(2)Z_{i-2} + \dots
 \tag{Formula 5.10}$$

with each element  $Z_i$  a normally distributed random variable with mean 0 and variance  $\sigma^2$ .

$r(i)$  is the time-discrete impulse response of the filter. For a 6th order Butterworth filter, the impulse response is given in the following figure:

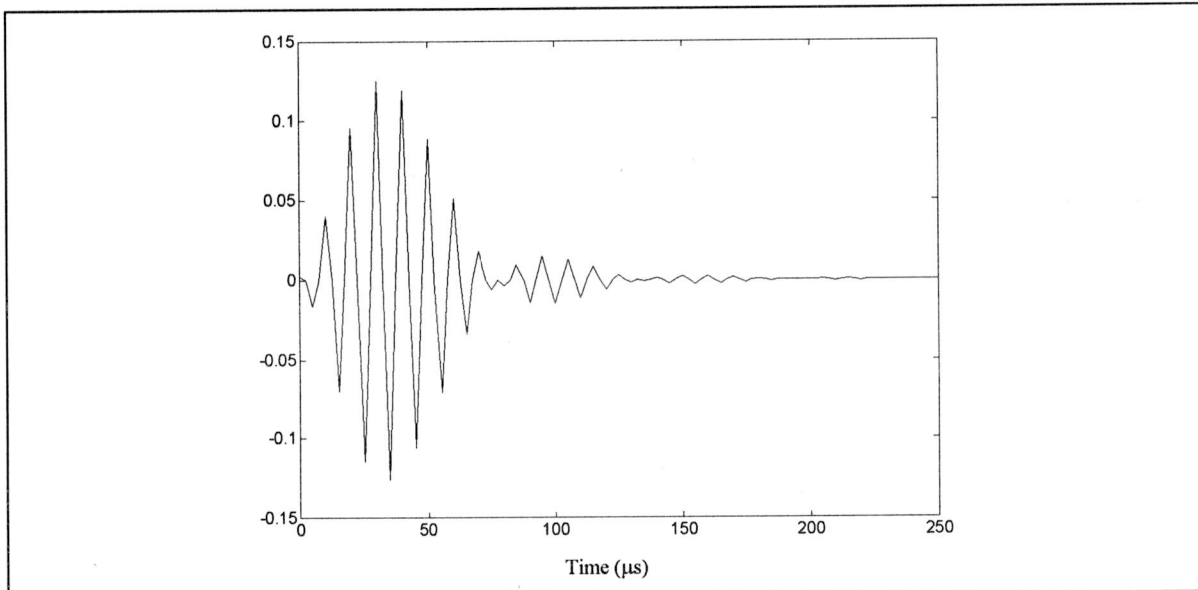


Figure 5.4: Impulse response of a 6th order 90-110 kHz bandpass Butterworth filter

As each element  $e_i$  is a linear combination of normally distributed random variables, it is itself a normally distributed random variable. Its variance is equal to the in-product of the impulse response times the original (i.e., before filtering) variance of the random signal. In formula form:

$$\text{var}(e_i) = \text{var}(Z) \cdot \sum_j r(j)^2 \quad \text{Formula 5.11}$$

For the 6th order Butterworth filter:

$$\sum_j r(j)^2 = 0.1043$$

which leads to the conclusion that the power of the random signal after filtering is roughly 10% of the power of the same signal before filtering.

Now, equation 5.9 can be plotted as a function of the SNR.

The probability of error for a linear cross-correlation receiver can be calculated. In the following figure, the pulse-error probability is plotted versus the SNR of the received signal:

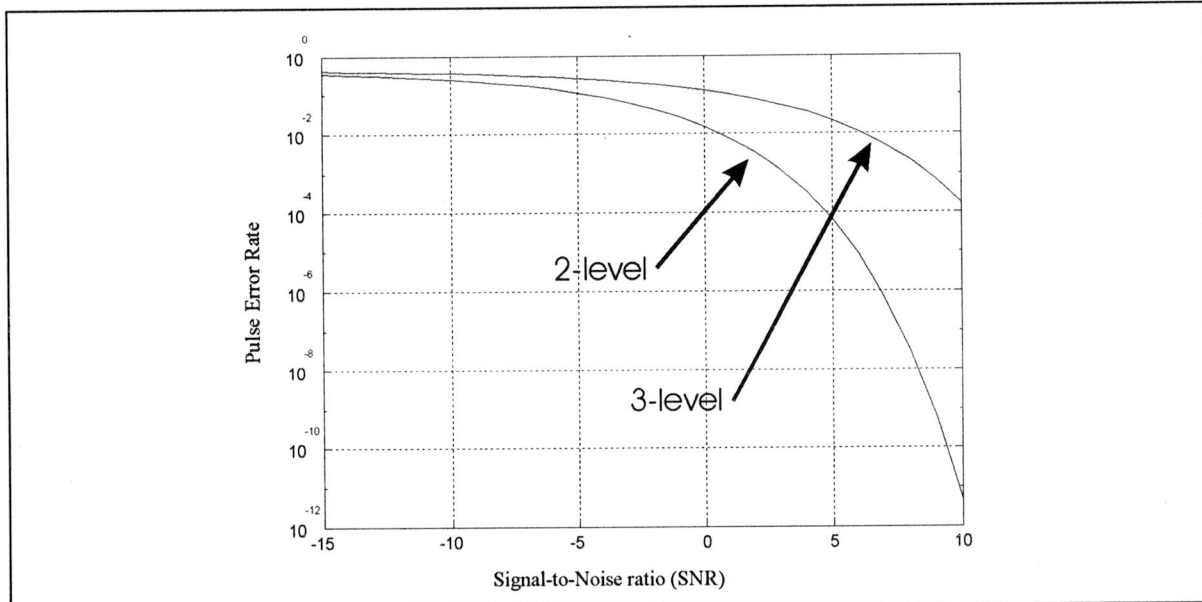


Figure 5.5: Probability of error versus SNR of the received signal for a linear cross-correlating receiver (2- and 3-level coding)

## 6. Testing of the proposed demodulator

In order to test different encoding and/or decoding methods for the Eurofix Datalink, it is desired to have a test-setup that simulates the reality as accurately as possible.

Ideally, the test-setup would be:

1. A 'live' transmission medium (including signals from other Loran-transmitters, atmospheric noise, electromagnetic disturbance due to lightning, etc.)
2. A Loran-transmitter transmitting real-time Eurofix data
3. A real-time Eurofix demodulator

### 6.1 The Transmission medium

The characteristics of the transmission medium can readily be monitored by putting up an antenna and inspecting the signals in the Loran-band (90-110 kHz). In this band, signals from other Loran-transmitters will be found, as well as signals that result from atmospheric conditions.

### 6.2 Acquiring Time-shifted Loran-pulses

It is quite difficult to have a real Loran-transmitter transmitting Eurofix data. In order to do this, an existing transmitter would have to be modified to transmit Eurofix data, which would politically and institutionally be very difficult. Furthermore, to be able to compute bit-error rates, a datalink (other than the Eurofix datalink) would have to be established between the transmitter and the demodulator to act as a reference datalink. Thirdly, this would have to be done for a number of transmitters to get a good grasp of the influence of parameters like distance to the transmitter, the GRI that is being operated on (as this could influence the type of Cross-rate that is experienced), the power of the transmitter etc.

The conclusion can be drawn that, at this stage of the research, it is not feasible to have a real Loran-transmitter transmitting Eurofix-data, just for test purposes.

An alternative can be found by looking into the nature of the Eurofix-modulation. Normally, the Loran-pulse would be transmitted at time  $T_0$  and received at time  $T_1$ , with its time-shifted variant being transmitted at time  $T_0 + \delta T$  and received at time  $T_1 + \delta T$ . But, if the Loran-pulse is transmitted at time  $T_0$ , its time-shifted version can also be found by looking at time  $T_1 - \delta T$ . In other words, instead of having the transmitter transmit the pulse later in time, it is also possible to have the receiver start receiving

earlier in time and vice versa. The concession that is made to the real-life situation is that all Cross-rate and noise appears to be time-shifted too.

In order to get a sampled version of a time-shifted Loran-pulse, a shiftable clock signal is needed. This clock signal needs to be adjustable in such a way that, for the duration of an entire Loran-C pulse, the clock is either  $1 \mu\text{s}$  early,  $0 \mu\text{s}$  early or  $1 \mu\text{s}$  late.

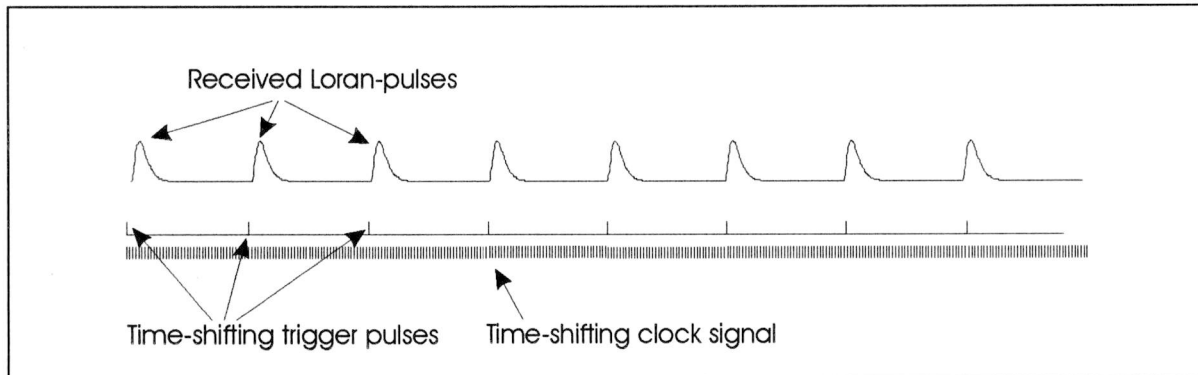


Figure 6.1: Timing diagram of the received pulses, the trigger signal and the sampling clock signal. The trigger pulses can be programmed to appear  $1 \mu\text{s}$  early,  $0 \mu\text{s}$  early or  $1 \mu\text{s}$  late.

Using this method, any normal Loran-C transmitter can be made to look like it is time-shifting its pulses, from the demodulator's viewpoint. This is illustrated in figure 6.1.

In order to get this clock, a Loran-C simulator is used. This simulator can produce 1 trigger pulse per Loran-signal. Furthermore, since the Loran-C simulator that is used can transmit Eurofix-modulated pulses as well, the trigger pulses are time-shiftable as well. The simulator is utilized just to produce trigger pulses - the actual Loran-C signals coming out of the simulator are not used. A separate PC is used to produce the control data for the simulator that determines how the trigger pulses are to be time-shifted.

An atomic frequency standard keeps the test-setup locked to the real Loran-C signals that are being tracked. No other tracking mechanism is used.

The 400 kHz signal that is needed is realized using a 10 MHz frequency (obtained from a 5 MHz atomic frequency standard) and a 25-counter. Each (400 kHz) clock cycle, the 25-counter starts at 25, counting down at 10 MHz. When the 25-counter hits 5, it raises its output - when it hits 0, it lowers its output again, thereby outputting a 400 kHz clock with a 20% high-time. The trigger pulse from the

Loran-C simulator is used to clear the 25-counter. By time-shifting the moment the trigger-pulse occurs by  $\delta T$ , the desired time-shifting clock is acquired.

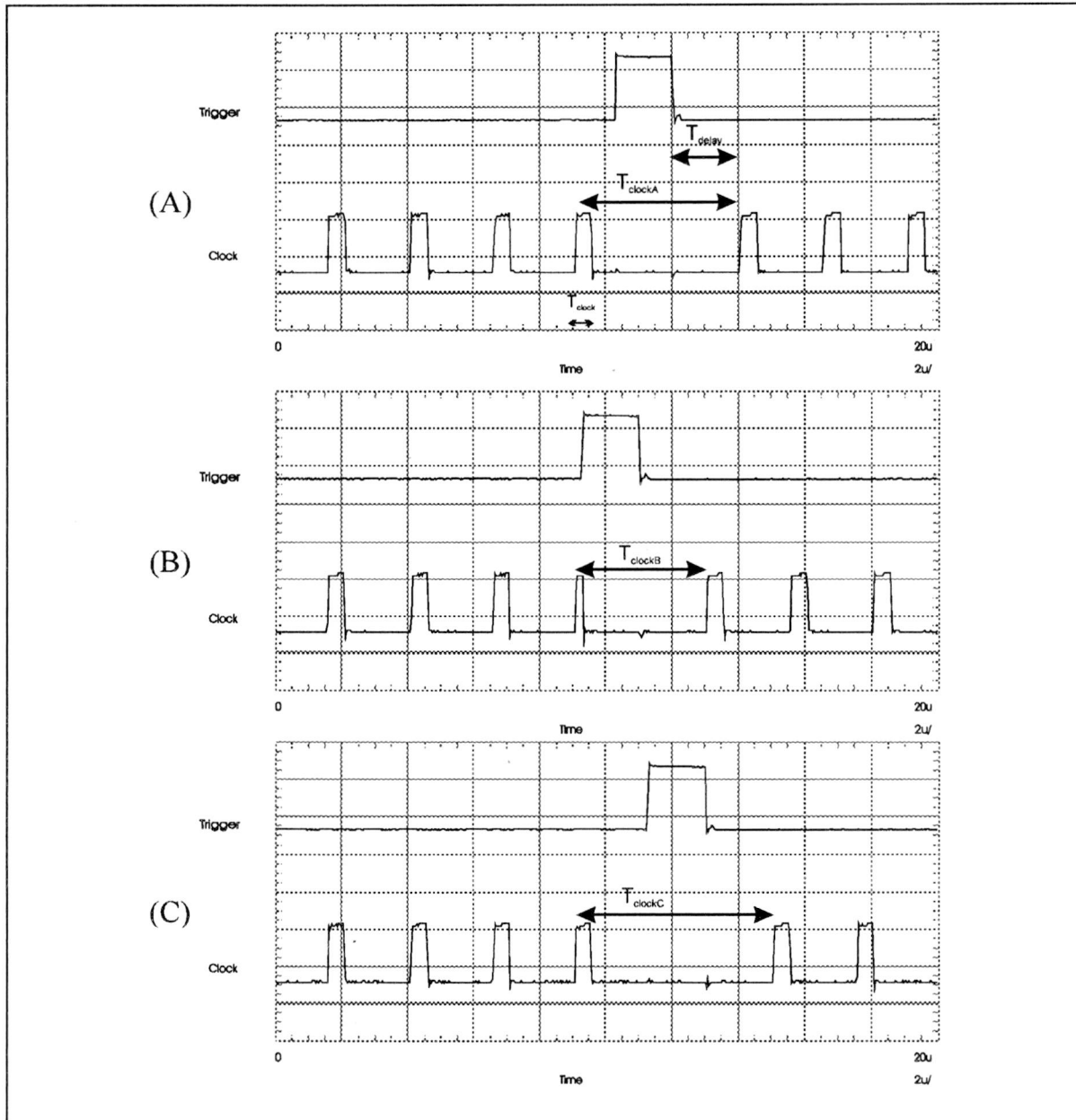


Figure 6.2: Timing of the clock signal with relation to the trigger pulse.

(A) is the diagram for a prompt-to-prompt clock transition,

(B) for a prompt-to-early transition and

(C) for a prompt-to-late transition.

$T_{delay} = 2 \mu s$ ,  $T_{clock} = 500 ns$ .  $T_{clockA} = 5 \mu s$ ,  $T_{clockB} = 4 \mu s$  and  $T_{clockC} = 6 \mu s$

This is illustrated in figure 6.2.

Unfortunately, 1 clock-pulse will always be lost because of the time  $T_{\text{delay}}$  being  $2 \mu\text{s}$ . This results in the fact that instead of  $8 \times 400$  samples, only  $8 \times 399$  samples are taken. The demodulator software has been modified to take this into account.

In 6.2(b), it can be seen that the 399th clock pulse is somewhat smaller than the others - this is also due to the fact that  $T_{\text{delay}}$  is  $2 \mu\text{s}$ . Since the received Loran-pulse must in its entirety lie between the occurrence of 2 trigger pulses, the received pulse will have 0 amplitude at the 399th clock pulse, so the timing for this clock pulse is not critical.

### 6.3 The Demodulator

The proposed demodulator of Chapter 5 has been implemented in software. The underlying hardware mainly consists of a 486 DXII-66MHz PC equipped with a 12 bit, 400 kHz A/D converter board. The timing for this board is provided by the Loran-C simulator, which produces the necessary trigger pulses from which the shifting clock is derived.

The demodulator as it has been programmed and tested differs from the demodulator as was proposed in Chapter 5 in the following respects:

- The shifter section has not been implemented due to lack of processing time. The PC is only just capable of performing all the other tasks (detecting distortion, cross-correlating and updating the reference figures) in the repetition time of the Loran-C pulses (the GRI).

This means that the reference figures for the early, prompt and late pulse can only be updated when the demodulator has decoded the received pulse as having the corresponding timeshift. This results in a reduced update rate of the reference figures. It also introduces an initialization problem: the reference figure of the prompt pulse can initially be built by using the first 2 pulses of the Loran-burst (since these pulses are never Eurofix-modulated), but there is no way to build the early and late reference figures. This is circumvented by always starting the tests with the transmission of a known synchronization pattern - the demodulator knows how the pattern is Eurofix-modulated and builds all 3 reference figures from this pattern.

The problem mentioned above could be resolved by using hardware that is more appropriate for the task of signal processing (e.g., a high-speed Digital Signal Processor) or, alternatively, by using a faster PC.

- The tolerance band of the distortion detecting filter is not applied to the envelope of the received signal, but rather to the square of the envelope of the received signal. The real-time calculation of the square root of this envelope proved to be an, as yet unresolved, problem.
- No notch filters have been used in the test-setup, resulting in the fact that CWI is not suppressed. During the tests, however, no effects of CWI were detected.
- No tracking mechanism was used other than an atomic frequency standard, which kept the timing of the test-setup synchronized to the timing of the Loran-C transmitters. As a result, no tracking errors were made - a situation that will not apply when a real-life Loran-C receiver is used.
- The used filter is a 5th order instead of a 6th order Butterworth filter.

#### 6.4 The Test-setup

The test setup as it has been used in the tests is depicted in the following figure:

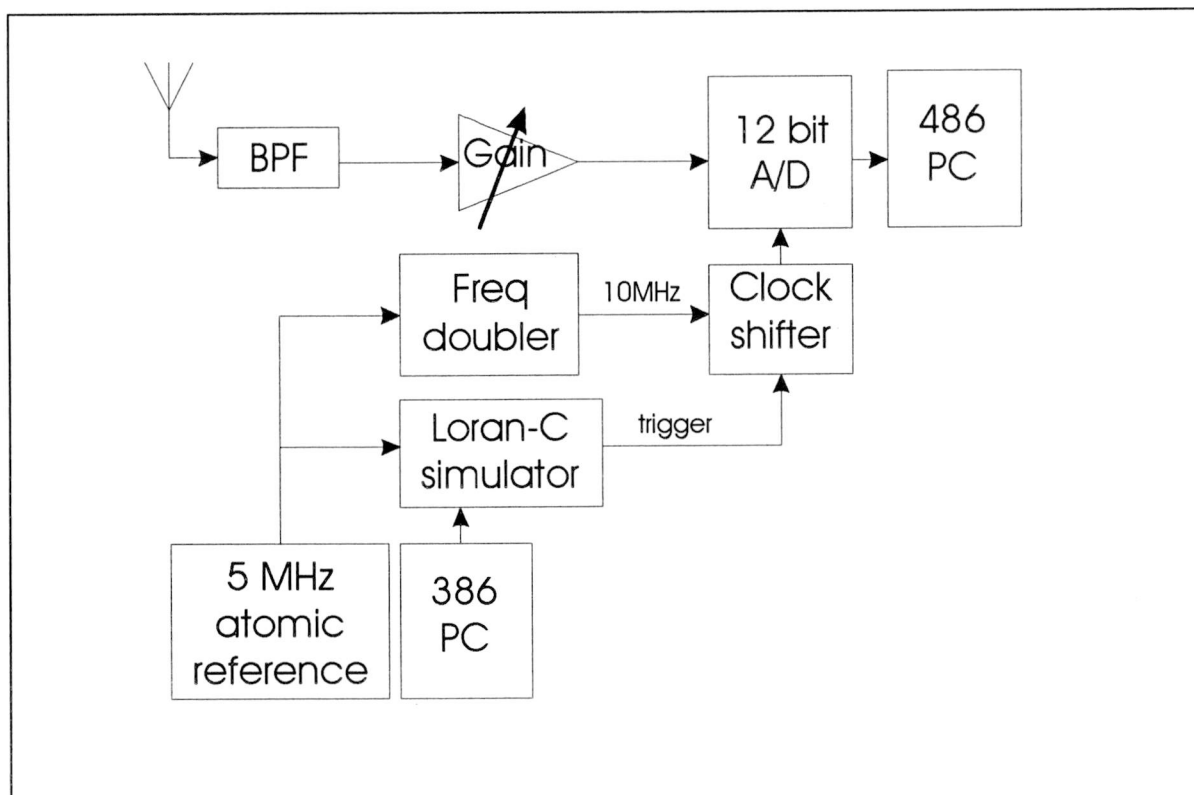


Figure 6.3: The test-setup. The block layout diagram of the software for the '486 PC' resembles figure 5.2.



## Testing of the proposed demodulator

---

The band-pass filter (BPF) that has been used is a 5th order Butterworth filter, with a center frequency of 100 kHz and a bandwidth of 17 kHz.

The 5 MHz atomic reference was provided by a 5 MHz rubidium frequency standard.

## 7. Results

In this chapter, the results of my research are presented.

For the tests, signals from the following 3 transmitters have been used: the Sylt-station in Germany, the Lessay-station in France and the Soustons-station, also in France.

The following table gives the distances from the transmitters to the Delft University of Technology, where the measurements were taken. The estimated SNR (based on the amplitude of the pulses) as it was received in Delft is also given, relative to the Sylt signal.

<b>Station:</b>	<b>Distance to Delft (km):</b>	<b>Transmitter power (kW):</b>	<b>Estimated SNR:</b>
Sylt	407.68 km	250	0 dB
Lessay	523.11 km	250	-3 dB
Soustons	1013.43 km	250	-15 dB

*Table 7.1: Distance, transmitted power and SNR for the Loran-C stations used for the tests. The measurements were all taken at the Delft University of Technology. The estimated SNR is relative to the Sylt signal.*

Detailed information about the location of these and other Loran-C stations can be found in Appendix B.

In all figures in this chapter, the horizontal scale is the time of day, measured in hours, modulo 24. So, for instance, if the time is 32 then this corresponds to 8.00 am, 1 day after the start of the test.

All Erasure Rates and Pulse Error Rates that are plotted in the figures are averaged over 1 minute (60 seconds).



## 7.1 The effect of the distortion detecting filter

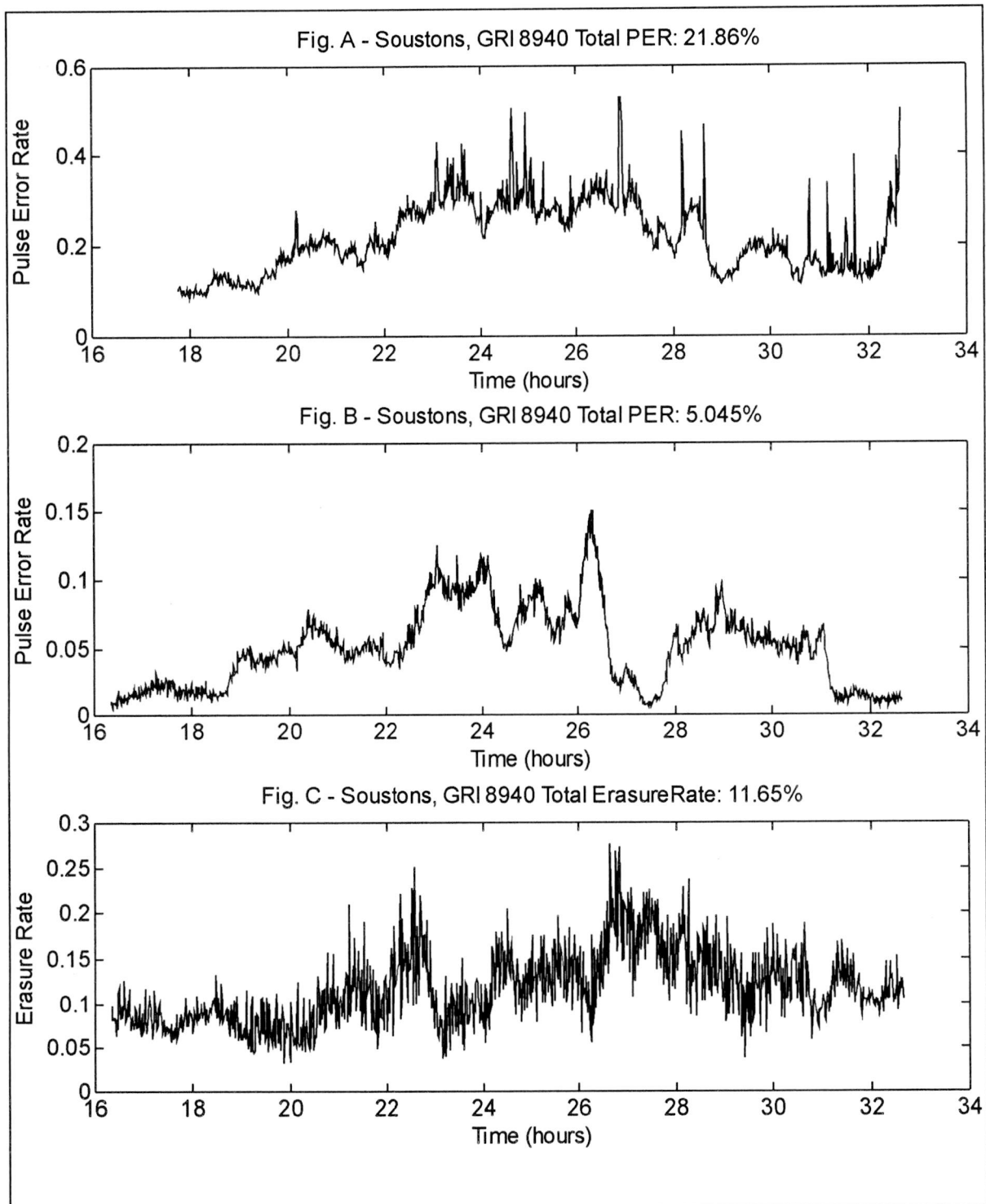


Figure 7.1: Effect of the distortion detecting filter on the Soustons-signals. Fig. (A) is the pulse error rate of the demodulator without distortion detection; fig. (B) and (C) are the pulse error rate and the erasure rate of a demodulator with distortion detection. 3-level coding is used. The measurement plotted in fig.(A) was done on 15 october '95; measurements (B) and (C) were done on 13 october '95.

## Results

---

The effect of the distortion detecting filter can be seen in figure 7.1. Without distortion detection, 21.86% of the received pulses is demodulated incorrectly. With distortion detection, only 5.05% is demodulated incorrectly - although 11.65% of the received pulses are declared as being an erasure. During this test, the erasure threshold factor  $E_{\text{thresh}}$  was set to 0.6 (i.e., when less than 60% of the Loran-pulse was undistorted, it was declared an erasure).

It should be noted, however, that the data was collected on separate occasions. The atmospheric conditions tend to change from night to night, and therefore the pulse error rates and erasure rates for signals from the same transmitter also change from night to night.

During other tests, it was noticed that the skywave-propagation changes quite severely during the night; much more than during daytime. Although only 1 night and only a part of a day has been plotted, this effect can, to some extent, also be seen in these plots: the pulse error rate (fig. B) is much higher between 20 and 29 hours (8.00 pm and 5.00 am the next day) than in the other parts of the plot. This effect can more clearly be seen in other plots in this chapter.

## 7.2 Sylt - 2-level coding

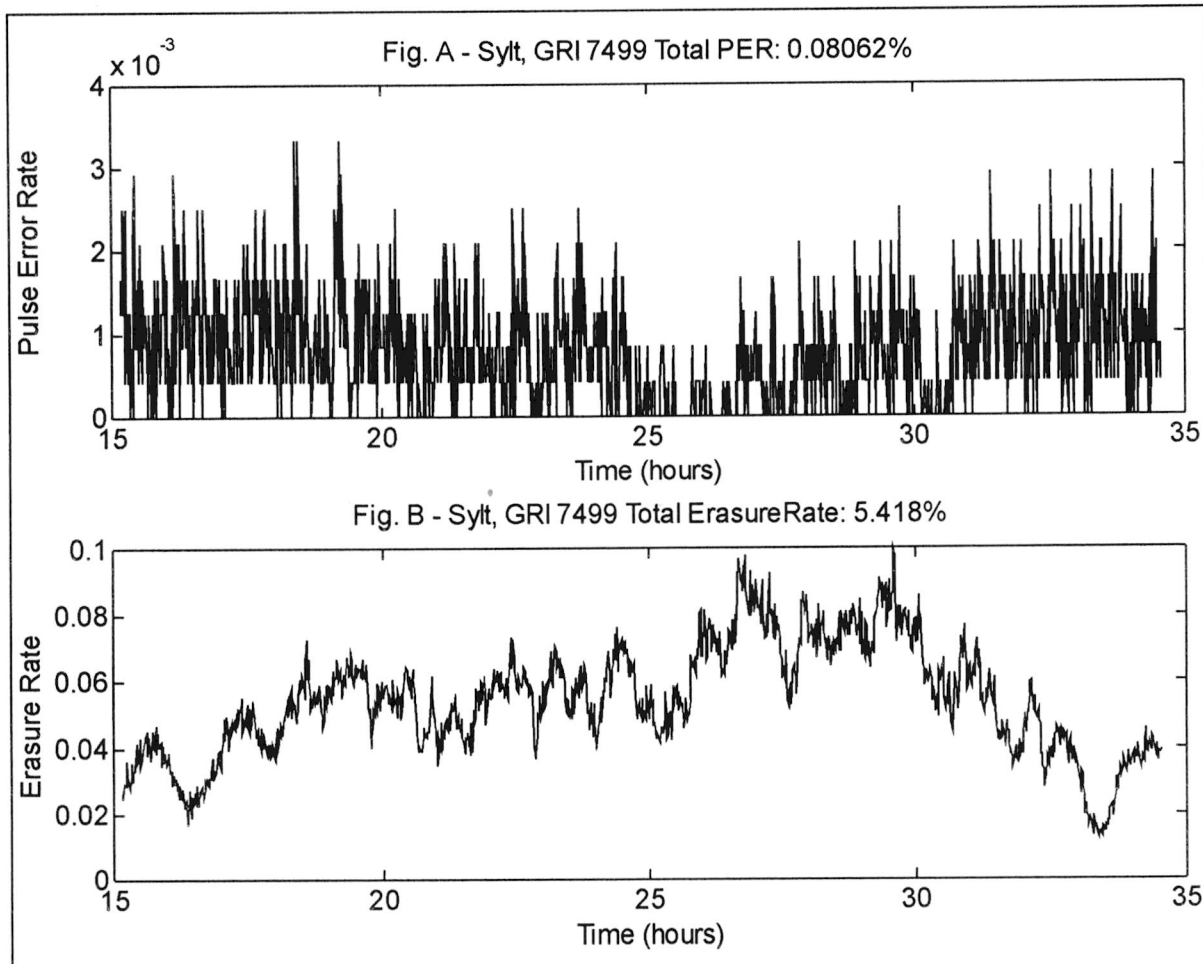


Figure 7.2: Pulse error rate (fig.A) and erasure rate (fig.B) of the Sylt-signal using 2-level modulation. The measurement was done on 7 november 1995.

In figure 7.2, the pulse error rate and the erasure rate of the Sylt signal are plotted. The measurements were done from 3.00 pm until 11.00 am the next day.

The pulse error rate using 2-level modulation is low - only 0.08% of the pulses are in error. This is not surprising, considering the fact that the distance from Sylt transmitter to Delft is only about 400 km, which is not far away in Loran-C terms (the typical coverage range for a Loran-C transmitter is roughly 1500 km).

It can be seen from the plot that the pulse error rate jumps to discrete levels. This is because the number of errors is averaged over 1 minute - since only a discrete number of pulses per minute can be in error, then when the error rate is low (as it is in this case), this can be seen in the resulting plot.

On average, 5.4% of the pulses have been detected as being hit by Cross-rate or severe atmospheric conditions.

### 7.3 Sylt - 3-level coding

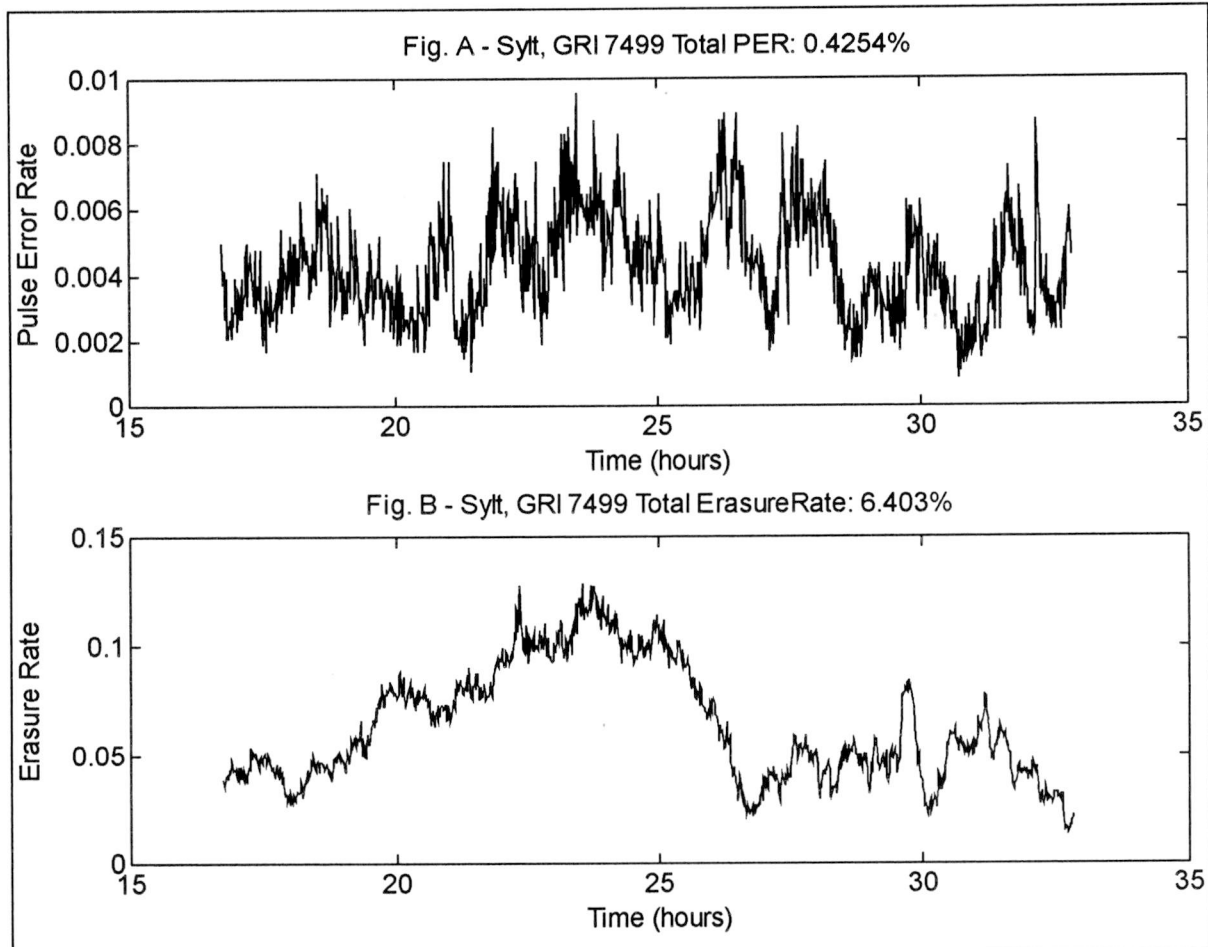


Figure 7.3: Pulse error rate (fig.A) and erasure rate (fig.B) of the Sylt-signal using 3-level modulation. The measurement was done on 8 november 1995.

The 3-level modulation scheme has a higher probability of being demodulated incorrectly than the 2-level modulation scheme under similar circumstances.

This effect can be seen in figure 7.3 - when compared with figure 7.2, the pulse error probability for the 3-level modulation scheme is about 5 times larger than the PER of the 2-level scheme.

On average, the erasure rate is comparable to the erasure rate in the previous plot. This is expected, since the distortion detection is independent from the modulation scheme used.

#### 7.4 Lessay - 2-level coding

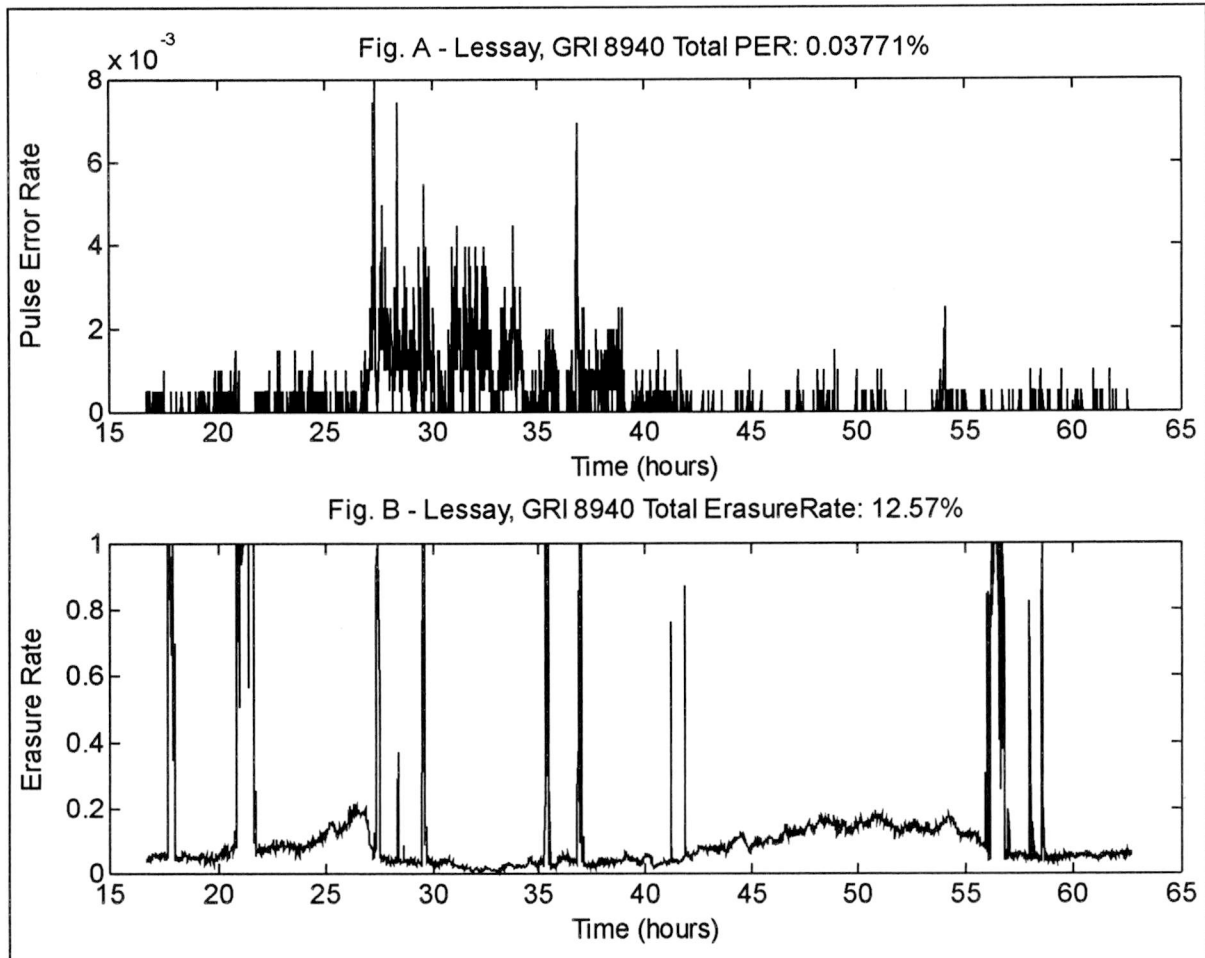


Figure 7.4: Pulse error rate (fig.A) and erasure rate (fig.B) of the Lessay-signal using 2-level modulation. The measurement was done on 17 november 1995.

In figure 7.4, the pulse error rate and erasure rate of the 2-level modulation scheme are plotted using the Lessay signal. Again, as was the case with the Sylt signal, the discrete levels in the PER-plot can be distinguished.

The average PER for Lessay is *lower* than the PER for the Sylt signal. This is surprising, since Sylt is located closer to Delft than Lessay and the SNR of the Sylt signal is higher than the SNR of the Lessay signal. An explanation could be that, when this measurement was done, atmospheric conditions were better than when the Sylt measurement was taken.

Another interesting phenomenon can be seen from the erasure rate - on several occasions, the erasure rate approaches 1, meaning that all pulses are flagged as being distorted. This is not a normal situation. However, when this measurement was taken, it was noticed that during some periods of time, an unknown, very loud signal was indeed interfering with the normal Loran-C signals. It is as yet unknown whether this really was the case, or if, maybe, some component in the test-setup broke down.

### 7.5 Lessay - 3-level coding

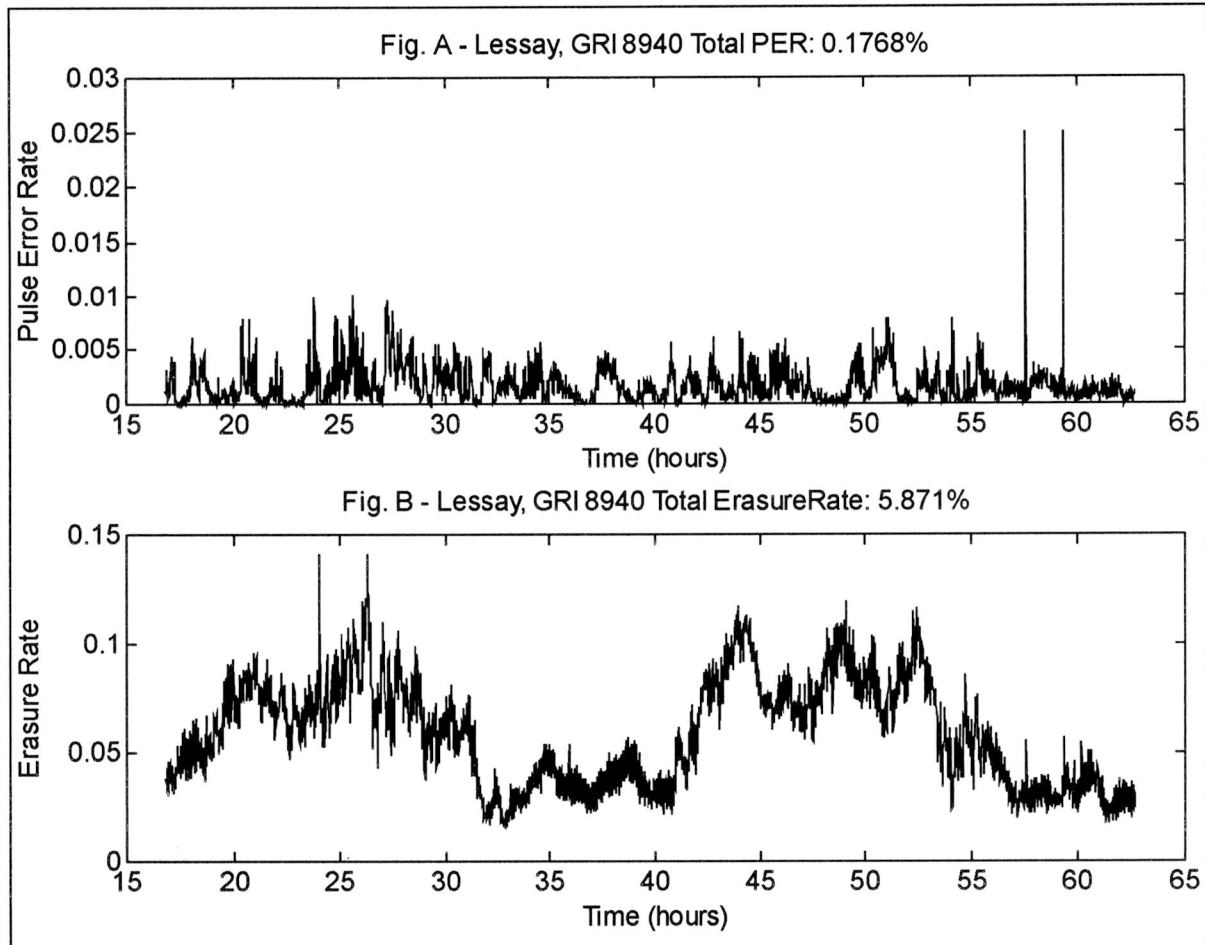


Figure 7.5: Pulse error rate (fig.A) and erasure rate (fig.B) of the Lessay-signal using 3-level modulation. The measurement was done on 18 October 1995.

In figure 7.5, the pulse error rate and erasure rate of the Lessay-signal using 3-level modulation are plotted.

Again, as was the case with the Sylt-signal, for Lessay the PER of the 3-level coding scheme is about 5 times larger than the PER of the 2-level coding scheme. However, in this case the average erasure rate during the 2-level run is higher than the erasure rate of the 3-level run. This is partly due to the peaks that occurred during the 2-level run, and also partly because the atmospheric conditions were not the same for the two runs.

The cause of the peaks in the plot of the PER around 58h is unknown. A possible reason can be a timing-adjustment in the Loran-C transmitter - if suddenly the timing is adjusted, it will take a while for the reference figures in the demodulator to follow the change in the received pulse. While this adjustment is taking place, the pulse-error rate will be higher.

## 7.6 Soustons - 2-level coding

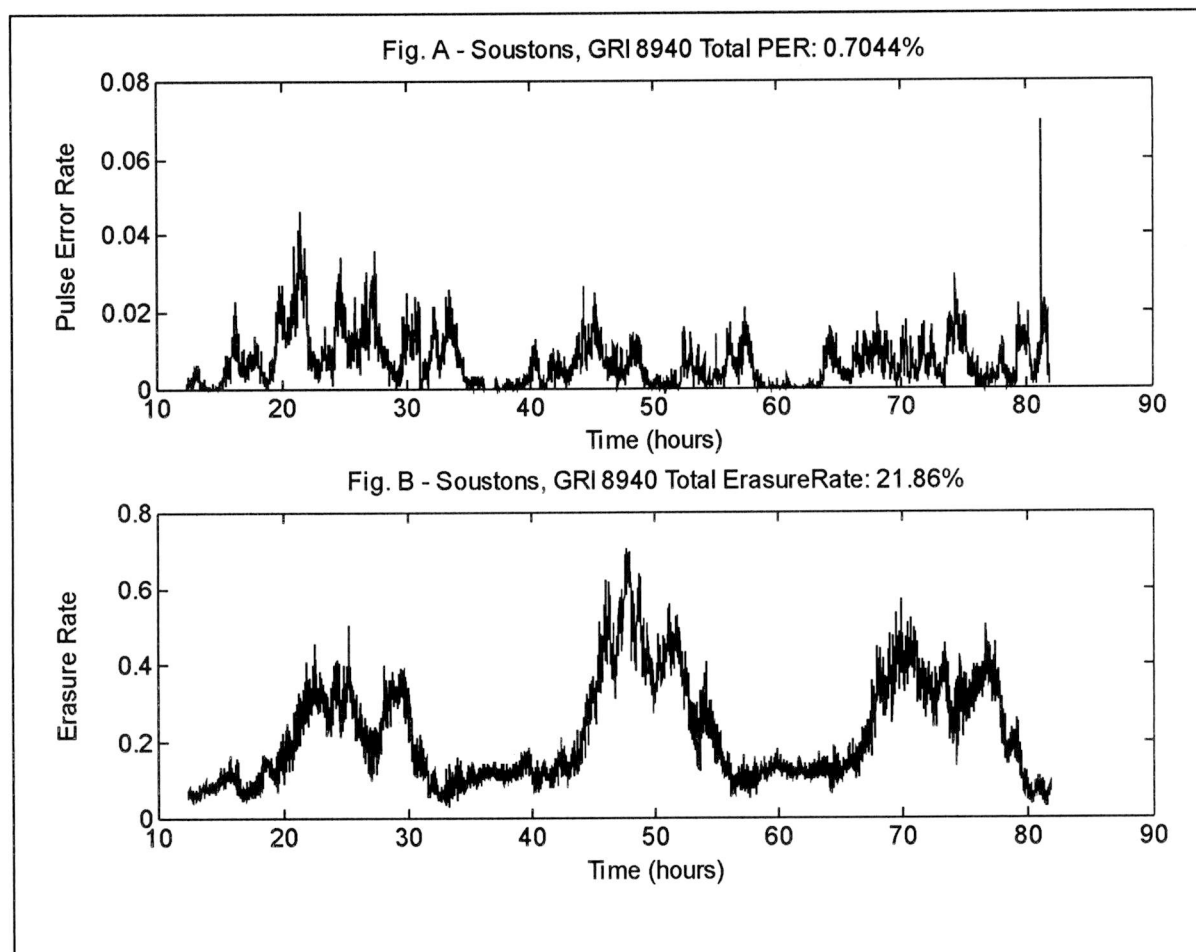


Figure 7.6: Pulse error rate (fig.A) and erasure rate (fig.B) of the Soustons-signal using 2-level modulation. The measurement was done on 3 november 1995.

Finally, tests with 2- and 3-level coding were done with the Soustons transmitter (located about 1000 km away from Delft).

These tests were done over a longer period of time; about 70 hours (2.9 days). In figure 7.6, the difference in erasure rate between daytime and nighttime can be seen clearly. This is most probably caused by the fact that skywave activity goes up during the night. This causes the interfering Cross-rate signals to be more powerful during the night than during the day, thereby distorting more desired pulses.

### 7.7 Soustons - 3-level coding

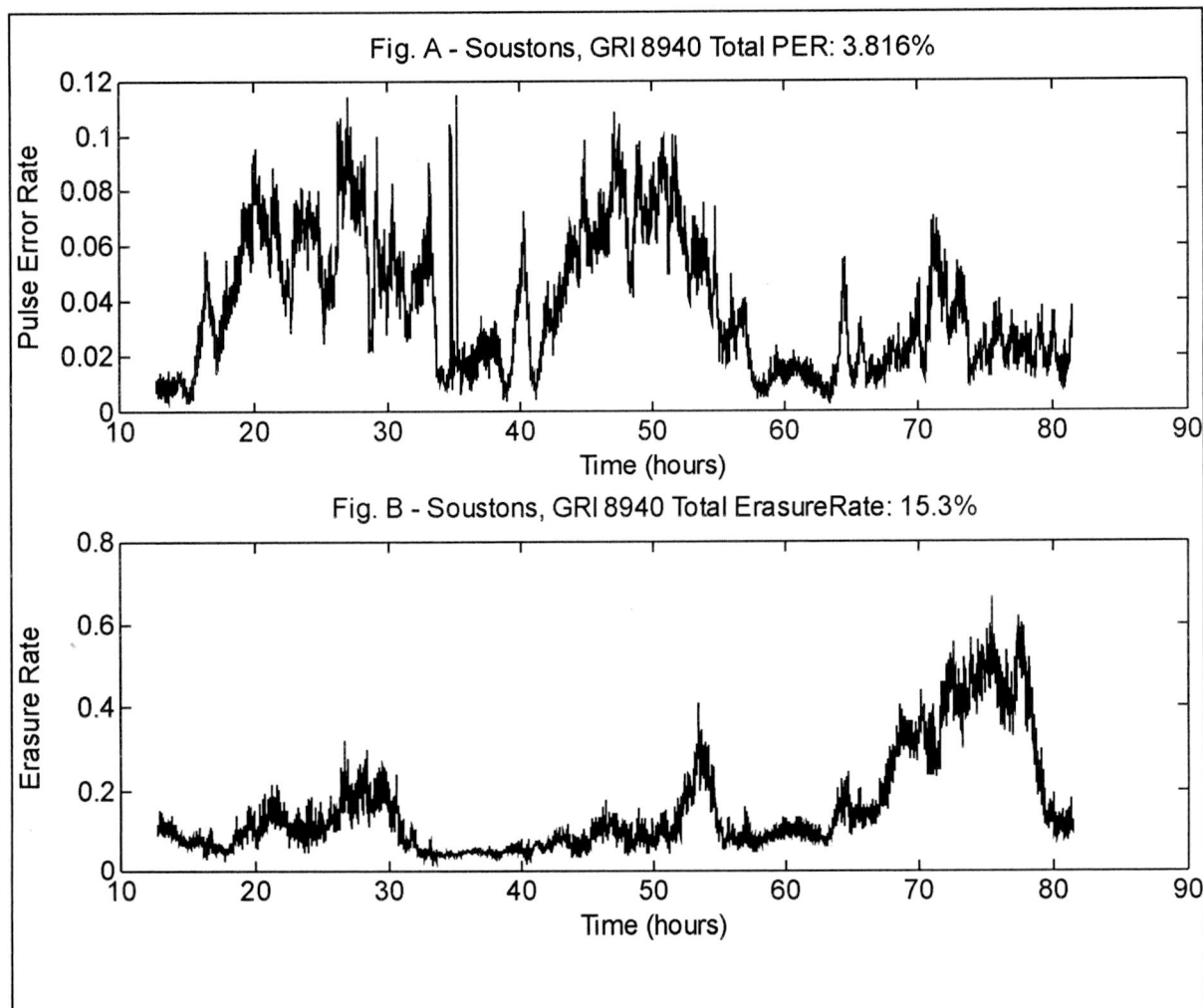


Figure 7.7: Pulse error rate (fig.A) and erasure rate (fig.B) of the Soustons-signal using 3-level modulation. The measurement was done on 26 October 1995.

In figure 7.7, the pulse error rate and erasure rate of the Soustons-signal using 3-level modulation are plotted.

As was expected, the PER for the 3-level modulation is higher than the PER for the 2-level modulation.

Again, the change in erasure rate between nighttime and daytime can be seen, although not as clearly as in figure 7.6. During the last night, however, it can be seen that the erasure rate goes up to 60%. It is doubtful that an error-correcting code can be developed that can still correct for 60% erasures.

## 7.8 Comparison between measurements and the theoretical analysis

When comparing the resulting pulse error rates from the measurements with the expected values of the PER as it is plotted in figure 5.5, the following conclusions can be drawn:

As was expected, the PER using 2-level modulation is lower than the PER using 3-level modulation. The measurements and the theoretical analysis agree on this.

The difference in error rate between the 2- and 3-level coding as has been measured, however, is less than was expected from figure 5.5. In the Lessay case, for example, the measured 2-level PER was 0.037%. From figure 5.5, the corresponding 3-level PER should be about 2%. The value from the measurement is 0.18%.

Apparently, most of the pulse errors are caused by effects other than Gaussian noise, like (weak) Cross-rate or atmospheric conditions.

It is also noted that the expected PER for the stronger transmitters (Sylt and Lessay) still is a fair bit higher than can be expected, given the PER of the weak Soustons transmitter.

No satisfying explanation for this effect can be given, other than the fact that the effects that have not been taken into account in the theoretical analysis, still have severe impact in the real-life situation.

Some effects that differ in the real-life situation from the theoretical analysis are:

- The atmospheric noise was supposed to be Gaussian, which in reality it is not.
- CW interference. No CWI-reducing methods have been used in the test-setup. In the theoretical analysis, CWI influence was not taken into account.
- A different filter was used in the test-setup than in the analysis.
- No pulse errors due to weak Cross-rate were considered in the analysis.

## 8. Conclusions and Recommendations

In this report, an effort was made to devise a Eurofix-demodulator capable of demodulating Eurofix-modulated Loran-C pulses. If the demodulator is unable to decode a Loran-C pulse correctly, it is better to recognize this fact than to make a wrong decision.

To develop such a demodulation scheme, and to test the resulting demodulator, several new techniques were introduced:

- 3-level coding
- Distortion detection
- A linear cross-correlating receiver with moving average reference figures
- A way of testing Eurofix demodulators without modification of normal Loran-C transmitters

### 8.1 Conclusions

With respect to 3-level coding:

Three-level coding has advantages over two-level coding:

- More data can be transmitted in the same time
- The coding scheme can be better balanced

The disadvantages of three-level vs. two-level coding are:

- The pulse-error rate will go up, resulting in more data errors.
- The demodulator becomes more complex

In the light of decreasing cost and increased performance of hardware, the last disadvantage is probably easy to overcome.

The assumption that the main reason for pulse errors would be Cross-rate interference seems to hold: the PER for 2-level coding is about 5 times lower than the PER for 3-level coding for both the Soustons and the Sylt signal ( $\text{SNR}_{\text{Sylt}} - \text{SNR}_{\text{Soustons}} \approx 15\text{dB}$ ). If the majority of errors were caused by thermal noise, this factor would be different for signals with different SNR's.

With respect to distortion detection:

Distortion detection is certainly beneficial for the Eurofix datalink: the total number of pulses that cannot be demodulated correctly remains roughly the same, but with distortion detection the majority of pulses that are demodulated incorrectly can be *identified* as such, whereas without distortion detection these pulses could not be distinguished from undistorted pulses.

With respect to the linear cross-correlation receiver with moving average reference figures:

Linear cross-correlation appears to be the receiver structure which has the best performance compared to other demodulator structures. The fact that the reference figures have to be continually updated does not seem to be a drawback on this technique. Linear cross-correlation utilizes the received signal to the maximum possible extent: all power in the received signal - even the power in skywaves that may be received along with the signal - is used.

With respect to the demodulator as it has been used to provide the test-results:

The general effects that were expected in the theoretical analysis have also been noticed in the test-results that were acquired using the demodulator. The absolute values of the PER, however, differ from the figures derived from the test-results. This is believed to be caused by factors that were not considered in the theoretical discussion (such as CWI), by the fact that some effects in real life differ from how they were used in the model (such as atmospheric noise and weak Cross-rate), and by the fact that the test-setup differed from the system assumed in the theoretical discussion.

With respect to the method of testing Eurofix-demodulators:

Time-shifting the clock-signal of the A/D converter seems to be a good way of acquiring time-shifted versions of a normal Loran-C pulse without having to modify a normal Loran-C transmitter to transmit time-shifted pulses. Various system parameters, such as the modulation index and the number of levels used, can easily be modified for test-purposes. Very little concessions to the real-life situation are made.

## 8.2 Recommendations

A lot of new system parameters were introduced, especially with the distortion-detecting filter. An optimum value will have to be found for all these parameters. To find the optimum values, it would be interesting to investigate a large number of cases where the distortion detecting filter starts adjusting



samples, or declares an erasure. By manually investigating the reason for the filter to do this, the filter parameters can probably be optimized to make the filter adjust only in cases where adjustment is needed. It is expected that the erasure threshold factor  $E_{\text{thresh}}$  should be adjusted depending on the SNR of the station that is being tracked. An algorithm will have to be developed to make this adjustment to be performed automatically.

Without any doubt, an error-correcting code will have to be used on the Eurofix datalink. Since erasures are very likely to occur in bursts, the error-correcting code should have strong burst-error-correcting capabilities. The performance of the error-correcting code, given the types of errors and erasures made by the demodulator, will have to be tested.

Tests of the proposed demodulator under moving (dynamic) conditions will also have to be done to investigate amplitude changes due to dynamic effects. Furthermore, in a real-life demodulator a tracking mechanism for the Loran-C signals will have to be used. The effect of tracking errors on the Eurofix demodulator should also be investigated. The performance of the tracking mechanism may be improved by so-called remodulation of the Eurofix-modulated Loran-C signals, which means that the tracking mechanism can compensate for the time-shifts introduced by the Eurofix modulation rather than just relying on a balanced modulation scheme.

Finally, the effect of Eurofix-modulation on conventional Loran-C navigation equipment should be investigated. The number of shifting levels used, and the shifting levels itself, need to be chosen such that this conventional Loran-C equipment can still use the system effectively.

## 9. References

1. D. van Willigen, Radio Plaatsbepaling, *Lecture notes*, Delft University of Technology.
2. R. Vroeijenstijn, *Eurofix and GNSS: The possibility of integrating Glonass into Eurofix*, Thesis report, Delft University of Technology, August 1995.
3. RTCM Special Committee No. 70, *Minimum Performance Standards for Marine Loran-C Receiving Equipment*, Washington DC, 1977
4. L.J. Beekhuis and D. van Willigen, *Eurofix*, Proceedings of the 6th International Technical Meeting of the Satellite Division of the Institute of Navigation, Salt Lake City, September 1993.
5. G.W.A. Offermans, *Modulation Schemes for the Eurofix Datalink*, Thesis report, Delft University of Technology, September 1994.
6. P. de Koning, *Ternary modulation and error control coding*, Thesis report, Delft University of Technology, December 1995
7. Loran-C User Handbook, Department of Transportation, United States Coast Guard, Washington DC, November 1992.
8. Robert Huysmans, *Asynchronous quadrature sampling of LORAN-C pulses*, Thesis report, Delft University of Technology, December 1995.
9. J. de Zwart, *Testing and Optimizing the Eurofix Datalink*, Thesis report, Delft University of Technology, July 1994.
10. T. Coenen, *private communications*, 1995.

## Appendix A - Overview of used software

A number of programs have been written to acquire the test-results as they have been described in this report. The following two programs are the most interesting to anyone who wants to be able to reproduce, or continue to work on, the test-setup:

First, there is the program that controls the Loran-C simulator. It can program the Loran-C simulator to operate on any GRI desired. Furthermore, it can make the Loran-C simulator produce Eurofix-modulated Loran-C pulses. It does this 'real time', meaning that it can control the Eurofix-modulation of every Loran-C pulse individually. The Eurofix-modulation that is imposed on the Loran-C pulses can be either 2- or 3-level, with a configurable modulation index. The program is configurable via a datafile. If the pulse-trigger output of the Loran-simulator is used for the shifting-clock circuit, this program can be used to provide a time-shifting clock as described in Chapter 6.

The latest version of this program is called SIMUL2.EXE. It is available, including its sources, through the SourceSafe source-distribution system.

The second program is the implemented version of the proposed demodulator. It programs the A/D card to use external clock and triggering signals, and does all the signal processing, including the distortion detecting filter. It is also informed of the data patterns that are being transmitted by the Loran-C transmitter, to be able to compute pulse error rates.

In the source, all A/D card routines have been gathered in a separate module, providing an easy-to-use interface to the programmer. All band-filtering routines are also put in a separate module.

The latest version of this program is called LOGSKY.EXE. Like the previous program, it is also available, including its sources, through the SourceSafe source-distribution system.

## Appendix B - Location, power and distances of Loran-C transmitters to the Delft University of Technology

The Loran-C antenna at the Delft University of Technology is located at:

51°59'56.696" N (51.9990821° N)

4°22'24.140" E (4.3733721° E)

<b>Station:</b>	<b>Latitude:</b>	<b>Longitude:</b>	<b>Power (kW):</b>	<b>Distance (km):</b>	<b>Propagation time to Delft (μs)</b>
Sylt	54°48'29.975" N	08°17'36.856" E	250	407.68	1360.95
Lessay	49°08'55.224" N	01°30'17.029" W	250	523.11	1743.14
Soustons	43°44'23.099" N	01°22'49.584" W	250	1013.43	3381.62
Bø	68°38'06.216" N	14°27'47.350" E	400	1929.56	6443.08
Jan Mayen	70°54'51.478" N	08°43'56.525" W	250	2208.99	7374.53
Vaerlandet	61°17'49.435" N	04°41'46.618" E	250	1035.54	3457.22
Ejde	62 17'59.837" N	07°04'26.079" W	400	1335.75	4457.91

# Design and Testing of an Advanced Eurofix Demodulator

Arthur  
Helwig

Delft University of Technology

Department of Electrical Engineering

Telecommunications and

Traffic Control Systems Group

## **Design and Testing of an Advanced Eurofix Demodulator**

Author: Arthur W.S. Helwig

Thesis Report

64 pages

November 1995

Professor: D. van Willigen  
Mentor: G.W.A. Offermans  
Code: A - 687  
Period: April - November 1995

Keywords: Eurofix  
Loran-C  
Linear cross-correlation demodulation  
Distortion detection

## Preface

This report concludes the research that I did on the development of a demodulation scheme for a Eurofix datalink receiver. The Eurofix project is part of the Beek program 'Integrated Navigation for Traffic and Transportation'. A lot of work still needs to be done before Eurofix will be up and running, but I hope that my research has helped in the process.

I would like to express my gratitude to professor van Willigen for the way he motivates people in his group, including me. I would also like to thank all the students of the P&N-group for always creating a pleasant atmosphere in the lab.

A special word of thanks goes out to Cor van der Knaap, for helping me out whenever the hardware needed adjustment. Finally, I would like to express my sincere gratitude to Gerard Offermans, for the way he assisted me along the way.

Arthur Helwig

November 1995

## Summary

In the Eurofix system, DGPS corrections are transmitted using an already existing infrastructure: the Loran-C system. Primarily, this provides a cost-effective way to supply coverage for DGPS-corrections over a large area. Secondly, the use of the Loran-C navigation system in combination with normal GPS will yield a combined system with improved integrity and availability.

In this report, the capabilities of the Eurofix datalink are investigated. The goal is to optimize the datalink for speed and error-rate. Both 2-level and 3-level Eurofix coding are investigated.

The Eurofix datalink is a difficult one: there is a number of factors limiting the performance. The largest reduction in performance is caused by a phenomenon that is inherent to the way that Loran-C operates: Cross-rate. Secondly, atmospheric effects can overpower the normal Loran-C signal.

A method is devised to detect whether individual Loran-C pulses are distorted by Cross-rate or severe atmospheric conditions. Then, a demodulation scheme is presented that is capable of demodulating both 2- and 3-level Eurofix modulation.

A new method of testing is developed that allows normal (unmodulated) Loran-C signals to appear to the demodulator under test as if they were modulated. This method is very realistic.

The 2-level coding scheme gives a lower pulse error rate than the 3-level coding scheme. On the other hand, the transmitted Loran-C signals can be more balanced with 3-level than with 2-level modulation.

Distortion detecting certainly prevents the demodulator from making incorrect decisions. Since it is easier for an error-correcting code to deal with erasures than with errors, distortion detection will improve the performance of the Eurofix datalink.

The proposed demodulator works as expected. It is difficult, however, to develop a theoretical model that accounts for all effects to which the Eurofix datalink is subjected.

## Abbreviations

CRI	Cross-Rate Interference
CW	Continuous Wave
CWI	Continuous Wave Interference
DGPS	Differential GPS
I-Q	In phase and Quadrature
Loran	Long Range Navigation
LF	Low Frequency
GPS	Global Positioning System
PER	Pulse Error Rate
PDF	Probability Density Function
RTCM	Radio Technical Commission for Maritime Services
RTCM-SC	RTCM Special Committee
SNR	Signal-to-Noise Ratio

# Table of Contents

Preface .....	iii
Summary .....	iv
Abbreviations .....	v
1. Introduction .....	1
2. The Eurofix datalink .....	3
2.1 Loran-C .....	3
2.2 GPS .....	3
2.3 Using the Loran-C system for data transmission.....	4
2.3.1 Modulation of the Loran-C system .....	4
2.3.2 Pulse-position modulation - 2-level .....	4
2.3.3 Pulse-position modulation - 3-level .....	5
3. Performance of the Eurofix datalink .....	6
3.1 Signal-to-Noise ratio of the Loran-C pulse.....	6
3.2 Thermal noise.....	7
3.3 Atmospheric noise.....	7
3.4 Cross-rate interference.....	8
3.5 Continuous Wave Interference.....	9
4. Pulse distortion detection and reduction .....	10
4.1 Noise sources .....	10
4.1.1 Gaussian noise .....	10
4.1.2 Cross-rate & Lightning .....	10
4.2 Counteracting Cross-rate and Lightning - pulse distortion detection.....	11
4.2.1 Using the envelope of the received signal as a means to detect distortion.....	11

4.3 Changes in the envelope not caused by distortion.....	13
4.3.1 Differences between received and expected envelope caused by Eurofix modulation ...	14
4.3.2 Envelope detection of the signal - Quadrature sampling.....	15
4.3.3 Skywaves.....	16
4.3.4 Dynamics.....	18
4.3.5 Thermal noise and Gaussian atmospheric noise.....	19
4.3.6 Consequences for the distortion detection.....	19
4.4 The Reference Figure .....	20
4.5 Extending the distortion detection to erasure detection .....	21
4.6 Parameters of the pulse distortion-detecting and reducing algorithm .....	23
<b>5. The Demodulator.....</b>	<b>25</b>
5.1 Demodulator structures .....	25
5.1.1 Hard-limited single point demodulators.....	25
5.1.2 Linear single point demodulator.....	26
5.1.3 Hard-limited cross-correlation demodulator .....	26
5.1.4 Linear cross-correlation demodulator.....	27
5.2 Demodulation of Eurofix-modulated pulses using linear cross-correlation.....	27
5.3 A Linear cross-correlation demodulator.....	29
5.3.1 The Pulse Shifter .....	30
5.3.2 The reference figures.....	32
5.4 Thermal noise influence on the linear cross-correlation method.....	32
<b>6. Testing of the proposed demodulator .....</b>	<b>36</b>
6.1 The Transmission medium .....	36
6.2 Acquiring Time-shifted Loran-pulses .....	36
6.3 The Demodulator .....	39
6.4 The Test-setup .....	40
<b>7. Results.....</b>	<b>42</b>
7.1 The effect of the distortion detecting filter .....	44

7.2 Sylt - 2-level coding.....	46
7.3 Sylt - 3-level coding.....	47
7.4 Lessay - 2-level coding.....	48
7.5 Lessay - 3-level coding.....	49
7.6 Soustons - 2-level coding.....	50
7.7 Soustons - 3-level coding.....	51
7.8 Comparison between measurements and the theoretical analysis.....	52
<b>8. Conclusions and Recommendations .....</b>	<b>53</b>
8.1 Conclusions.....	53
8.2 Recommendations .....	54
<b>9. References.....</b>	<b>56</b>
<b>Appendix A - Overview of used software .....</b>	<b>57</b>
<b>Appendix B - Location, power and distances of Loran-C transmitters to the Delft University of Technology .....</b>	<b>58</b>

## 1. Introduction

At the time of this writing, GPS is dominating the world as the leading navigation system. Apparently, the accuracy of the system and the global coverage it provides, combined with easy-to-use, cheap receivers is appealing to a lot of people and organizations. The GPS certainly has raised the people's interest in the world of radionavigation.

The accuracy of GPS by itself, though, is not terribly high: its  $2\sigma$ -accuracy is limited to about 100 m. For example, this is not accurate enough for ships that want to do harbour-approaches. Furthermore, at the moment many questions are being raised about the integrity of the GPS system.

Eurofix can be used to overcome both problems: the normal Loran-C system can be used as a backup to the GPS system, thereby improving the integrity of the combined system. In addition to this, by modulating the Loran-C signal, DGPS data and integrity information can be transmitted.

This thesis concentrates on how to design different modules of a Eurofix demodulator such that, given the limitations, the maximum performance is achieved. The following effects are dealt with:

- The Eurofix datalink is mostly disturbed by atmospheric noise and Cross-rate interference. To counteract these effects, special algorithms are designed to deal with just these sources of interference.
- The shape of the Loran-C signals can change substantially - especially during the night - by skywave influences. Although this effect is generally regarded as undesirable, a demodulator is developed that uses the received signal - including possible skywaves - to the maximum extent.

After a brief introduction to the Eurofix system and its components in Chapter 2, the sources of interference for the Eurofix datalink are discussed in Chapter 3.

In Chapter 4, a method is introduced that is able to detect which part of the received signal is distorted by Cross-rate or lightning.

Chapter 5 describes a demodulator capable of demodulating multi-level Eurofix modulation.

In Chapter 6, a method is described for real-time testing of the Eurofix datalink. The results of these tests are presented in Chapter 7.

Finally, in Chapter 8 conclusions are drawn from the tests regarding the performance of the newly introduced concepts.



## 2. The Eurofix datalink

This chapter will give a short introduction to the Eurofix datalink.

The reader is assumed to have knowledge of radionavigation principles, and of existing radionavigation systems. This chapter only describes the basic properties of the Eurofix datalink - more detailed information on Eurofix and its components can be obtained from the references.

### 2.1 Loran-C

The Loran-C system is a two-dimensional terrestrial radio navigation system, meaning that the transmitters are located on the surface of the earth, and that the user does not get height information. Loran-C operates at a low frequency, i.e. 100 kHz. These low-frequency signals can be received at distances up to 1500 km from the transmitter.

Loran-C transmitters transmit pulses with a carrier frequency of 100 kHz. Each Loran-C transmitter transmits 8 consecutive pulses, all separated 1 ms. Such a group of 8 Loran-C pulses is called a *Loran-burst*. The Loran-C transmitter repeats this burst with a certain repetition time, called the Group Repetition Interval (GRI). The GRI is used as one of the means by which the receiver can identify the origin of the pulses it is receiving. GRI's range from 40.00 ms to 100.00 ms. By requirement, a GRI is always a multiple of 10  $\mu$ s.

The coverage of Loran-C includes the entire United States, Japan, Saudi-Arabia, Northern Europe and, although not yet fully operational, Western Europe.

The 2d-rms accuracy of Loran is 450 m at the border of the coverage area of Loran-C. In general, though, its accuracy is much better.

More information about Loran-C can be found in [1].

### 2.2 GPS

The Global Positioning System (GPS) is fully operational since July 1995. It makes use of 24 satellites orbiting the globe.

The horizontal  $2\sigma$  (95%) accuracy of normal GPS is specified to be 100 m.

The accuracy of GPS can greatly be improved by providing the user with correction information for each satellite, the so-called Differential GPS (DGPS) data. A more in-depth discussion about contents of this DGPS data can be found in [2].

### 2.3 Using the Loran-C system for data transmission

By modulating the pulses broadcast by a Loran-C transmitter, the Loran-C system can be used to transmit data. Modulating the Loran-C pulses, however, will inevitably lead to a decreased signal-to-noise ratio (SNR) for the existing Loran-C receivers. The modulation needs to be chosen such that this loss of performance does not cause the existing receivers to fail the requirements on Loran-C navigation specified by the RTCM SC-70 [3].

#### 2.3.1 Modulation of the Loran-C system

One of the possible types of modulation of the Loran-C pulses is pulse-position modulation. By applying a little variation to the time of transmission of normal Loran-pulses, data can be broadcast. The first 2 pulses of each burst, however, can not be modulated, as they are used to indicate malfunction of the Loran-C system (blinking). Therefore, only 6 out of 8 pulses can be modulated.

#### 2.3.2 Pulse-position modulation - 2-level

The Eurofix datalink as described in [4] proposes 2-level pulse-position modulation for the Loran-C pulses. The modulation index  $\mu$  is proposed to be  $1 \mu\text{s}$  (10% of the cycle time of the 100 kHz signal). This means that the time of transmission of each Loran-C pulse is either advanced by  $1 \mu\text{s}$  (an *early* pulse) or delayed by  $1 \mu\text{s}$  (a *late* pulse). To ensure proper functioning of existing Loran-C receivers, however, the number of advanced pulses must equal the number of late pulses on average - the transmitted pattern must be *balanced*. This puts restrictions on the number of possible early/late combinations that can be used to encode the data with. Balanced and nearly-balanced coding schemes are investigated in [5].

The value of  $1 \mu\text{s}$  for the modulation index is subject to further investigation. It is a compromise between the degradation of the normal Loran-C system and the admissible Pulse Error Rate of the Eurofix datalink.

### 2.3.3 Pulse-position modulation - 3-level

Rather than transmitting only early and late pulses, it is also possible to increase the number of levels of the time-shift for each Loran-C pulse. With a 3-level modulation scheme, for instance, each Loran-C pulse can either be transmitted  $1 \mu\text{s}$  early (an early pulse),  $1 \mu\text{s}$  late (a late pulse), or on time (a prompt pulse).

Using the same number of Loran-pulses, more data can be sent with 3-level coding than with 2-level coding. Furthermore, there are more balanced early/prompt/late patterns than balanced early/late patterns, making it feasible to develop a coding scheme that is balanced for each burst. With 3-level coding and 6 pulses to be modulated, there are  $3^6=729$  (9.5 bit) possible combinations, 141 (7.1 bit) of which are balanced. With 2-level coding, there are  $2^6=64$  (6 bit) combinations, of which only 20 (4.3 bit) are balanced. So, if an integer number of bits per pattern is assumed, upgrading from 2-level to 3-level coding yields a  $9/6$  (50%) increase in transmission speed. If balanced codes are considered, the increase of the transmission speed is  $7/4$  (75%). More information about 2- and 3-level coding schemes can be found in [6].

Increasing the number of levels of the time-shift, however, will inevitably lead to an increased probability of demodulating a pulse incorrectly, and hence an increased Pulse Error Rate (PER). It is anticipated, however, that the majority of pulses that are incorrectly demodulated will be distorted in such a way that the pulse can not correctly be demodulated at all - no matter how small the number of possible levels.

In this report, 3-level coding as well as 2-level coding is investigated. The time-shifts that are used for the 2-level coding are  $-1 \mu\text{s}$  (early) and  $+1 \mu\text{s}$  (late). For the 3-level coding, time-shifts of  $-1 \mu\text{s}$  (early),  $0 \mu\text{s}$  (prompt) and  $+1 \mu\text{s}$  (late) are used.

### 3. Performance of the Eurofix datalink

In this chapter, the possible sources of interference on the Loran-C signal are investigated. First, the meaning of the term Signal-to-Noise ratio for the Loran-C pulse will be discussed.

#### 3.1 Signal-to-Noise ratio of the Loran-C pulse

Since the Loran-C pulse is not a continuous wave (CW) signal, standard formulas for calculating its received signal power do not apply.

The RTCM SC-70 [3] defines the signal-to-noise ratio of the Loran-C pulse as the signal-to-noise ratio of a single CW carrier having the same amplitude as the Loran-pulse at the so-called 'standard sample-point' (25  $\mu\text{s}$ ).

This is illustrated in the following figure:

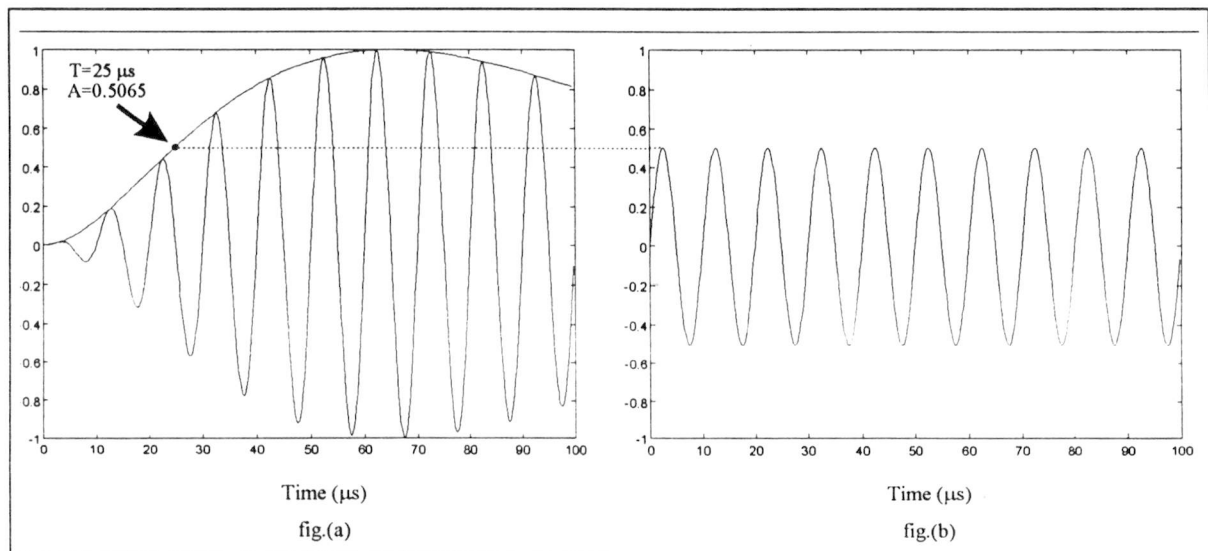


Figure 3.1: (a) Amplitude of the Loran-C pulse at  $T=25 \mu\text{s}$ , and (b) sinusoidal wave with the same amplitude

If the maximum envelope of the Loran-C pulse is normalized to 1, the envelope at  $T=25 \mu\text{s}$  is 0.5065. Furthermore, the averaged normalized power contained in a general sinusoidal waveform  $A \cdot \sin(\omega \cdot t)$  is equal to  $\frac{1}{2}A^2$ .

This yields the following formula for the power of a Loran-C pulse:

$$P_{Signal} = \frac{(0.5065 \cdot A_{max})^2}{2} \approx 0.1283 \cdot A_{max}^2 \quad \text{Formula 3.1}$$

where  $A_{max}$  is the maximum value of the envelope of the Loran-C pulse.

The power contained in bandpass-filtered Gaussian noise is:

$$P_{noise} = N_0 B = \sigma^2 \quad \text{Formula 3.2}$$

with  $N_0$  the normalized spectral density,  $B$  the bandwidth and  $\sigma^2$  the variance of the noise.

### 3.2 Thermal noise

As is the case with any real-life radio-signal, thermal noise will be present on the Loran-C signal. This thermal noise is assumed to be Gaussian, with variance  $\sigma^2$ . In the coverage area of a Loran-C transmitter the SNR of the received signal is at least -10 dB [7]. Normal Loran-C receivers can integrate the received signal for a certain period of time to get a better SNR. With the Eurofix datalink, however, this is not possible since each received pulse carries data which must be demodulated. The minimum SNR that yields an acceptable Pulse Error Rate (PER) for the Eurofix datalink is subject to further investigation.

### 3.3 Atmospheric noise

Atmospheric noise is caused by electrostatic discharges in the atmosphere. These discharges can have tremendous power compared with the received Loran-C signals. Lightning is a form of atmospheric noise.

If the power of the electrostatic discharge is weak, it can be treated as weak Cross-rate. If it is weaker, it can probably be treated as thermal noise. If the power is large, however, it will be impossible to demodulate the Loran-C pulse without a high error-probability.

The effect of thermal noise is negligible compared to atmospheric noise - very weak electrostatic discharges will still easily overpower the thermal noise. Unfortunately, though, the effect of the electrostatic discharges is hard to model. Therefore, in the remainder of this report, weak atmospheric noise will be considered to be Gaussian.

### 3.4 Cross-rate interference

Probably the most important source of interference will be Cross-rate interference: due to the fact that all Loran-C stations share the same frequency, some of the pulses from a Loran-C station transmitting at one GRI will be received at the same time as pulses from another Loran-C station transmitting at another GRI. Since the receiver can not distinguish between the 2 pulses, the probability of incorrect demodulation of the received signal will be high.

The effect of Cross-rate is illustrated in figure 3.2.

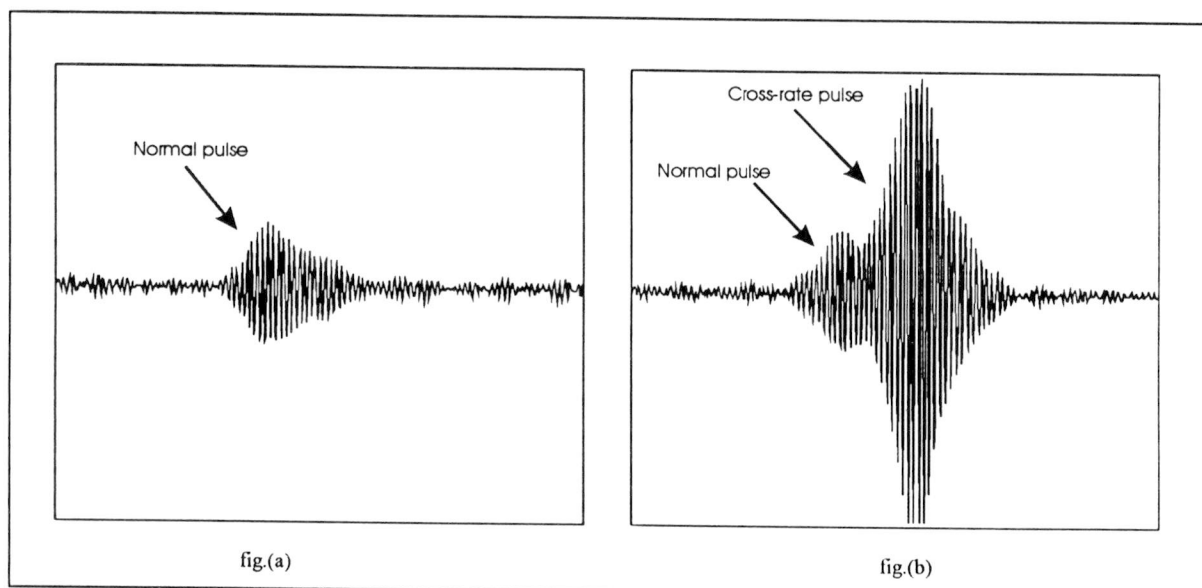


Figure 3.2: Example of the effect of Cross-rate.

Figure (a) is the undistorted signal received from the Soustons transmitter.

In (b), the last part of the pulse is clearly hit by Cross-rate from another (stronger) transmitter.

If the power of the interfering signal is relatively small, its effect will be negligible. If it is relatively large, the probability of correctly demodulating the signal will be low, but the fact that the received pulse is hit by another signal is easy to acknowledge.

Cross-rate has its worst influence if the power of the interfering signal is comparable to the power of the desired signal; that is, when the power is too large to have a negligible influence, and too small to be recognized as an interfering signal.



### **3.5 Continuous Wave Interference**

Interference caused by radio transmitters operating at frequencies close to the Loran-C band (90-110 kHz) is called continuous wave interference (CWI). However, as described in [5], CWI can successfully be suppressed by notch-filters in addition to the standard Loran-C bandfilter. In the remainder of this report, the effects of CWI are assumed to be sufficiently suppressed by such filters to be negligible.

## 4. Pulse distortion detection and reduction

In this chapter, a method is proposed to detect whether (and if so, which part of) a particular Loran-C pulse is distorted by Cross-rate or lightning. Then, this method is extended to reducing the effect of the distortion on the received Loran-C pulse.

### 4.1 Noise sources

As discussed in the previous Chapter, the received signal from a particular Loran-C transmitter can be distorted by the following sources:

- Gaussian noise (thermal noise and weak atmospheric noise)
- Cross-rate
- Strong atmospheric noise (Lightning)
- Continuous Wave Interference

In this report, only Gaussian noise, Cross-rate and lightning will be discussed further.

#### 4.1.1 Gaussian noise

Thermal noise and weak atmospheric noise are assumed to be Gaussian, which means that the probability density function (PDF) of the noise has a normal distribution, a mean value of 0 and a standard deviation of  $\sigma$ , where  $\sigma^2$  equals the power of the noise signal. One of the means to reduce the effects of Gaussian noise is to average the desired signal over a certain period of time. Because the desired signal is averaged coherently, and the noise signal is averaged incoherently, this effectively leads to an increase of the signal-to-noise ratio (SNR).

#### 4.1.2 Cross-rate & Lightning

Both Cross-rate and lightning differ significantly from Gaussian noise, in the respect that Gaussian noise is always present. Cross-rate and lightning, however, tend to distort only individual pulses. This means that one can expect at least a reasonable number of pulses that is not affected in any way by Cross-rate or lightning. This type of interference is quite rare in normal communication channels. Counteracting it, therefore, requires a special approach.

## 4.2 Counteracting Cross-rate and Lightning - pulse distortion detection

Even *if* a pulse has been hit by Cross-rate, it is usually hit only partially: in general, the interfering signal will not be lengthy enough to distort the entire desired pulse. (In some cases, Cross-rate *will* hit the entire pulse. This can happen if the start of the interfering pulse arrives at the receiver at the exact moment the desired pulse arrives, or, more likely, when the interfering pulse is longer than the desired pulse due to skywaves). The performance of a demodulator may be increased by being able to identify which part of the pulse is still undistorted. The part of the pulse that is apparently hit by some sort of interference can then be processed keeping in mind that that part of the received signal possibly differs significantly from how it was transmitted by the Loran-transmitter.

If a Loran-pulse is hit by another Loran-pulse (as is the case when Cross-rate occurs), or when a Loran-pulse is distorted by an electromagnetic pulse caused by lightning, the interfering signal is generally received with an amplitude that differs from the pulses originating from the transmitter that is being tracked (i.e., the desired signal). When this amplitude is much lower than the amplitude of the desired pulse, its disturbing effect will be negligible. We will therefore focus on the case where the interfering signal has a larger amplitude than the desired pulse.

### 4.2.1 Using the envelope of the received signal as a means to detect distortion

If, at any particular point in time, the amplitude of the received signal differs significantly from the amplitude that can be expected given the shape of the pulses as they were received ‘in the past’, that part of the pulse must have been hit either by Cross-rate or by lightning.

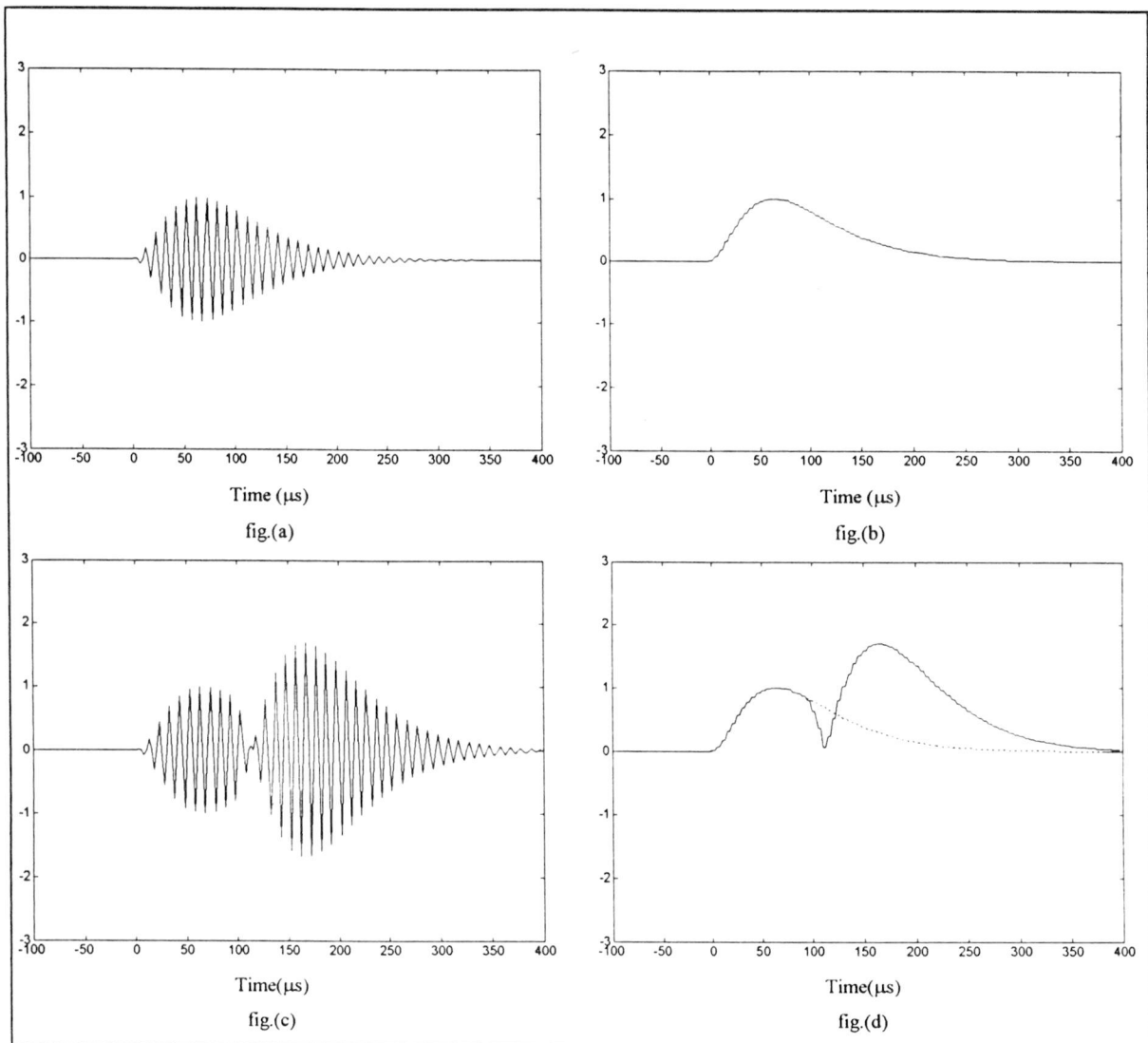


Figure 4.1:

(a) A 'normal' Loran-pulse.

(b) Envelope of the 'normal' Loran-pulse.

(c) A Loran-pulse hit by Cross-rate. The Cross-rate signal is +6dB, and interferes from  $t=95 \mu\text{s}$ .

(d) Envelope of the Loran-pulse hit by Cross-rate, compared with figure (b) (dashed).

Figure 4.1 illustrates this by merging a 'normal' pulse with Cross-rate signal which is 6 dB stronger and interferes from  $t=95 \mu\text{s}$ . In 4.1(d), the difference between the envelopes of the desired pulse and the distorted pulse can clearly be seen.

By comparing the envelope of the expected pulse with the envelope of the received signal, the part of the signal which is distorted can be identified. To avoid that part of the signal having influence on the demodulator, the signal is suppressed (i.e., all samples are made 0) when the envelope differs 'significantly' from the expected envelope.

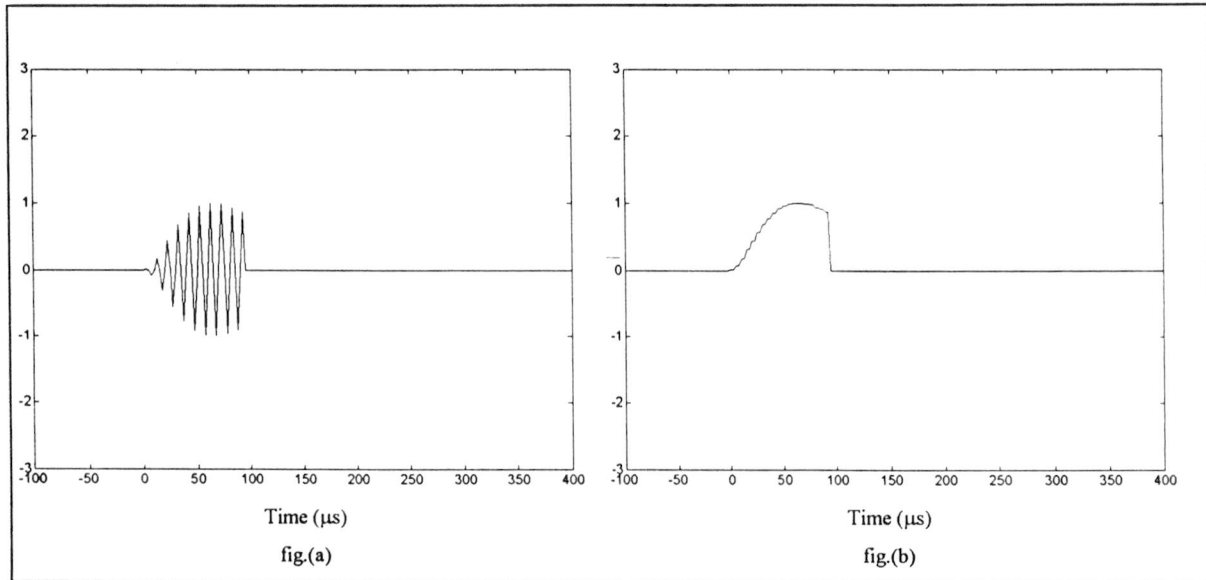


Figure 4.2: The modified pulse after distortion detection (a), with the resulting envelope (b).

By ‘nulling’ the signal at those points where distortion is suspected, the remaining pulse shape has a high probability of being undistorted. This proves to give a large reduction of errors in the demodulator, because the demodulator can now use only the samples at those points where the signal is (supposed to be) undistorted.

### 4.3 Changes in the envelope not caused by distortion

It was stated in the previous section that the sample values of the received signal were nulled when the envelope differed ‘significantly’ from the expected envelope. This term will now be defined more strictly.

There are certain predictable effects that cause a change in the envelope of the signal. The effects causing the changes investigated in this report are:

- Changes in the expected envelope caused by Eurofix modulation
- Accuracy of the envelope-detecting algorithm
- Changes in envelope caused by skywaves
- Changes in envelope caused by the dynamics of the receiver.

Of course, changes in envelope caused by these effects should not result in any modifications by the distortion-detecting algorithm.

After investigating each of these sources, the term 'significantly' can be given a numerical value.

#### 4.3.1 Differences between received and expected envelope caused by Eurofix modulation

If the received Loran-pulse is Eurofix-modulated, its envelope will have a certain time-shift compared to the non-modulated pulse. When the envelopes are compared without taking this time-shift into account, the envelopes appear to differ:

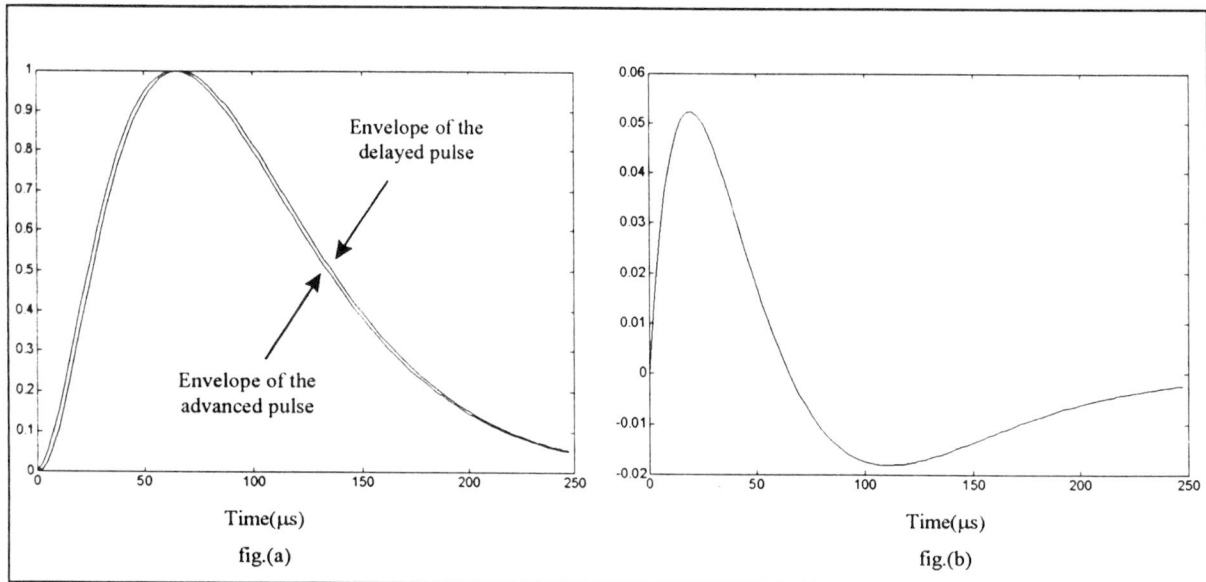


Figure 4.3: (a) Envelopes of an 'early' pulse and of a 'late' pulse, and (b) the difference between the two envelopes.

From figure 4.3 it can be seen that the maximum difference between the two envelopes caused by Eurofix modulation is 0.052 (or 5.2%), at  $t=20 \mu\text{s}$ .

A difference of 5.2% between the received envelope and the expected envelope can thus be caused by Eurofix modulation.

### 4.3.2 Envelope detection of the signal - Quadrature sampling

When the received signal is sampled taking both an in-phase and a quadrature sample at a rate higher than the Nyquist-frequency (so called Quadrature sampling), the envelope of the signal can be acquired by using the formula:

$$E_k = \sqrt{i_k^2 + q_k^2} \quad \text{Formula 4.1}$$

where

$E_k$  = the envelope at the  $k$ 'th samplepoint

$i_k$  = the  $k$ 'th in-phase sample

$q_k$  = the  $k$ 'th quadrature sample

Note that although  $i_k$  and  $q_k$  ideally should be taken at the same moment in time, this is generally not feasible. In most practical applications when A/D converters are used, only one sample can be taken at any moment in time (since taking more samples at the same moment in time requires multiple A/D converters, and hence increased cost). This is circumvented by rather than taking 2 samples at the same moment in time at the Nyquist rate, 1 sample is taken at twice the Nyquist rate. So, in reality:

$$i_k = s_{2k}$$

$$q_k = s_{2k+1}$$

$s$  = a vector of samples taken at 2 times the Nyquist-frequency.

If (as is the case with Loran-pulses) the envelope of the signal is not constant, the envelope of the signal is changed between the moment  $i_k$  was taken and the moment  $q_k$  was taken. This introduces an error on this method of envelope detection.

The carrier frequency of the Loran-pulse is 100 kHz. The Nyquist rate is therefore 200 kHz, and the single A/D converter has to have a sample frequency of 400 kHz. This means that a sample has to be taken every 2.5  $\mu$ s.

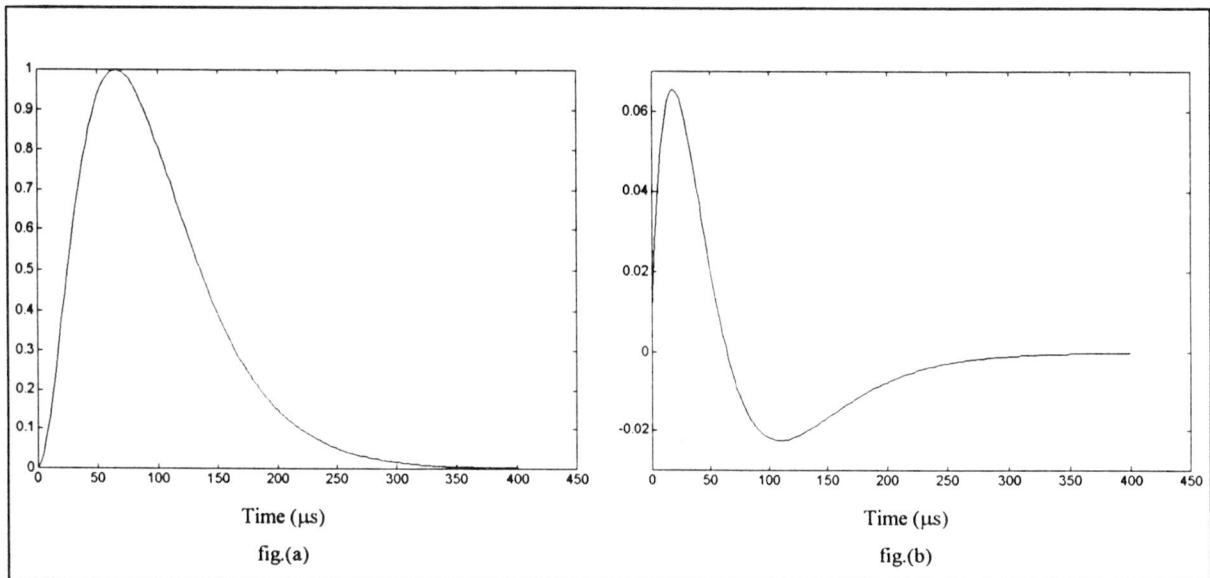


Figure 4.4: (a) Envelope of the Loran-C pulse (sampled at 400 kHz), (b) its derivative

From figure 4.4(b), it can be seen that the maximum difference in amplitude between 2 consecutive samples is 0.065 (or 6.5%), and that this occurs at  $t=17.5 \mu\text{s}$ .

This means that in the worst case the envelope detected by this method can be off 6.5%. The method is, however, accurate within 0.5% for 90% of the duration of the Loran-pulse.

The error could be suppressed by time-shifting both the in-phase and the quadrature set of samples by using an interpolating filter. More information on Quadrature sampling can be found in [8].

A difference of 6.5% between the received envelope and the expected envelope can thus be caused by the method by which the envelope of the received signal is determined.

### 4.3.3 Skywaves

Another reason for changes of the envelope of the received pulse are changes in the ionosphere. These changes cause the skywaves that are always received in combination with the groundwave-signal of the Loran-pulse to change. Since the received pulse consists of the addition of both the groundwave and skywaves, the envelope of the received pulse also changes.

Unfortunately, little is known about the way in which the ionosphere changes. The ionosphere is affected by sunlight and other atmospheric conditions - all of which are hard to model. Furthermore, the resulting effect of a changing atmosphere on skywave propagation is equally hard to model.

To get some idea of changes in the received pulse shape over time due to changing skywaves, data of ‘live’ Loran-C signals was collected, and the pulse shape was monitored from GRI to GRI over a long period of time. It was noted that during daytime, the received pulse shape remained fairly constant - even for signals originating from distant transmitters at about 1,000 km (and therefore are influenced quite severely by skywaves).

During the night, however, the received pulse shape can change relatively fast. It was noted that, in the worst cases, in a few minutes the pulse shape could change completely. This is especially true for those cases where the received signal consisted mainly of skywaves (i.e., when the transmitter was far away). In these cases where the groundwave signal could easily be recognized in the received signal, it was noted that that portion of the signal hardly changed.

The effect of skywaves can be seen from the following figure:

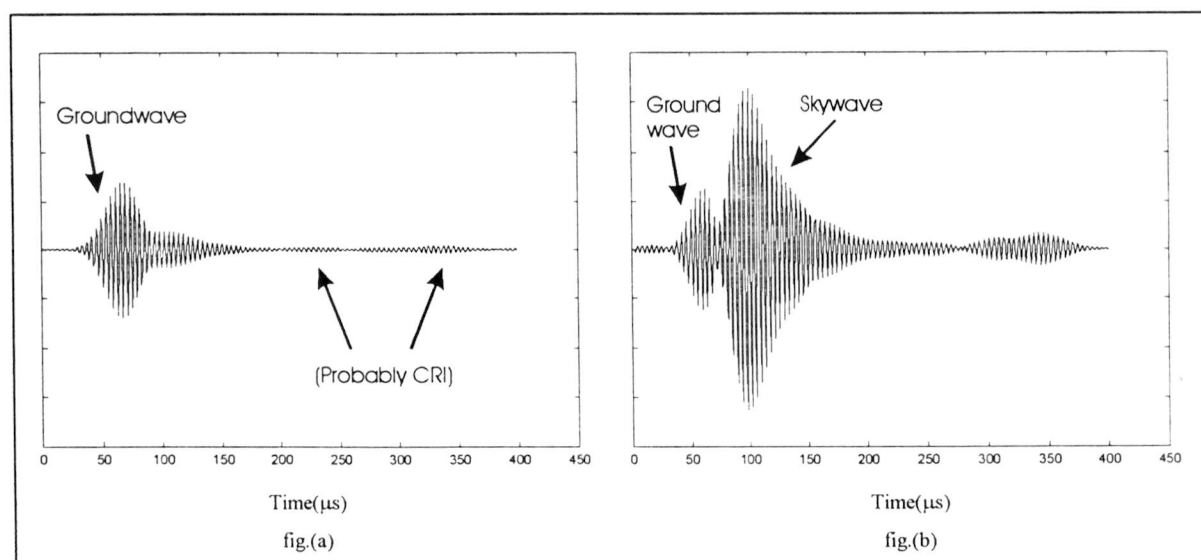


Figure 4.5: Effect of skywaves.

Fig. (a) represents the signal as it is received from Soustons at 12.00 pm (noon).

Fig. (b) is the signal from the same transmitter received at 1.00 am. The effect of the skywave can clearly be seen.

For calculation of the percentual change in the envelope between GRI's, it is assumed (based on the measurements mentioned above) that in the worst case, in 3 minutes less than 10% of the original envelope remains. If the time between two GRI's is assumed to be 100 ms, then the percentual change in envelope between two GRI's is:

$$1 - \frac{180s}{100ms} \sqrt[3]{0.1} \approx 1 - 0.9987 \approx 0.13\%$$

This is negligible compared to changes in the envelope between GRI's caused by other factors.

#### 4.3.4 Dynamics

When the receiver moves geographically, the received signal strength (and thus the received envelope) will vary. However, these changes are quite small over time, compared to changes in the envelope due to other reasons, as the following example will illustrate:

Suppose that the receiver is moving at about 100 km/h (or 27 m/s). Suppose further that the distance from the receiver to the transmitter is 1 km (1000 m). If the receiver moves another 1000 m away from the transmitter, the received power will be one quarter of what it was before, since the received power decreases quadratically with distance. The envelope will then be 0.5 times the original envelope. It will take the receiver  $1000/27 \approx 37$  seconds to cover this distance.

The speed of 100 km/h and the distance of 1000 m can safely be used as limits as to the maximum speed of the receiver and the minimum distance between the receiver and the transmitter. A more typical distance between receiver and transmitter would be 100 km.

The time between 2 Loran-bursts is typically in the order of 100 ms. This time is very short compared with the time of 37 seconds calculated above. The percentual change in envelope between 2 bursts is:

$$1 - \frac{37s}{100ms} \sqrt[3]{0.5} \approx 1 - 0.9981 \approx 0.19\%$$

This is negligible compared to changes in the envelope between GRI's caused by other factors.

Other dynamic effects (for example, when driving in a city) can probably also cause large changes in the amplitude of the received signal. These effects remain to be investigated - if the changes in envelope

caused by dynamics become unacceptably large (i.e., larger than the changes caused by skywaves), then the received pulse probably needs to be scaled to achieve a maximum fit with the reference envelope.

#### 4.3.5 Thermal noise and Gaussian atmospheric noise

The received pulse will also contain a certain amount of random noise. This will also cause a change in the envelope. Contrary to the previous causes, however, the amount of random noise that is received does not change with the received Loran-C signal strength or the momentary envelope of the Loran-pulse. Its influence is therefore measured as a fixed value; rather than a percentage of the expected envelope.

#### 4.3.6 Consequences for the distortion detection

From the previous paragraphs it can be concluded that the largest changes in envelope that are not caused by distortion, are caused by:

- the error in the method of envelope-detection (6.5%), and
- the change in the expected envelope caused by the Eurofix-modulation (5.2%)

These two errors are independent from each other - the errors can add up. So, the error that is made in the worst case is  $(1.065 \cdot 1.052 - 1) = 0.12$ , or about 12%. This is the allowed percentual change in the tolerance band, called  $T_{\text{perc}}$ .

The envelope of a received pulse must therefore differ at least 12% from the expected envelope before it can safely be concluded that the pulse in fact is hit by Cross-rate or lightning.

The pulse needs only to be adjusted (i.e., nulled) at those points where the influence of the distortion is severe. If the pulse is hit by, for instance, very weak Cross-rate, an adjustment of the pulse is not necessary. Therefore, the tolerance band can be extended so that a larger difference is still tolerated.

Furthermore, to accommodate for a certain amount of random noise the tolerance band must be extended by a fixed value. This is the allowed fixed change in the tolerance band, called  $T_{\text{fixed}}$ .

An example of the resulting expected envelope, including its tolerance band, is given in the following figure:

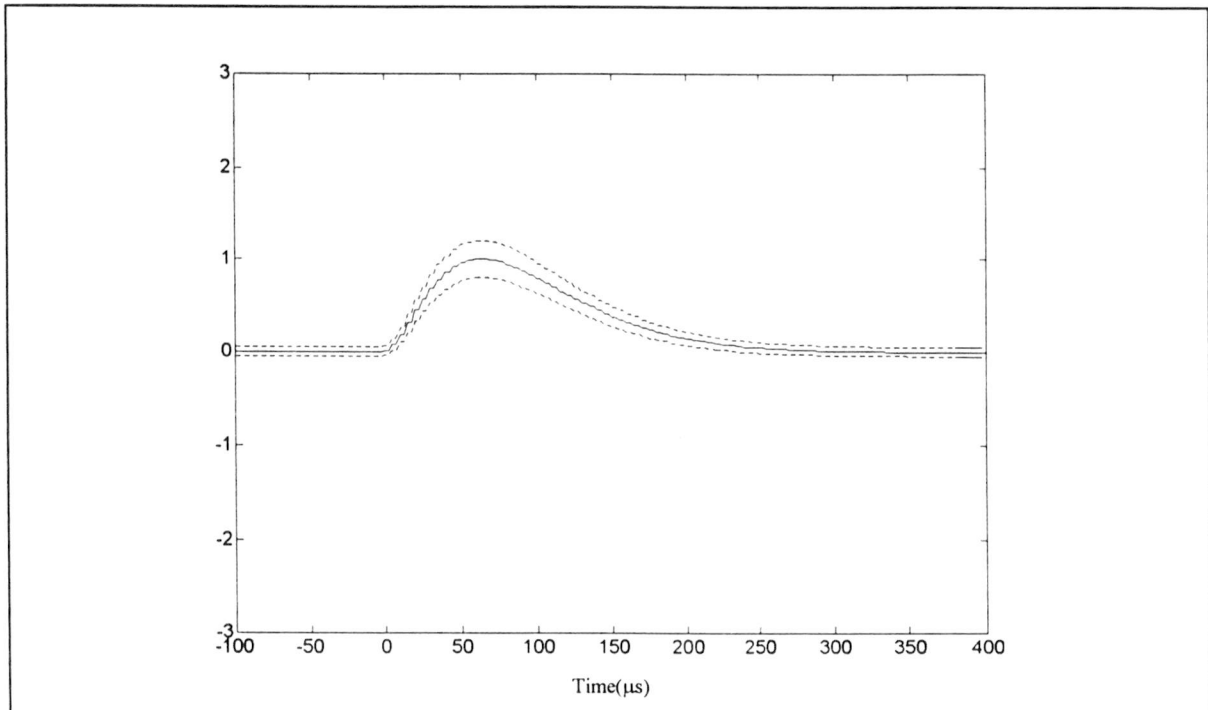


Figure 4.6: The expected envelope, with a tolerance band (the area enclosed between the dashed lines)

At all points where the envelope of the received pulse does not lie within the area enclosed by the two dashed lines, the samples are nulled (as described in section 4.2.1).

#### 4.4 The Reference Figure

The receiver will have to ‘know’ the shape of the pulse it can expect. For this purpose, a reference figure that contains the expected envelope is kept in the memory of the receiver. Pulse shapes that differ significantly from this reference figure are assumed to be distorted.

As described in the previous sections, there are influences that can cause the expected envelope to change slowly. This is the case when:

- skywaves occur, or
- the receiver moves geographically.

The differences will not vary much between successive pulses, but the expected envelope will slowly drift over time. Of course, signals that differ slightly from the expected signal must not be interpreted by the receiver as signals distorted by interference.

The reference figure will therefore have to be continually adjusted over time to make sure that it keeps resembling the momentary pulse shape if it is received without interference. The reference figure is chosen to be a moving average over the received envelope shapes.

In formula form:

$$R_k = q_{hold} \cdot R_{k-1} + (1 - q_{hold}) \cdot X_k \quad \text{Formula 4.2}$$

where:

- $R_k$  = the reference figure
- $X_k$  = the envelope of the received signal, averaged over 1 GRI (8 pulses)
- $q_{hold}$  = a parameter that controls how fast changes in the received signal are incorporated in the reference figure

If we state that all pulses that were received more than  $n$  GRI's ago must have an influence less than 0.1% on the reference figure, the parameter  $q_{hold}$  can be calculated as follows:

$$q_{hold} = \sqrt[n]{0.001},$$

which can be calculated by

$$q_{hold} = e^{\frac{\ln(0.001)}{n}} \quad \text{Formula 4.3}$$

*Example:*

Suppose we are listening to GRI 8940, and we want all pulses that occurred more than 1 minute ago to have an influence of less than 0.1% on the reference figure.

In 1 minute (60 seconds),  $60 \cdot (1/8940e-5) = 671$  GRI's occur.

$q_{hold}$  is then calculated by  $q_{hold} = e^{\frac{\ln(0.001)}{671}} = 0.9898$ .

#### 4.5 Extending the distortion detection to erasure detection

After detecting which parts of the received pulse are being affected by Cross-rate or lightning, it is not difficult to determine a measure to indicate whether the received pulse still has a fair chance of being decoded correctly. If it is determined that the chance of incorrect decoding the pulse is large, it is better

to accept this fact and not even attempt decoding. The symbol can then be marked as an 'erasure'. Erasures are easier to correct by error-correcting codes than errors.

The power of the part of the signal that is not distorted (and therefore has not been 'nulled' by the distortion detecting algorithm) can be used as a measure for erasure-detection. If this amount of power becomes small compared to the total amount of power of a complete Loran-pulse, the received pulse is badly damaged and demodulation can only be done with an increased probability of making a wrong decision.

In other words:

If  $P_{\text{received signal}} < E_{\text{thresh}} \cdot P_{\text{reference figure}}$ , then the received pulse is marked as an erasure. The factor  $E_{\text{thresh}}$  is called the Erasure threshold factor. It is a compromise between the number of erasures and the number of errors. If it is chosen too low, then the erasure rate will go down, at the cost of the pulse error rate going up. If it is chosen too high, the pulse error rate will be lower, but the erasure rate will go up.

If the distance to the transmitter is small (i.e., the received signal power is high), then the factor  $E_{\text{thresh}}$  can be relatively low, because even if only a small portion of the received pulse is undistorted, this undistorted portion will still carry enough information to decode the pulse correctly. If the received signal power is smaller, then  $E_{\text{thresh}}$  will have to be chosen higher, since random noise will have a larger influence on the undistorted portion of the pulse, which leads to an increased probability of incorrect demodulation of the pulse.  $E_{\text{thresh}}$  should therefore be dependent on the SNR of the received signal.

The erasure threshold factor can be used to balance the amount of erasures received, and the number of received pulse errors. The higher the factor, the less pulse errors will be received, but many pulses will be marked as an erasure. If the factor is lowered, the erasure rate goes down, but the pulse error rate will go up.

Since the (modified) envelope of the received signal is already available, the power of the undistorted part of the signal can easily be calculated by squaring the envelope and integrating it over the length of the entire pulse.

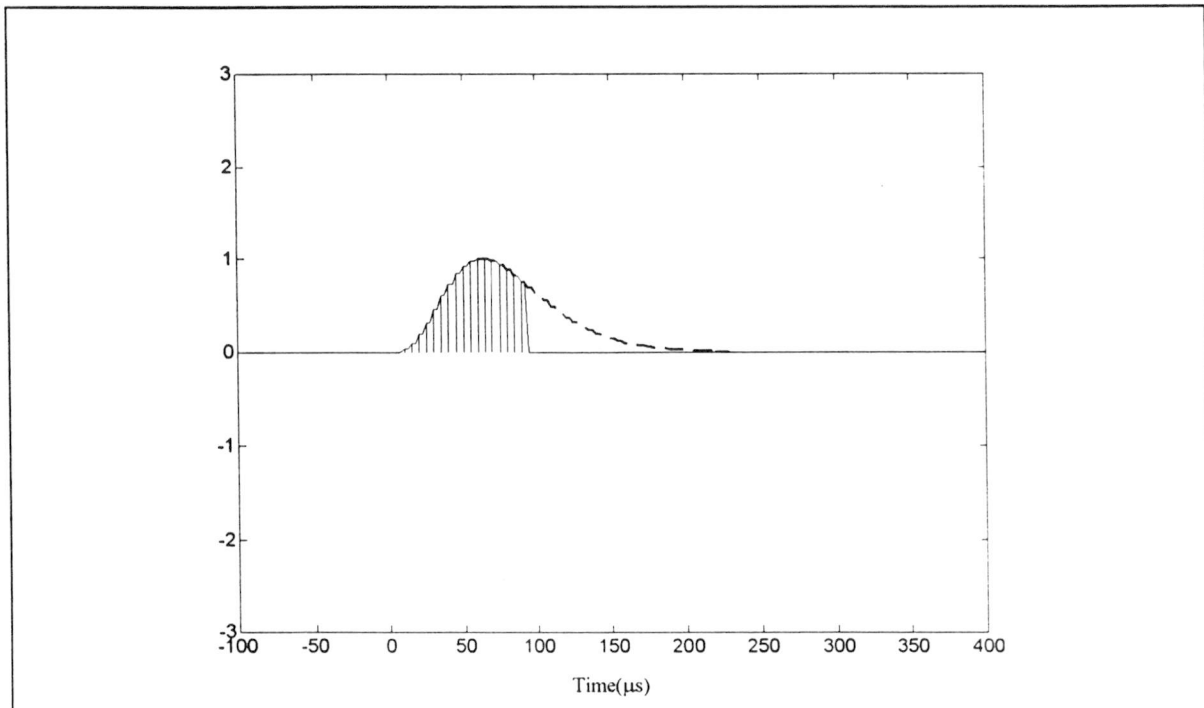


Figure 4.7: Power of the undistorted part of the received signal (dashed area)

From figure 4.7 the amount of power contained in the undistorted part of the received signal from figure 4.1(c) can be seen as the dashed area.

#### 4.6 Parameters of the pulse distortion-detecting and reducing algorithm

A number of parameters were presented with the introduction of the pulse distortion-detecting and reducing algorithm. All relevant parameters, and their influences, are described below:

- The width of the tolerance band, composed of:

$T_{perc}$ : the allowed percentual change in the expected envelope. This factor must be chosen such that all changes in the expected envelope caused by non-distorting phenomena (like Eurofix modulation and the error in the envelope detection) all have an impact on the received envelope that is less than  $T_{perc}$  times the expected envelope. If this factor is chosen too low, pulses will be marked as being hit by Cross-rate when they are not. If it is chosen too high, pulses distorted by Cross-rate or severe atmospheric noise will not be detected as such.

$T_{fixed}$ : the allowed random change in the envelope. This factor allows a certain amount of random signals (such as thermal noise, weak atmospheric noise and weak Cross-rate) to be present on the received signal. If this factor is chosen too low, the tolerance band will be very small on the points when the expected envelope is small in amplitude. This means

that all changes in the envelope at those points (for instance, by a skywave building up over time) will be marked as distorted, which is undesirable. If the factor is chosen too high, pulses that are distorted by Cross-rate or atmospheric conditions will pass unnoticed.

- $q_{\text{hold}}$ : the expected envelope hold factor. This factor controls how fast changes in the received envelope are incorporated in the reference (expected) envelope. The lower  $q_{\text{hold}}$ , the faster the reference envelope follows changes in the received envelope. This factor should be low enough to follow the fastest changes in the received envelope caused by skywaves and dynamics, but high enough not to allow envelope-changes caused by Cross-rate or lightning to have any impact on the stored reference envelope.
- $E_{\text{thresh}}$ : the erasure threshold factor. This factor determines how much of the power of a Loran-pulse must remain undistorted before an erasure is declared. This factor balances the erasure rate and the pulse error rate - if  $E_{\text{thresh}}$  is lowered, the pulse error rate will go up and the erasure rate will go down - if  $E_{\text{thresh}}$  is increased, the opposite happens.  $E_{\text{thresh}}$  should be inversely proportional to the mean SNR, as explained in section 4.5.

## 5. The Demodulator

In this chapter, a demodulator for the Eurofix datalink is developed. First, the possible demodulator structures are discussed.

### 5.1 Demodulator structures

There is a number of possible Loran-C receiver structures that can decode Eurofix modulation:

- Single point receivers
  - Hard-limited single point receivers
  - Linear single point receivers
- Cross-correlation receivers
  - Hard-limited cross-correlation receivers
  - Linear cross-correlation receivers

All these receiver structures are described more extensively in [9]. For completeness, a short description of each demodulator type is given here:

#### 5.1.1 Hard-limited single point demodulators

A hard-limited single point demodulator takes only one sample of each Loran-C pulse, and uses only the sign (positive or negative) of this sample. The sample is taken at a point in the Loran-pulse where no skywaves are assumed to be present. If the transmitted signal was early, the sign will be negative - if it was late, the sign will be positive. If the transmitted code was balanced, then on average the number of positive samples and negative samples must be zero. This provides a tracking mechanism for the Loran-C receiver, since if the average is not equal to zero, the sample-moment must be adjusted. More information about tracking can be found in [5].

This demodulator is appealing because of its simplicity - its implementation is very simple, and the hardware needed is very cheap. It is, however, quite susceptible to noise, because a certain amount of noise on the sample point results directly in increased probability of incorrect decoding of the pulse.

This technique can be used to demodulate Eurofix 2-level coding, but is unusable for demodulation of 3- or more level coding schemes, because only 1 bit of information per Loran-C pulse is acquired.

### 5.1.2 Linear single point demodulator

This type of demodulator also takes only one sample per Loran-C pulse, but it acquires more information than the hard-limited case because it uses the value of the sample rather than just the sign of the sample. This demodulator structure is still quite simple, and thus cheap.

This demodulator structure is capable of decoding 3- or more level Eurofix coding, since the value of the sample provides a measure on how much the transmitted pulse was advanced or delayed. However, a 'moving average' set of reference values (1 per level) is needed to determine the level of shifting of the transmitted Loran-pulse, because influences other than Eurofix-modulation (for instance, the signal strength) will affect the value of the sample that is taken.

For exactly the same reason as was given for the hard-limited case, this demodulator is also quite susceptible to noise.

### 5.1.3 Hard-limited cross-correlation demodulator

This type of demodulator takes a large number of samples per Loran-C pulse, and cross-correlates the signs of this set of samples with a stored reference set. Then, the demodulator cross-correlates the same signs of the received set of samples with a time-shifted version of the stored reference set. The demodulator repeats this process for each possible level of modulation. The time-shift of the received signal is then determined by the time-shift of the reference set that yields the highest correlation.

Cross-correlation demodulators use much more information per pulse than single-point demodulators do. Theoretically, since on average the (Gaussian) noise that is always present at each sample taken is zero, the more samples per Loran-C pulse are taken, the more the noise influence is reduced considered over all of the samples taken.

Practically, however, a band filter will have to be used in the receiver. The filter causes the noise influence on consecutive samples to be correlated to a certain extent. This puts an upper limit to the number of samples that can be taken, above which further reduction in noise influence is negligible.

#### 5.1.4 Linear cross-correlation demodulator

This type of demodulator uses the same concept as the hard-limited cross-correlation demodulator, but instead of only using the signs of the sample values, the sample values itself are being used for the received pulse and the reference figures. This way, the information that is contained in the amplitude of the received signal is also taken into account, yielding a higher performance.

This demodulator structure has the highest complexity of all types of demodulators presented here. Its performance, however, will be better than that of the other demodulator structures. This demodulator acquires the largest amount of information about the signal compared with the other demodulators.

In the light of the continuing increase in speed and decrease in cost of computing hardware, the complexity of this demodulator will not have a large impact on its price - costwise, it will probably be competitive with the simpler types of demodulators presented. Therefore, this type of demodulator is the most promising of the types presented here.

#### 5.2 Demodulation of Eurofix-modulated pulses using linear cross-correlation

The demodulator calculates the correlation value of the incoming pulse with stored reference figures: one for each level of shift. The reference figure that yields the highest correlation value with the incoming pulse is assumed to have the same timeshift as the received pulse.

The following figure is a graph of the 3 autocorrelation functions of an early, a prompt and a delayed pulse.

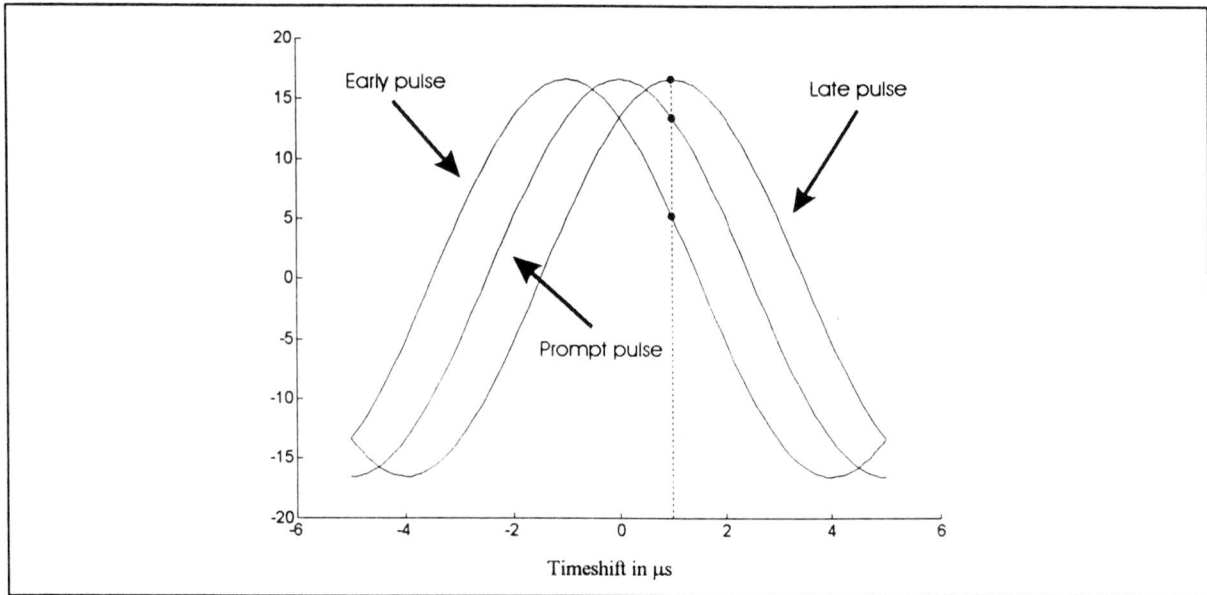


Figure 5.1: Cross-correlation values: correlation function of a normalized early, a prompt and a delayed pulse with a time-shifted Loran-C pulse - all sampled at 400 kHz

As an example, a Loran-C pulse with a time-shift of 1  $\mu\text{s}$  is represented as a dashed line. The correlation values between the Loran-C pulse and the 3 reference figures are represented as black dots. Since the correlation value with the ‘late’ pulse is highest, the pulse will be decoded as a ‘late’ pulse.

For our purposes, the most interesting values that can be seen from this figure are the correlation values at the points of intersection between all possible levels of shifting of the pulses. The difference between these values is a measure of the selectivity of the demodulator. These are summarized in the following table:

shift	-1 $\mu\text{s}$ (early)	0 $\mu\text{s}$ (prompt)	1 $\mu\text{s}$ (late)
-1 $\mu\text{s}$ (early)	16.635 (1.000)	13.456 (0.809)	5.137 (0.309)
0 $\mu\text{s}$ (prompt)	13.456 (0.809)	16.635 (1.000)	13.456 (0.809)
1 $\mu\text{s}$ (late)	5.137 (0.309)	13.456 (0.809)	16.635 (1.000)

Table 5.1: Correlation values and factors of normalized Loran-C pulses (sampled at 400 kHz) with different levels of shifting. The correlation factors are bracketed.

It can be seen from the table that the correlation between an early and a prompt pulse yields a much higher value than the correlation between an early and a late pulse. Since the correlation value is the only criterion used to classify a received pulse as an early, a prompt or a late pulse, we can expect to

find that the probability that an early pulse will be decoded as a prompt pulse is much higher than the probability that the same pulse is decoded as a late pulse.

This table illustrates a well-known principle in telecommunications: the greater the alphabet of symbols that can be transmitted over any telecommunications channel, the higher the possibility that an error is made in the demodulation of a given symbol, and hence an increased Symbol Error Rate (SER). The question whether the increase in speed outweighs the increased SER is subject to investigation.

### 5.3 A Linear cross-correlation demodulator

The concept of the linear cross-correlation demodulator is given in the following figure. 3-level Eurofix coding is assumed.

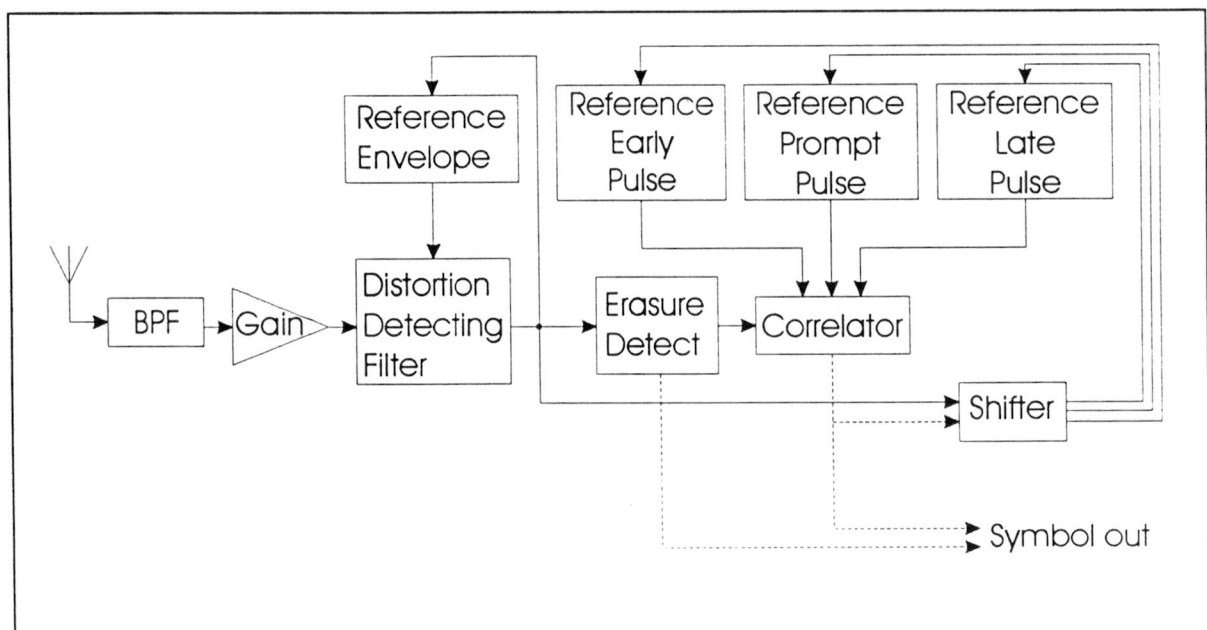


Figure 5.2: The demodulator structure. The solid lines display the signal path; the dashed lines display the control path

The Loran-C signal is received by the antenna, and fed through a band-pass filter to filter out all frequencies outside the Loran-C band (90-110 kHz). The signal is then fed through the distortion-detecting filter that was introduced in Chapter 5. If the filter did not detect the received pulse as being an erasure, the filtered signal is correlated with 3 reference figures. The correlator decides which of the 3 reference figures yields the highest correlation with the received (filtered) signal, and outputs the result.

The shifter takes the received (filtered) pulse, and calculates from this data 3 new sets of data: 1) one that matches the pulse had it been transmitted early, 2) one set had it been transmitted prompt and 3) one had it been transmitted late.

The symbol output can be either a valid symbol, or an erasure. This data can further be processed by a decoder that can extract messages from the data, correcting errors and erasures from the demodulator with an error-correcting protocol.

Two of the components used in this demodulator structure will be discussed a bit more in-depth in the following paragraphs. These are:

- The pulse shifter, and
- The reference figures

### 5.3.1 The Pulse Shifter

The pulse shifter is used to calculate ‘shifted versions’ of a particular set of data. For instance, if the received set of data is the sampled version of a prompt pulse, and represented by:

$$p_i = S_i * T_{\text{sample}} \quad \text{Formula 5.1}$$

where:

$p$  is the set of sample values of the prompt pulse,

$S_T$  is the received signal sampled at time  $T$ , and

$1/T_{\text{sample}}$  is the sampling frequency (assumed to be 400 kHz),

then the shifter should calculate:

$$e_i = S_i * T_{\text{sample} + 1 \mu\text{s}} \quad \text{Formula 5.2}$$

$$l_i = S_i * T_{\text{sample} - 1 \mu\text{s}} \quad \text{Formula 5.3}$$

where:

$e_i$  is the set of sample values of the early pulse,

$l_i$  is the set of sample values of the late pulse,

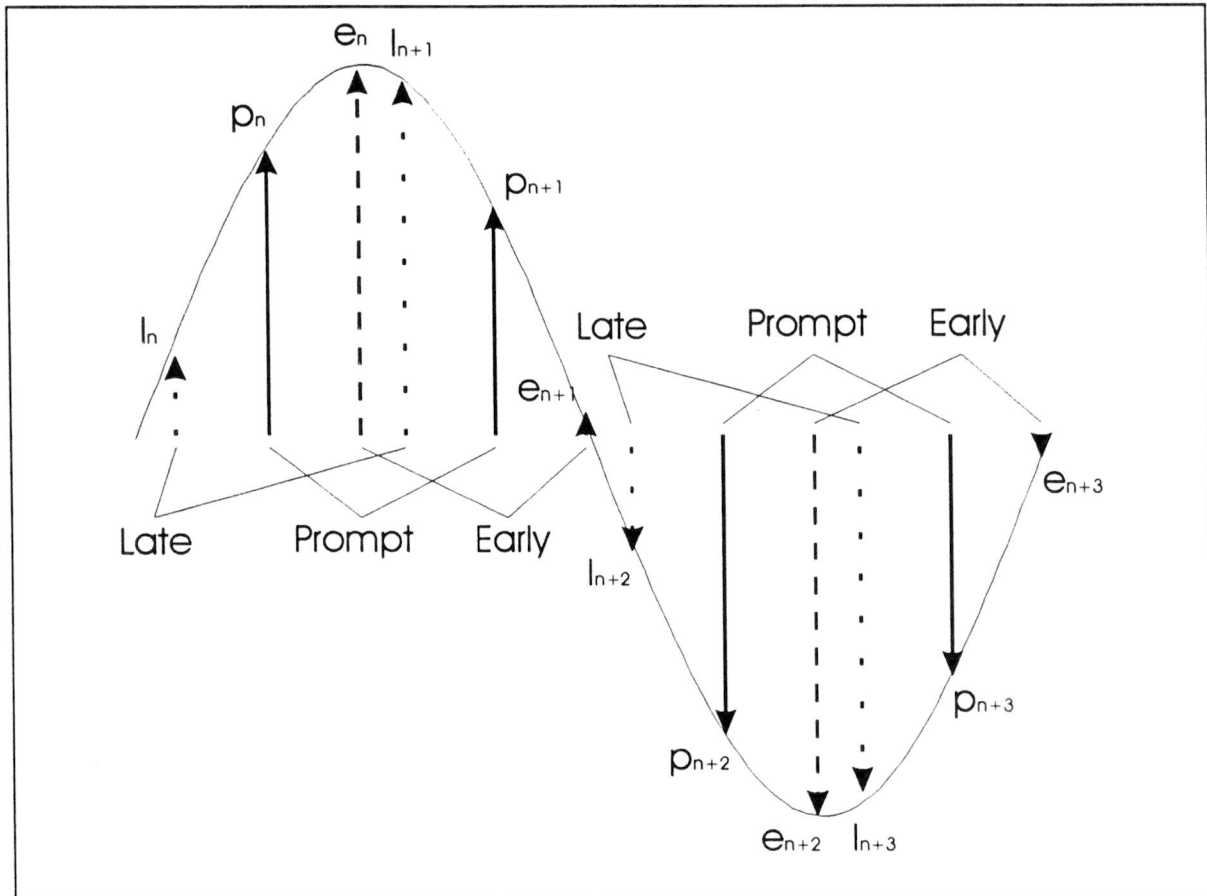


Figure 5.3: Graphical representation of the function the Shifter performs: given the Prompt samples, the shifter calculates the Late and the Early sample values.

In other words, the shifter should interpolate the values of the received signal at those points in time where the real samples would have been taken when the signal was early or late.

Given the fact that the samples are taken at twice the Nyquist frequency, this is theoretically possible, since all information about the signal is contained in the samples.

Its practical implementation, however, is not trivial: theoretically, to calculate any interpolated samplepoint, all other sample points need to be included in the calculation, making this a very lengthy process.

By cleverly giving weight factors to the samplepoints, however, it is possible to design a filter for shifting Loran-pulses that uses only 6 coefficients [10]. The difference between an advanced pulse that has been calculated by shifting a prompt pulse and a normal advanced pulse is smaller than  $1.5e-4$ .

### 5.3.2 The reference figures

The reference figures that are used to store the representations of an early, a prompt and a late Loran-C pulse bear a great similarity to the reference figure used for the distortion detecting, as described in section 5.4. This means that the update rate of the reference figures should be slow enough to minimize the influence of non-consistent disturbances, but fast enough to follow consistent changes in the shape of the Loran-C pulse due to skywaves.

### 5.4 Thermal noise influence on the linear cross-correlation method

To find the probability of the linear cross-correlation method of making an incorrect decision due to thermal (Gaussian) noise, the result of this Gaussian noise on the received signal is investigated first.

The probability of an incorrect decision using the linear cross-correlation method can be expressed as a function of the signal-to-noise ratio of the received signal.

A sampled version of the Loran-C signal is expressed as:

$$x_i = \left(\frac{t}{t_p}\right)^2 \cdot \exp\left(2 - \frac{2t}{t_p}\right) \cdot \sin\left(2\pi \cdot t \cdot 100 \cdot 10^3\right), \quad \text{Formula 5.4}$$

with  $t=i \cdot 2.5 \mu\text{s}$ ,  $t_p=65 \mu\text{s}$  and  $i=0..399$ .

The samples of the received signal are represented by the vector  $y_i$ . The corresponding values of the reference figure are denoted as  $x_i$ . The correlation  $C$  is then calculated by:

$$C = \sum_i x_i \cdot y_i \quad \text{Formula 5.5}$$

We can assume a certain amount of Gaussian distributed noise on each of the samples  $y_i$ , denoted by  $e_i$ . Each element of  $e_i$  is a normally distributed random value with  $m=0$  and variance  $\sigma^2$ . So:

$$y_i = x_i + e_i \quad \text{Formula 5.6}$$

Equation 5.5 now becomes:

$$\begin{aligned}
 C &= \sum_i x_i \cdot (x_i + e_i) \\
 &= \sum_i x_i^2 + \sum_i x_i \cdot e_i
 \end{aligned}$$

Formula 5.7

The value of the first right-hand term in this equation can be found in table 5.1, and is equal to 16.635.

We want to calculate the probability that a pulse is demodulated incorrectly. Mathematically:

$$P\left(\sum_i x_i^B \cdot y_i > \sum_i x_i^A \cdot y_i\right)$$

Formula 5.8

where  $x^A$  and  $x^B$  represent two different reference figures. With equation 5.6, this can be rewritten as:

$$\begin{aligned}
 &P\left(\sum_i x_i^B(x_i^A + e_i) > \sum_i x_i^A(x_i^A + e_i)\right) = \\
 &P\left(\sum_i x_i^B x_i^A + \sum_i x_i^B e_i > \sum_i (x_i^A)^2 + \sum_i x_i^A e_i\right) = \\
 &P\left(\sum_i e_i(x_i^B - x_i^A) > \sum_i x_i^A(x_i^A - x_i^B)\right)
 \end{aligned}$$

Formula 5.9

In this formula,  $x^A$  and  $x^B$  are known. The problem, however, lies in the elements of  $e_i$ : because the thermal noise is bandpass filtered, these noise samples will not be statistically independent.

Instead, all samples  $e_i$  are dependent on a new random variable and all previous values of  $e_i$ .

$$e_i = r(0)Z_i + r(1)Z_{i-1} + r(2)Z_{i-2} + \dots$$

Formula 5.10

with each element  $Z_i$  a normally distributed random variable with mean 0 and variance  $\sigma^2$ .

$r(i)$  is the time-discrete impulse response of the filter. For a 6th order Butterworth filter, the impulse response is given in the following figure:

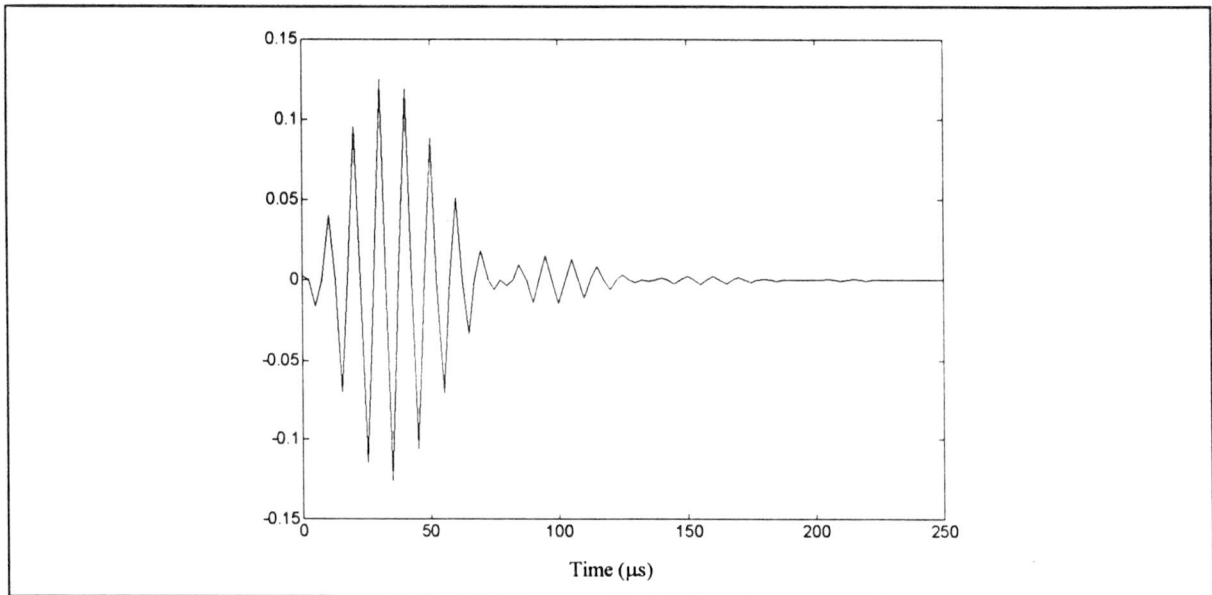


Figure 5.4: Impulse response of a 6th order 90-110 kHz bandpass Butterworth filter

As each element  $e_i$  is a linear combination of normally distributed random variables, it is itself a normally distributed random variable. Its variance is equal to the in-product of the impulse response times the original (i.e., before filtering) variance of the random signal. In formula form:

$$\text{var}(e_i) = \text{var}(Z) \cdot \sum_j r(j)^2 \quad \text{Formula 5.11}$$

For the 6th order Butterworth filter:

$$\sum_j r(j)^2 = 0.1043$$

which leads to the conclusion that the power of the random signal after filtering is roughly 10% of the power of the same signal before filtering.

Now, equation 5.9 can be plotted as a function of the SNR.

The probability of error for a linear cross-correlation receiver can be calculated. In the following figure, the pulse-error probability is plotted versus the SNR of the received signal:

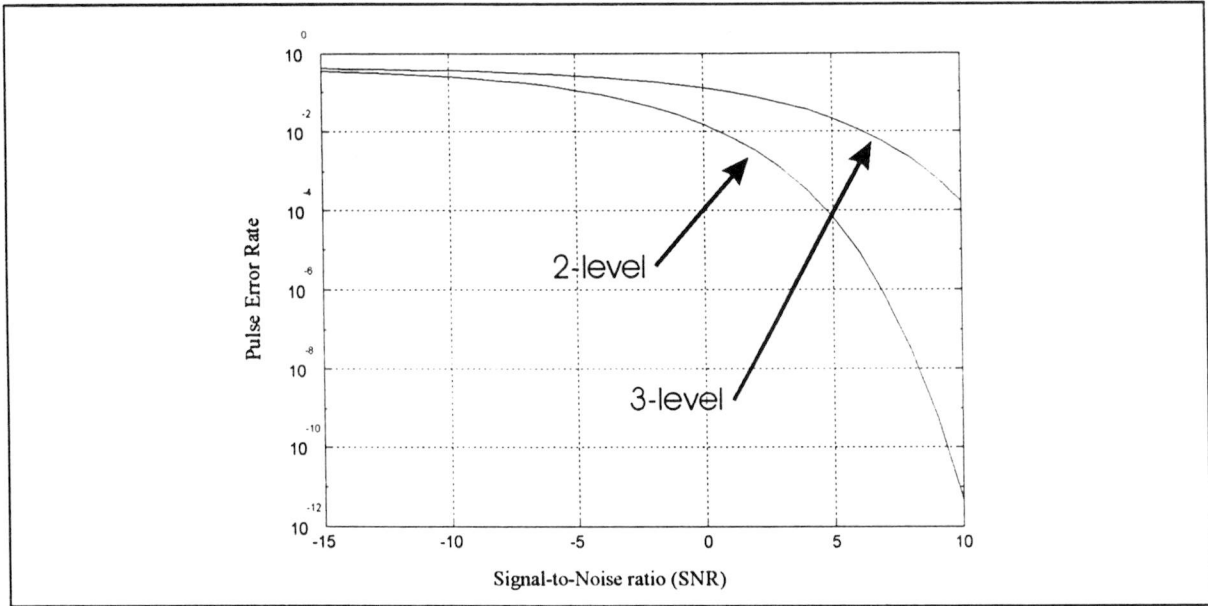


Figure 5.5: Probability of error versus SNR of the received signal for a linear cross-correlating receiver (2- and 3-level coding)

## 6. Testing of the proposed demodulator

In order to test different encoding and/or decoding methods for the Eurofix Datalink, it is desired to have a test-setup that simulates the reality as accurately as possible.

Ideally, the test-setup would be:

1. A 'live' transmission medium (including signals from other Loran-transmitters, atmospheric noise, electromagnetic disturbance due to lightning, etc.)
2. A Loran-transmitter transmitting real-time Eurofix data
3. A real-time Eurofix demodulator

### 6.1 The Transmission medium

The characteristics of the transmission medium can readily be monitored by putting up an antenna and inspecting the signals in the Loran-band (90-110 kHz). In this band, signals from other Loran-transmitters will be found, as well as signals that result from atmospheric conditions.

### 6.2 Acquiring Time-shifted Loran-pulses

It is quite difficult to have a real Loran-transmitter transmitting Eurofix data. In order to do this, an existing transmitter would have to be modified to transmit Eurofix data, which would politically and institutionally be very difficult. Furthermore, to be able to compute bit-error rates, a datalink (other than the Eurofix datalink) would have to be established between the transmitter and the demodulator to act as a reference datalink. Thirdly, this would have to be done for a number of transmitters to get a good grasp of the influence of parameters like distance to the transmitter, the GRI that is being operated on (as this could influence the type of Cross-rate that is experienced), the power of the transmitter etc.

The conclusion can be drawn that, at this stage of the research, it is not feasible to have a real Loran-transmitter transmitting Eurofix-data, just for test purposes.

An alternative can be found by looking into the nature of the Eurofix-modulation. Normally, the Loran-pulse would be transmitted at time  $T_0$  and received at time  $T_1$ , with its time-shifted variant being transmitted at time  $T_0+\delta T$  and received at time  $T_1+\delta T$ . But, if the Loran-pulse is transmitted at time  $T_0$ , its time-shifted version can be also be found by looking at time  $T_1-\delta T$ . In other words, instead of having the transmitter transmit the pulse later in time, it is also possible to have the receiver start receiving

earlier in time and vice versa. The concession that is made to the real-life situation is that all Cross-rate and noise appears to be time-shifted too.

In order to get a sampled version of a time-shifted Loran-pulse, a shiftable clock signal is needed. This clock signal needs to be adjustable in such a way that, for the duration of an entire Loran-C pulse, the clock is either 1  $\mu$ s early, 0  $\mu$ s early or 1  $\mu$ s late.

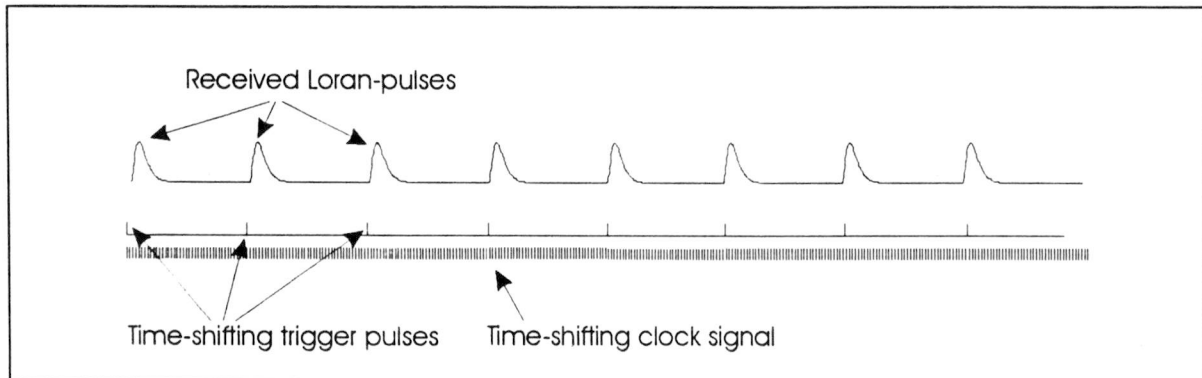


Figure 6.1: Timing diagram of the received pulses, the trigger signal and the sampling clock signal. The trigger pulses can be programmed to appear 1  $\mu$ s early, 0  $\mu$ s early or 1  $\mu$ s late.

Using this method, any normal Loran-C transmitter can be made to look like it is time-shifting its pulses, from the demodulator's viewpoint. This is illustrated in figure 6.1.

In order to get this clock, a Loran-C simulator is used. This simulator can produce 1 trigger pulse per Loran-signal. Furthermore, since the Loran-C simulator that is used can transmit Eurofix-modulated pulses as well, the trigger pulses are time-shiftable as well. The simulator is utilized just to produce trigger pulses - the actual Loran-C signals coming out of the simulator are not used. A separate PC is used to produce the control data for the simulator that determines how the trigger pulses are to be time-shifted.

An atomic frequency standard keeps the test-setup locked to the real Loran-C signals that are being tracked. No other tracking mechanism is used.

The 400 kHz signal that is needed is realized using a 10 MHz frequency (obtained from a 5 MHz atomic frequency standard) and a 25-counter. Each (400 kHz) clock cycle, the 25-counter starts at 25, counting down at 10 MHz. When the 25-counter hits 5, it raises its output - when it hits 0, it lowers its output again, thereby outputting a 400 kHz clock with a 20% high-time. The trigger pulse from the

Loran-C simulator is used to clear the 25-counter. By time-shifting the moment the trigger-pulse occurs by  $\delta T$ , the desired time-shifting clock is acquired.

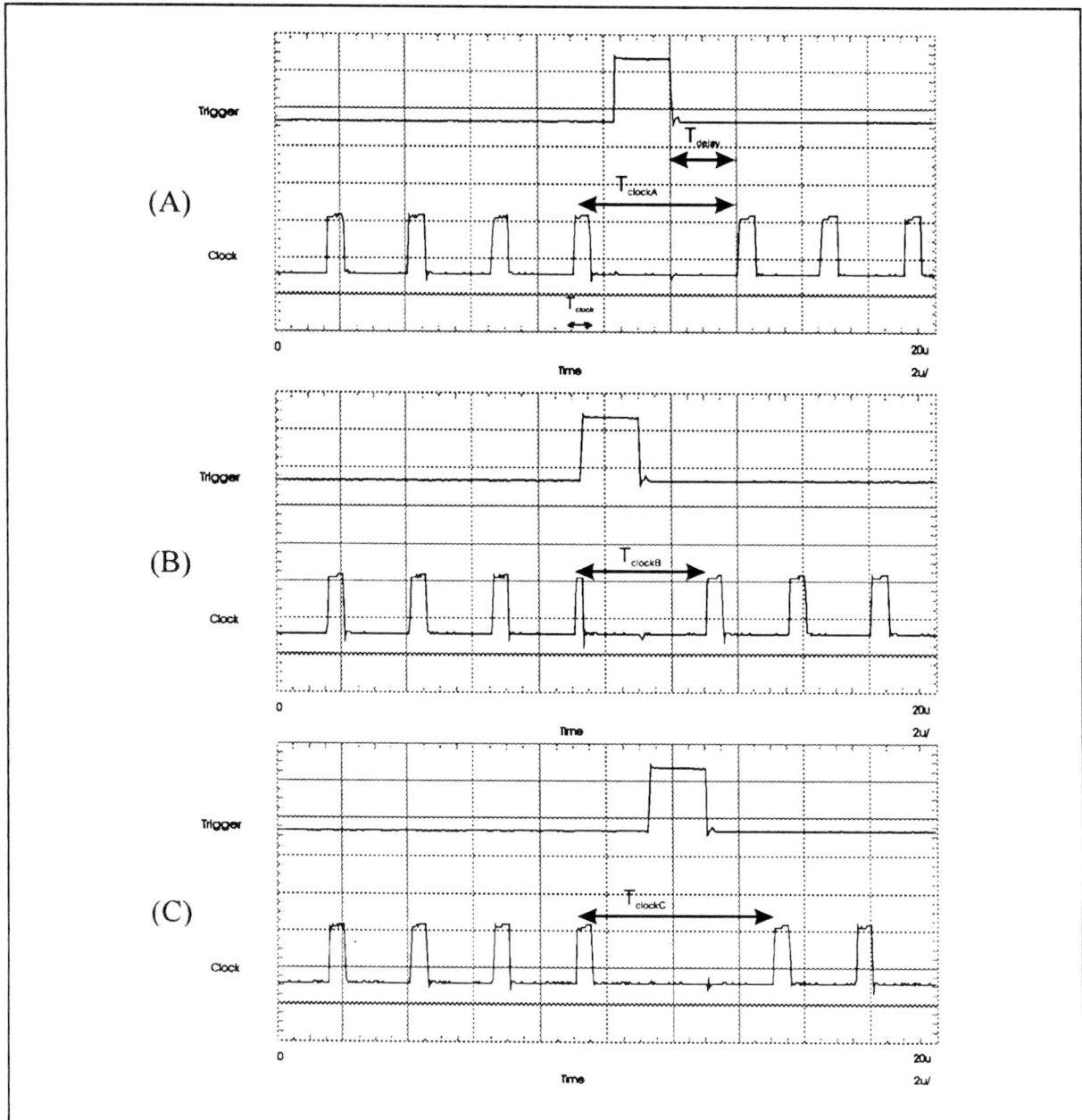


Figure 6.2: Timing of the clock signal with relation to the trigger pulse.

(A) is the diagram for a prompt-to-prompt clock transition,

(B) for a prompt-to-early transition and

(C) for a prompt-to-late transition.

$$T_{\text{delay}} = 2 \mu\text{s}, T_{\text{clock}} = 500 \text{ ns}, T_{\text{clockA}} = 5 \mu\text{s}, T_{\text{clockB}} = 4 \mu\text{s} \text{ and } T_{\text{clockC}} = 6 \mu\text{s}$$

This is illustrated in figure 6.2.

Unfortunately, 1 clock-pulse will always be lost because of the time  $T_{\text{delay}}$  being  $2 \mu\text{s}$ . This results in the fact that instead of  $8 \times 400$  samples, only  $8 \times 399$  samples are taken. The demodulator software has been modified to take this into account.

In 6.2(b), it can be seen that the 399th clock pulse is somewhat smaller than the others - this is also due to the fact that  $T_{\text{delay}}$  is  $2 \mu\text{s}$ . Since the received Loran-pulse must in its entirety lie between the occurrence of 2 trigger pulses, the received pulse will have 0 amplitude at the 399th clock pulse, so the timing for this clock pulse is not critical.

### 6.3 The Demodulator

The proposed demodulator of Chapter 5 has been implemented in software. The underlying hardware mainly consists of a 486 DXII-66MHz PC equipped with a 12 bit, 400 kHz A/D converter board. The timing for this board is provided by the Loran-C simulator, which produces the necessary trigger pulses from which the shifting clock is derived.

The demodulator as it has been programmed and tested differs from the demodulator as was proposed in Chapter 5 in the following respects:

- The shifter section has not been implemented due to lack of processing time. The PC is only just capable of performing all the other tasks (detecting distortion, cross-correlating and updating the reference figures) in the repetition time of the Loran-C pulses (the GRI).

This means that the reference figures for the early, prompt and late pulse can only be updated when the demodulator has decoded the received pulse as having the corresponding timeshift. This results in a reduced update rate of the reference figures. It also introduces an initialization problem: the reference figure of the prompt pulse can initially be built by using the first 2 pulses of the Loran-burst (since these pulses are never Eurofix-modulated), but there is no way to build the early and late reference figures. This is circumvented by always starting the tests with the transmission of a known synchronization pattern - the demodulator knows how the pattern is Eurofix-modulated and builds all 3 reference figures from this pattern.

The problem mentioned above could be resolved by using hardware that is more appropriate for the task of signal processing (e.g., a high-speed Digital Signal Processor) or, alternatively, by using a faster PC.

- The tolerance band of the distortion detecting filter is not applied to the envelope of the received signal, but rather to the square of the envelope of the received signal. The real-time calculation of the square root of this envelope proved to be an, as yet unresolved, problem.
- No notch filters have been used in the test-setup, resulting in the fact that CWI is not suppressed. During the tests, however, no effects of CWI were detected.
- No tracking mechanism was used other than an atomic frequency standard, which kept the timing of the test-setup synchronized to the timing of the Loran-C transmitters. As a result, no tracking errors were made - a situation that will not apply when a real-life Loran-C receiver is used.
- The used filter is a 5th order instead of a 6th order Butterworth filter.

#### 6.4 The Test-setup

The test setup as it has been used in the tests is depicted in the following figure:

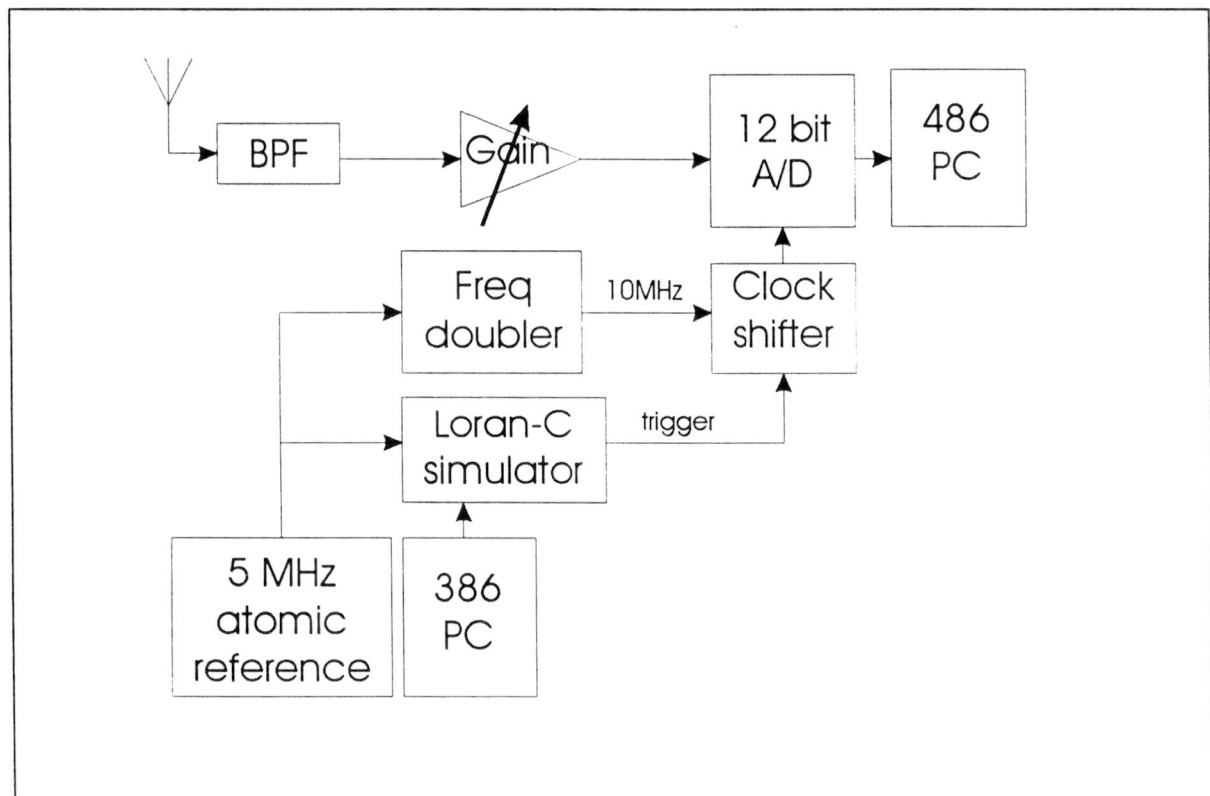


Figure 6.3: The test-setup. The block layout diagram of the software for the '486 PC' resembles figure 5.2.

## Testing of the proposed demodulator

---

The band-pass filter (BPF) that has been used is a 5th order Butterworth filter, with a center frequency of 100 kHz and a bandwidth of 17 kHz.

The 5 MHz atomic reference was provided by a 5 MHz rubidium frequency standard.

## 7. Results

In this chapter, the results of my research are presented.

For the tests, signals from the following 3 transmitters have been used: the Sylt-station in Germany, the Lessay-station in France and the Soustons-station, also in France.

The following table gives the distances from the transmitters to the Delft University of Technology, where the measurements were taken. The estimated SNR (based on the amplitude of the pulses) as it was received in Delft is also given, relative to the Sylt signal.

<b>Station:</b>	<b>Distance to Delft (km):</b>	<b>Transmitter power (kW):</b>	<b>Estimated SNR:</b>
Sylt	407.68 km	250	0 dB
Lessay	523.11 km	250	-3 dB
Soustons	1013.43 km	250	-15 dB

*Table 7.1: Distance, transmitted power and SNR for the Loran-C stations used for the tests. The measurements were all taken at the Delft University of Technology. The estimated SNR is relative to the Sylt signal.*

Detailed information about the location of these and other Loran-C stations can be found in Appendix B.

In all figures in this chapter, the horizontal scale is the time of day, measured in hours, modulo 24. So, for instance, if the time is 32 then this corresponds to 8.00 am, 1 day after the start of the test.

All Erasure Rates and Pulse Error Rates that are plotted in the figures are averaged over 1 minute (60 seconds).

## 7.1 The effect of the distortion detecting filter

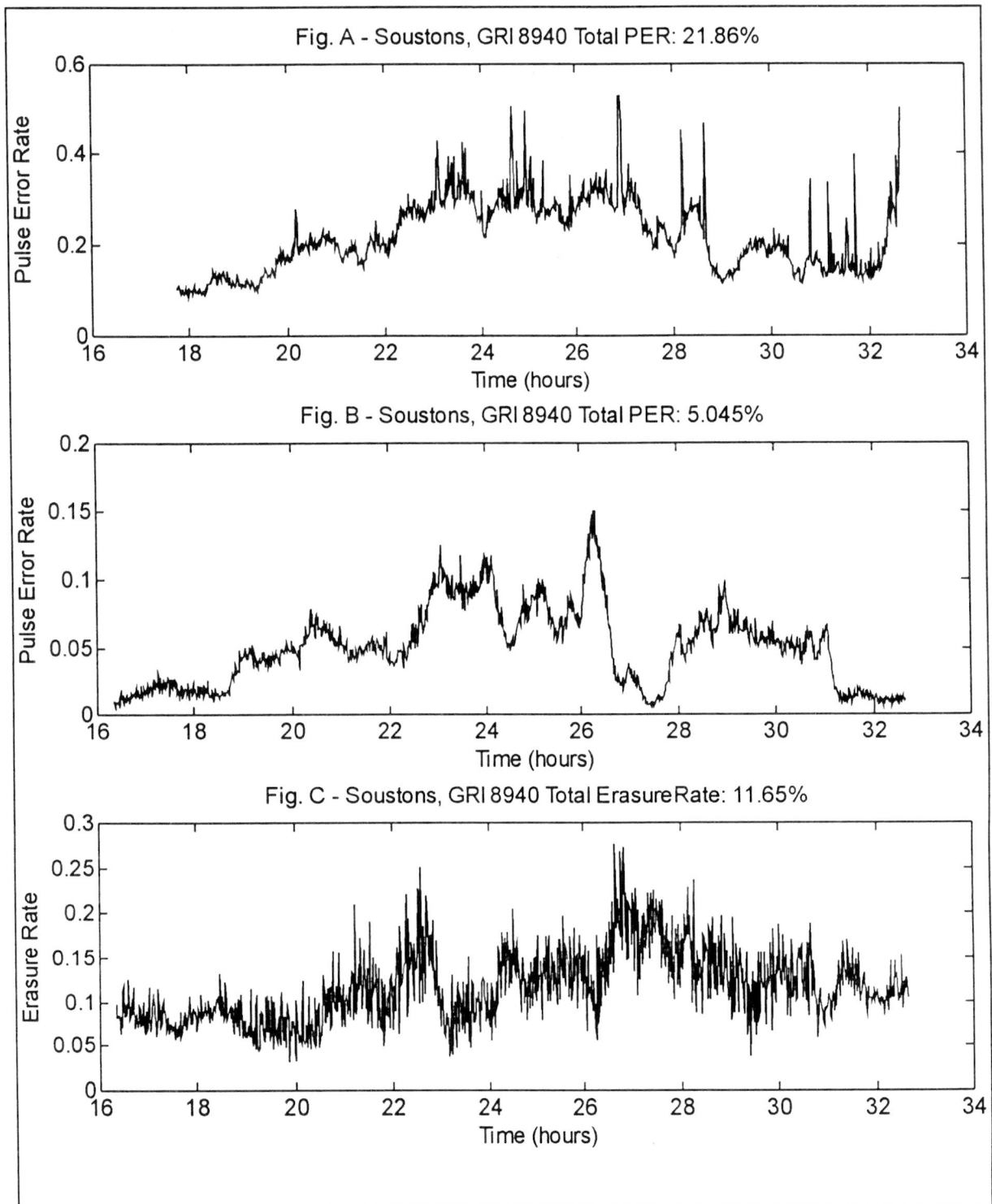


Figure 7.1: Effect of the distortion detecting filter on the Soustons-signals. Fig. (A) is the pulse error rate of the demodulator without distortion detection; fig. (B) and (C) are the pulse error rate and the erasure rate of a demodulator with distortion detection. 3-level coding is used. The measurement plotted in fig.(A) was done on 15 october '95; measurements (B) and (C) were done on 13 october '95.

## Results

---

The effect of the distortion detecting filter can be seen in figure 7.1. Without distortion detection, 21.86% of the received pulses is demodulated incorrectly. With distortion detection, only 5.05% is demodulated incorrectly - although 11.65% of the received pulses are declared as being an erasure. During this test, the erasure threshold factor  $E_{\text{thresh}}$  was set to 0.6 (i.e., when less than 60% of the Loran-pulse was undistorted, it was declared an erasure).

It should be noted, however, that the data was collected on separate occasions. The atmospheric conditions tend to change from night to night, and therefore the pulse error rates and erasure rates for signals from the same transmitter also change from night to night.

During other tests, it was noticed that the skywave-propagation changes quite severely during the night, much more than during daytime. Although only 1 night and only a part of a day has been plotted, this effect can, to some extent, also be seen in these plots: the pulse error rate (fig. B) is much higher between 20 and 29 hours (8.00 pm and 5.00 am the next day) than in the other parts of the plot. This effect can more clearly be seen in other plots in this chapter.

## 7.2 Sylt - 2-level coding

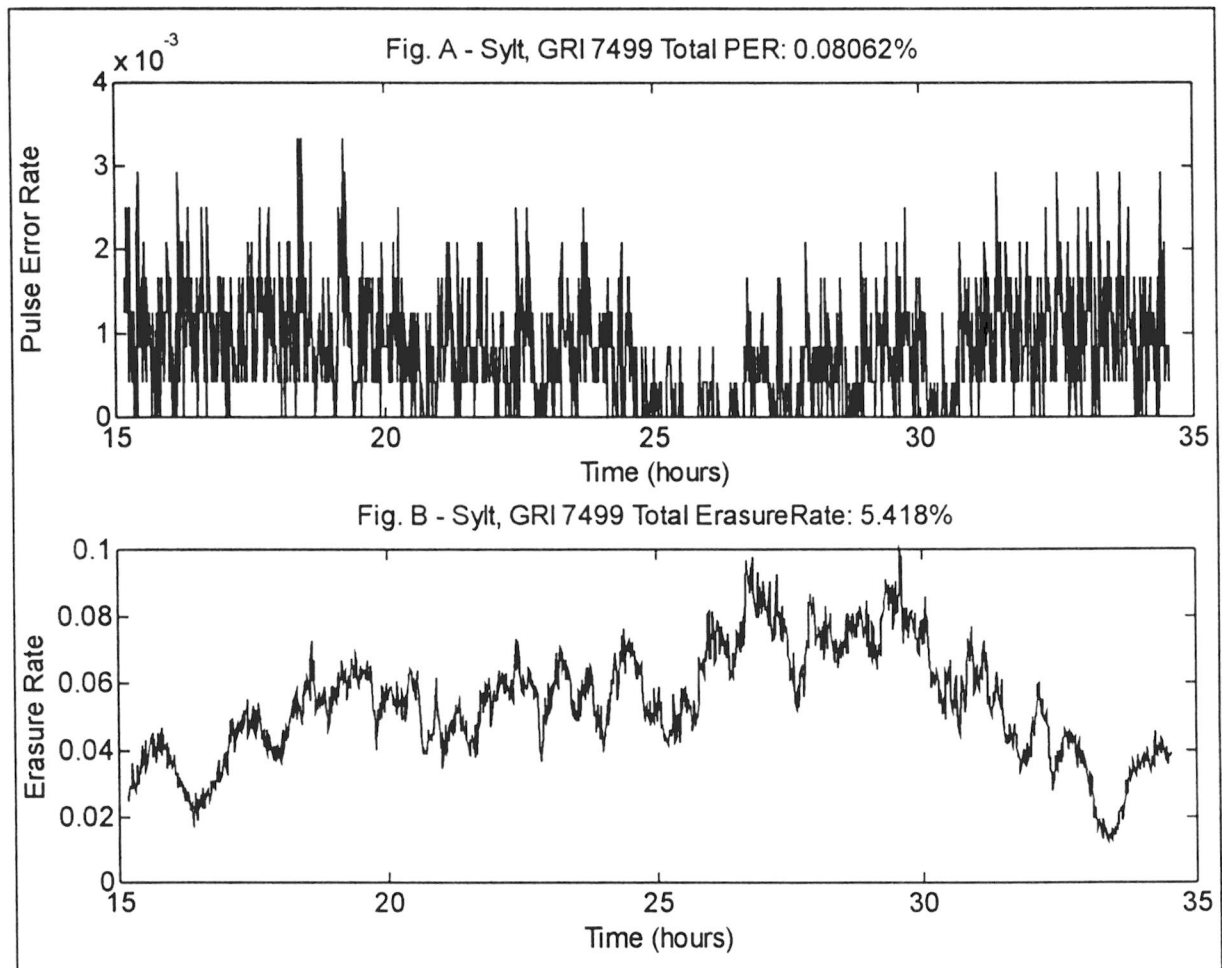


Figure 7.2: Pulse error rate (fig.A) and erasure rate (fig.B) of the Sylt-signal using 2-level modulation. The measurement was done on 7 november 1995.

In figure 7.2, the pulse error rate and the erasure rate of the Sylt signal are plotted. The measurements were done from 3.00 pm until 11.00 am the next day.

The pulse error rate using 2-level modulation is low - only 0.08% of the pulses are in error. This is not surprising, considering the fact that the distance from Sylt transmitter to Delft is only about 400 km, which is not far away in Loran-C terms (the typical coverage range for a Loran-C transmitter is roughly 1500 km).

It can be seen from the plot that the pulse error rate jumps to discrete levels. This is because the number of errors is averaged over 1 minute - since only a discrete number of pulses per minute can be in error, then when the error rate is low (as it is in this case), this can be seen in the resulting plot.

On average, 5.4% of the pulses have been detected as being hit by Cross-rate or severe atmospheric conditions.

### 7.3 Syllt - 3-level coding

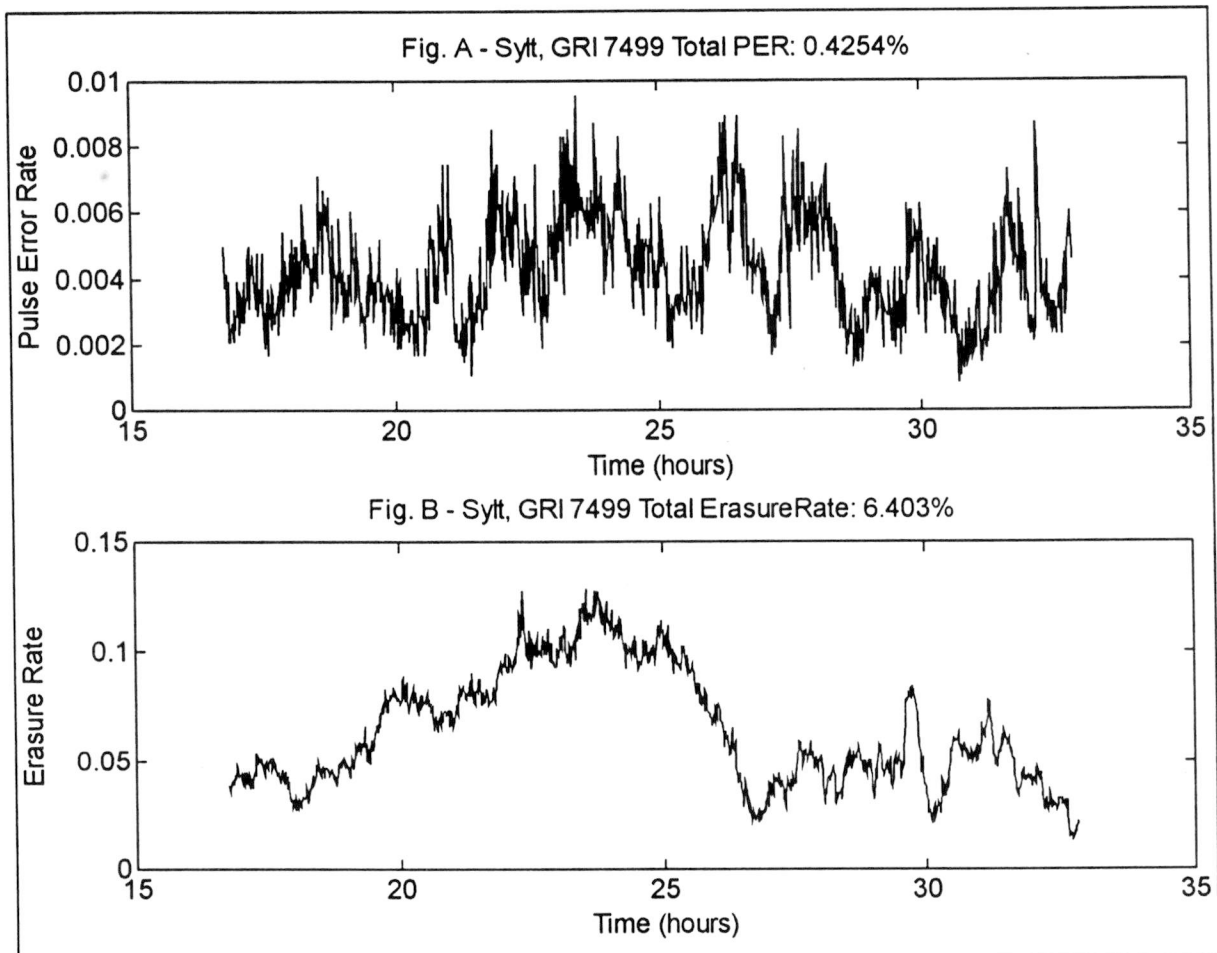


Figure 7.3: Pulse error rate (fig.A) and erasure rate (fig.B) of the Syllt-signal using 3-level modulation. The measurement was done on 8 november 1995.

The 3-level modulation scheme has a higher probability of being demodulated incorrectly than the 2-level modulation scheme under similar circumstances.

This effect can be seen in figure 7.3 - when compared with figure 7.2, the pulse error probability for the 3-level modulation scheme is about 5 times larger than the PER of the 2-level scheme.

On average, the erasure rate is comparable to the erasure rate in the previous plot. This is expected, since the distortion detection is independent from the modulation scheme used.

### 7.4 Lessay - 2-level coding

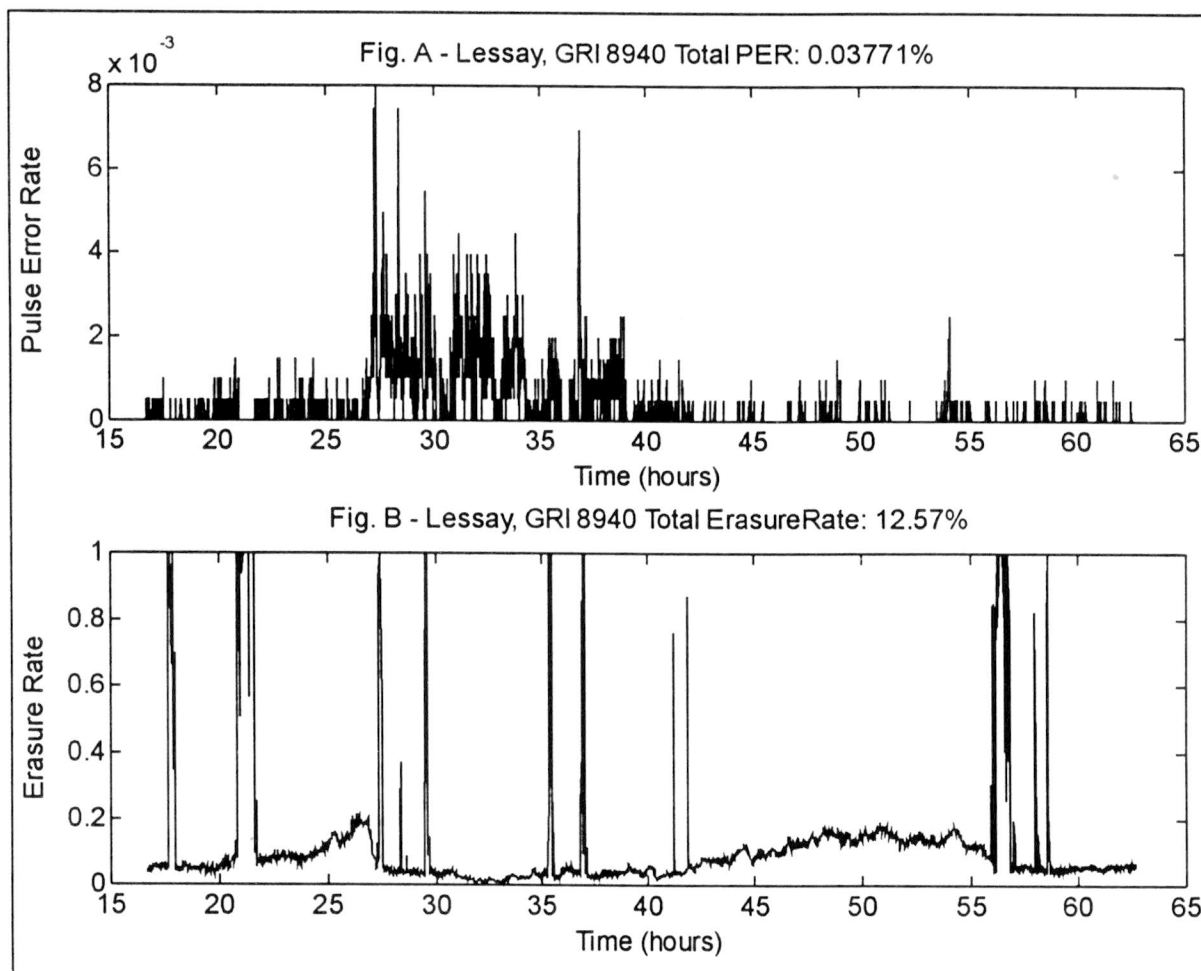


Figure 7.4: Pulse error rate (fig.A) and erasure rate (fig.B) of the Lessay-signal using 2-level modulation. The measurement was done on 17 november 1995.

In figure 7.4, the pulse error rate and erasure rate of the 2-level modulation scheme are plotted using the Lessay signal. Again, as was the case with the Sylt signal, the discrete levels in the PER-plot can be distinguished.

The average PER for Lessay is *lower* than the PER for the Sylt signal. This is surprising, since Sylt is located closer to Delft than Lessay and the SNR of the Sylt signal is higher than the SNR of the Lessay signal. An explanation could be that, when this measurement was done, atmospheric conditions were better than when the Sylt measurement was taken.

Another interesting phenomenon can be seen from the erasure rate - on several occasions, the erasure rate approaches 1, meaning that all pulses are flagged as being distorted. This is not a normal situation. However, when this measurement was taken, it was noticed that during some periods of time, an unknown, very loud signal was indeed interfering with the normal Loran-C signals. It is as yet unknown whether this really was the case, or if, maybe, some component in the test-setup broke down.

### 7.5 Lessay - 3-level coding

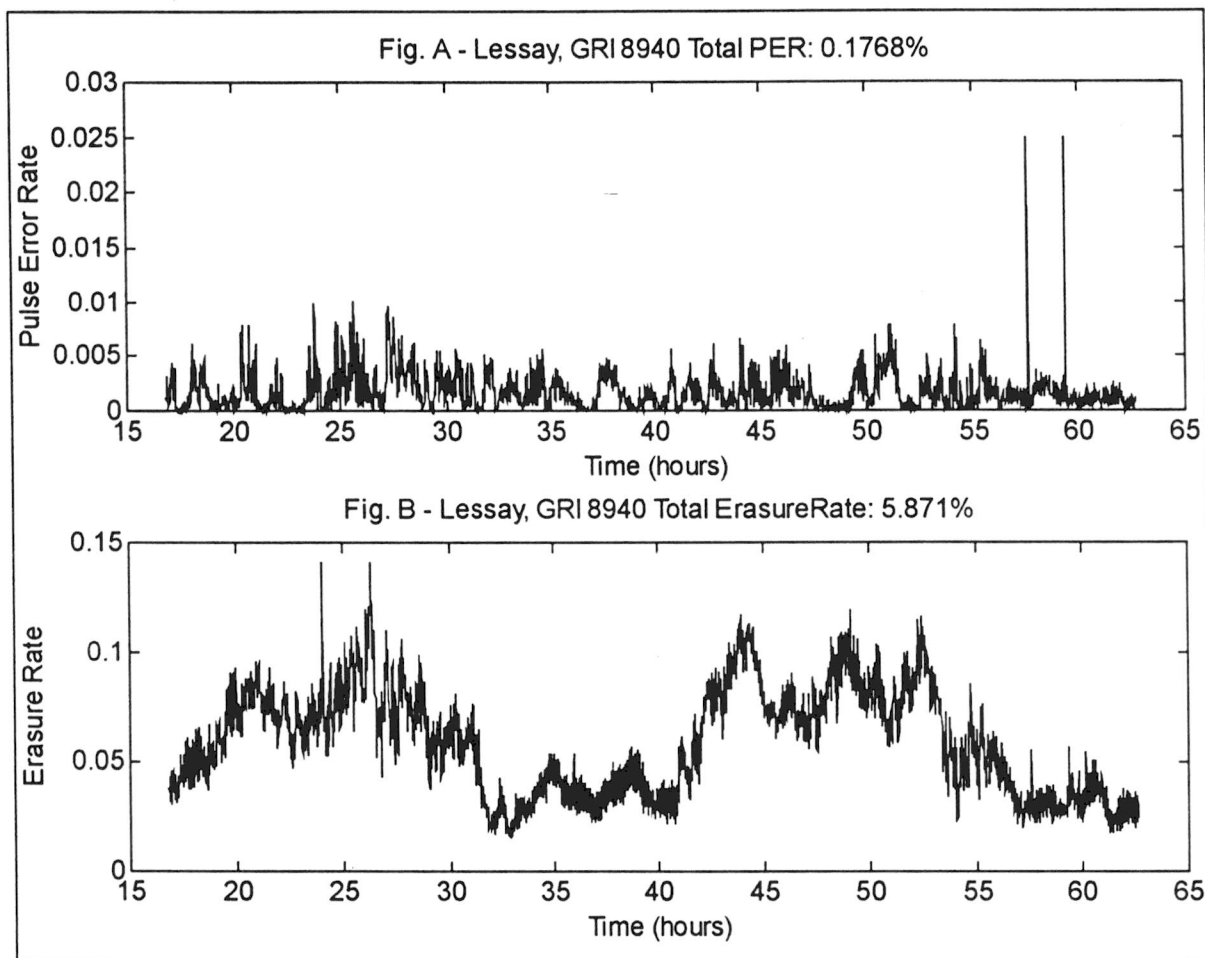


Figure 7.5: Pulse error rate (fig.A) and erasure rate (fig.B) of the Lessay-signal using 3-level modulation. The measurement was done on 18 October 1995.

In figure 7.5, the pulse error rate and erasure rate of the Lessay-signal using 3-level modulation are plotted.

Again, as was the case with the Sylt-signal, for Lessay the PER of the 3-level coding scheme is about 5 times larger than the PER of the 2-level coding scheme. However, in this case the average erasure rate during the 2-level run is higher than the erasure rate of the 3-level run. This is partly due to the peaks that occurred during the 2-level run, and also partly because the atmospheric conditions were not the same for the two runs.

The cause of the peaks in the plot of the PER around 58h is unknown. A possible reason can be a timing-adjustment in the Loran-C transmitter - if suddenly the timing is adjusted, it will take a while for the reference figures in the demodulator to follow the change in the received pulse. While this adjustment is taking place, the pulse-error rate will be higher.

## 7.6 Soustons - 2-level coding

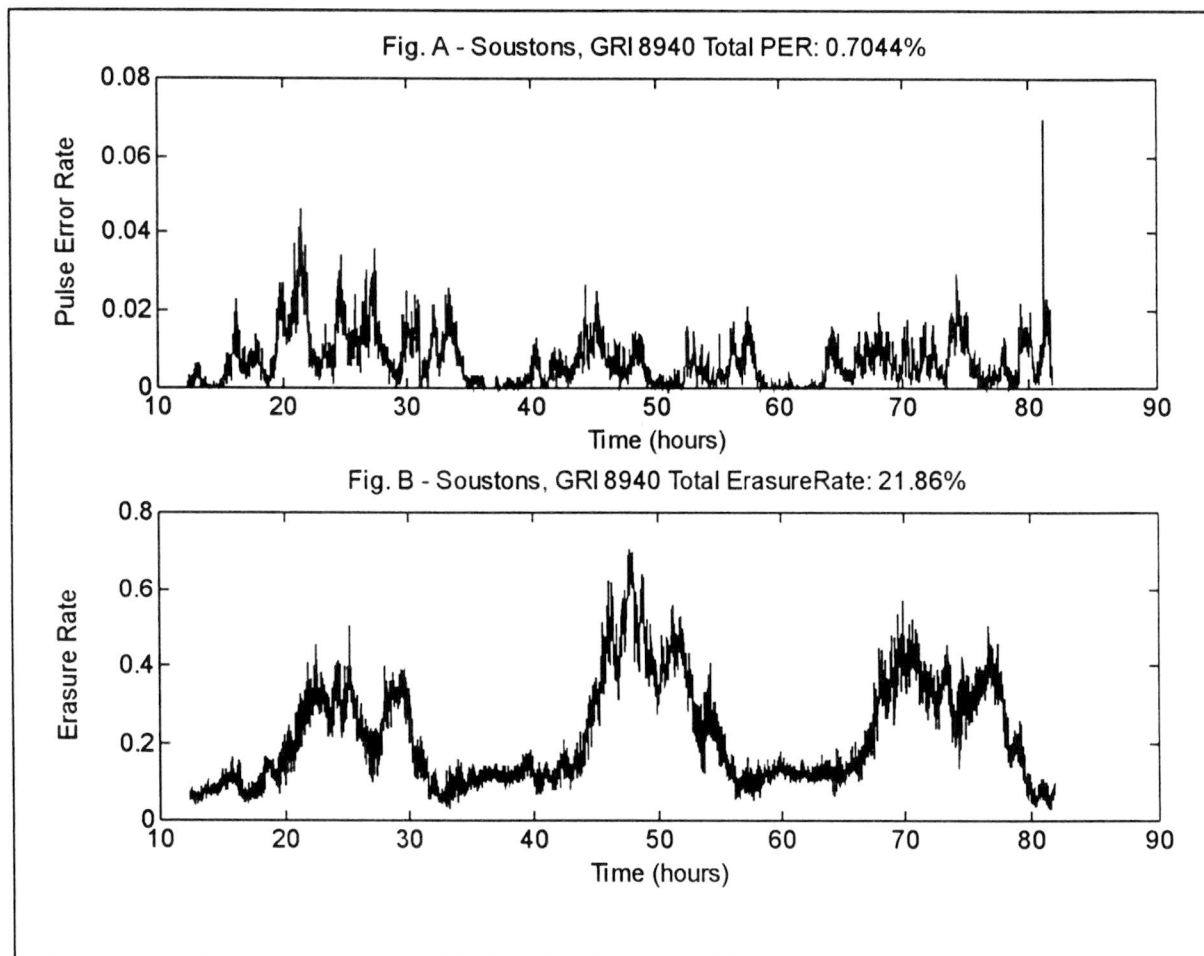


Figure 7.6: Pulse error rate (fig.A) and erasure rate (fig.B) of the Soustons-signal using 2-level modulation. The measurement was done on 3 november 1995.

Finally, tests with 2- and 3-level coding were done with the Soustons transmitter (located about 1000 km away from Delft).

These tests were done over a longer period of time; about 70 hours (2.9 days). In figure 7.6, the difference in erasure rate between daytime and nighttime can be seen clearly. This is most probably caused by the fact that skywave activity goes up during the night. This causes the interfering Cross-rate signals to be more powerful during the night than during the day, thereby distorting more desired pulses.

### 7.7 Soustons - 3-level coding

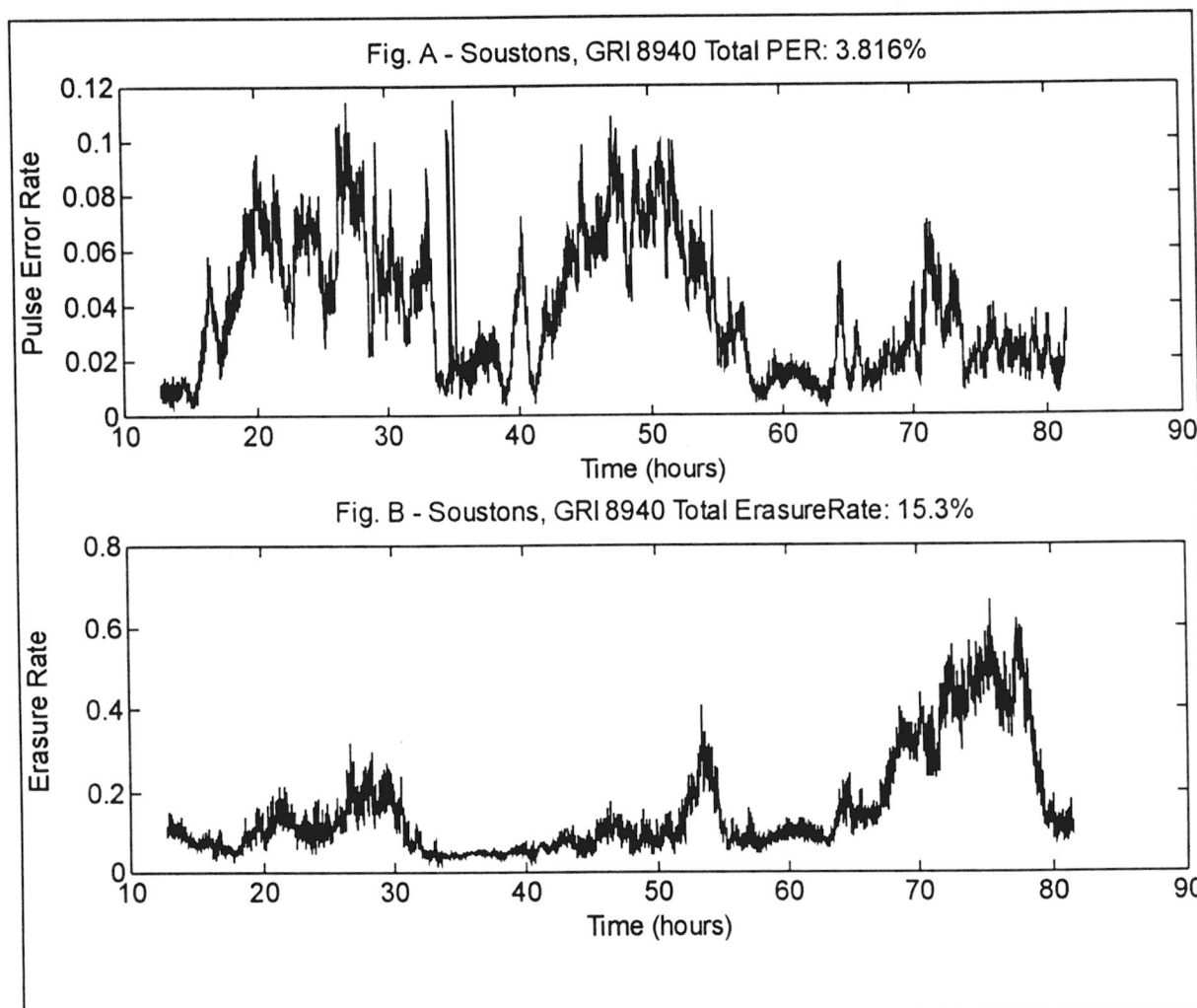


Figure 7.7: Pulse error rate (fig.A) and erasure rate (fig.B) of the Soustons-signal using 3-level modulation. The measurement was done on 26 October 1995.

In figure 7.7, the pulse error rate and erasure rate of the Soustons-signal using 3-level modulation are plotted.

As was expected, the PER for the 3-level modulation is higher than the PER for the 2-level modulation.

Again, the change in erasure rate between nighttime and daytime can be seen, although not as clearly as in figure 7.6. During the last night, however, it can be seen that the erasure rate goes up to 60%. It is doubtful that an error-correcting code can be developed that can still correct for 60% erasures.

## 7.8 Comparison between measurements and the theoretical analysis

When comparing the resulting pulse error rates from the measurements with the expected values of the PER as it is plotted in figure 5.5, the following conclusions can be drawn:

As was expected, the PER using 2-level modulation is lower than the PER using 3-level modulation. The measurements and the theoretical analysis agree on this.

The difference in error rate between the 2- and 3-level coding as has been measured, however, is less than was expected from figure 5.5. In the Lessay case, for example, the measured 2-level PER was 0.037%. From figure 5.5, the corresponding 3-level PER should be about 2%. The value from the measurement is 0.18%.

Apparently, most of the pulse errors are caused by effects other than Gaussian noise, like (weak) Cross-rate or atmospheric conditions.

It is also noted that the expected PER for the stronger transmitters (Sylt and Lessay) still is a fair bit higher than can be expected, given the PER of the weak Soustons transmitter.

No satisfying explanation for this effect can be given, other than the fact that the effects that have not been taken into account in the theoretical analysis, still have severe impact in the real-life situation.

Some effects that differ in the real-life situation from the theoretical analysis are:

- The atmospheric noise was supposed to be Gaussian, which in reality it is not.
- CW interference. No CWI-reducing methods have been used in the test-setup. In the theoretical analysis, CWI influence was not taken into account.
- A different filter was used in the test-setup than in the analysis.
- No pulse errors due to weak Cross-rate were considered in the analysis.

## 8. Conclusions and Recommendations

In this report, an effort was made to devise a Eurofix-demodulator capable of demodulating Eurofix-modulated Loran-C pulses. If the demodulator is unable to decode a Loran-C pulse correctly, it is better to recognize this fact than to make a wrong decision.

To develop such a demodulation scheme, and to test the resulting demodulator, several new techniques were introduced:

- 3-level coding
- Distortion detection
- A linear cross-correlating receiver with moving average reference figures
- A way of testing Eurofix demodulators without modification of normal Loran-C transmitters

### 8.1 Conclusions

With respect to 3-level coding:

Three-level coding has advantages over two-level coding:

- More data can be transmitted in the same time
- The coding scheme can be better balanced

The disadvantages of three-level vs. two-level coding are:

- The pulse-error rate will go up, resulting in more data errors.
- The demodulator becomes more complex

In the light of decreasing cost and increased performance of hardware, the last disadvantage is probably easy to overcome.

The assumption that the main reason for pulse errors would be Cross-rate interference seems to hold: the PER for 2-level coding is about 5 times lower than the PER for 3-level coding for both the Soustons and the Sylt signal ( $\text{SNR}_{\text{Sylt}} - \text{SNR}_{\text{Soustons}} \approx 15\text{dB}$ ). If the majority of errors were caused by thermal noise, this factor would be different for signals with different SNR's.

With respect to distortion detection:

Distortion detection is certainly beneficial for the Eurofix datalink: the total number of pulses that cannot be demodulated correctly remains roughly the same, but with distortion detection the majority of pulses that are demodulated incorrectly can be *identified* as such, whereas without distortion detection these pulses could not be distinguished from undistorted pulses.

With respect to the linear cross-correlation receiver with moving average reference figures:

Linear cross-correlation appears to be the receiver structure which has the best performance compared to other demodulator structures. The fact that the reference figures have to be continually updated does not seem to be a drawback on this technique. Linear cross-correlation utilizes the received signal to the maximum possible extent: all power in the received signal - even the power in skywaves that may be received along with the signal - is used.

With respect to the demodulator as it has been used to provide the test-results:

The general effects that were expected in the theoretical analysis have also been noticed in the test-results that were acquired using the demodulator. The absolute values of the PER, however, differ from the figures derived from the test-results. This is believed to be caused by factors that were not considered in the theoretical discussion (such as CWI), by the fact that some effects in real life differ from how they were used in the model (such as atmospheric noise and weak Cross-rate), and by the fact that the test-setup differed from the system assumed in the theoretical discussion.

With respect to the method of testing Eurofix-demodulators:

Time-shifting the clock-signal of the A/D converter seems to be a good way of acquiring time-shifted versions of a normal Loran-C pulse without having to modify a normal Loran-C transmitter to transmit time-shifted pulses. Various system parameters, such as the modulation index and the number of levels used, can easily be modified for test-purposes. Very little concessions to the real-life situation are made.

## 8.2 Recommendations

A lot of new system parameters were introduced, especially with the distortion-detecting filter. An optimum value will have to be found for all these parameters. To find the optimum values, it would be interesting to investigate a large number of cases where the distortion detecting filter starts adjusting

samples, or declares an erasure. By manually investigating the reason for the filter to do this, the filter parameters can probably be optimized to make the filter adjust only in cases where adjustment is needed. It is expected that the erasure threshold factor  $E_{\text{thresh}}$  should be adjusted depending on the SNR of the station that is being tracked. An algorithm will have to be developed to make this adjustment to be performed automatically.

Without any doubt, an error-correcting code will have to be used on the Eurofix datalink. Since erasures are very likely to occur in bursts, the error-correcting code should have strong burst-error-correcting capabilities. The performance of the error-correcting code, given the types of errors and erasures made by the demodulator, will have to be tested.

Tests of the proposed demodulator under moving (dynamic) conditions will also have to be done to investigate amplitude changes due to dynamic effects. Furthermore, in a real-life demodulator a tracking mechanism for the Loran-C signals will have to be used. The effect of tracking errors on the Eurofix demodulator should also be investigated. The performance of the tracking mechanism may be improved by so-called remodulation of the Eurofix-modulated Loran-C signals, which means that the tracking mechanism can compensate for the time-shifts introduced by the Eurofix modulation rather than just relying on a balanced modulation scheme.

Finally, the effect of Eurofix-modulation on conventional Loran-C navigation equipment should be investigated. The number of shifting levels used, and the shifting levels itself, need to be chosen such that this conventional Loran-C equipment can still use the system effectively.

## 9. References

1. D. van Willigen, Radio Plaatsbepaling, *Lecture notes*, Delft University of Technology.
2. R. Vroeijsstijn, *Eurofix and GNSS: The possibility of integrating Glonass into Eurofix*, Thesis report, Delft University of Technology, August 1995.
3. RTCM Special Committee No. 70, *Minimum Performance Standards for Marine Loran-C Receiving Equipment*, Washington DC, 1977
4. L.J. Beekhuis and D. van Willigen, *Eurofix*, Proceedings of the 6th International Technical Meeting of the Satellite Division of the Institute of Navigation, Salt Lake City, September 1993.
5. G.W.A. Offermans, *Modulation Schemes for the Eurofix Datalink*, Thesis report, Delft University of Technology, September 1994.
6. P. de Koning, *Ternary modulation and error control coding*, Thesis report, Delft University of Technology, December 1995
7. Loran-C User Handbook, Department of Transportation, United States Coast Guard, Washington DC, November 1992.
8. Robert Huysmans, *Asynchronous quadrature sampling of LORAN-C pulses*, Thesis report, Delft University of Technology, December 1995.
9. J. de Zwart, *Testing and Optimizing the Eurofix Datalink*, Thesis report, Delft University of Technology, July 1994.
10. T. Coenen, *private communications*, 1995.

## Appendix A - Overview of used software

A number of programs have been written to acquire the test-results as they have been described in this report. The following two programs are the most interesting to anyone who wants to be able to reproduce, or continue to work on, the test-setup:

First, there is the program that controls the Loran-C simulator. It can program the Loran-C simulator to operate on any GRI desired. Furthermore, it can make the Loran-C simulator produce Eurofix-modulated Loran-C pulses. It does this 'real time', meaning that it can control the Eurofix-modulation of every Loran-C pulse individually. The Eurofix-modulation that is imposed on the Loran-C pulses can be either 2- or 3-level, with a configurable modulation index. The program is configurable via a datafile. If the pulse-trigger output of the Loran-simulator is used for the shifting-clock circuit, this program can be used to provide a time-shifting clock as described in Chapter 6.

The latest version of this program is called SIMUL2.EXE. It is available, including its sources, through the SourceSafe source-distribution system.

The second program is the implemented version of the proposed demodulator. It programs the A/D card to use external clock and triggering signals, and does all the signal processing, including the distortion detecting filter. It is also informed of the data patterns that are being transmitted by the Loran-C transmitter, to be able to compute pulse error rates.

In the source, all A/D card routines have been gathered in a separate module, providing an easy-to-use interface to the programmer. All band-filtering routines are also put in a separate module.

The latest version of this program is called LOGSKY.EXE. Like the previous program, it is also available, including its sources, through the SourceSafe source-distribution system.

## Appendix B - Location, power and distances of Loran-C transmitters to the Delft University of Technology

The Loran-C antenna at the Delft University of Technology is located at:

51°59'56.696" N (51.9990821° N)

4°22'24.140" E (4.3733721° E)

<b>Station:</b>	<b>Latitude:</b>	<b>Longitude:</b>	<b>Power (kW):</b>	<b>Distance (km):</b>	<b>Propagation time to Delft (μs)</b>
Sylt	54°48'29.975" N	08°17'36.856" E	250	407.68	1360.95
Lessay	49°08'55.224" N	01°30'17.029" W	250	523.11	1743.14
Soustons	43°44'23.099" N	01°22'49.584" W	250	1013.43	3381.62
Bo	68°38'06.216" N	14°27'47.350" E	400	1929.56	6443.08
Jan Mayen	70°54'51.478" N	08°43'56.525" W	250	2208.99	7374.53
Vaerlandet	61°17'49.435" N	04°41'46.618" E	250	1035.54	3457.22
Ejde	62 17'59.837" N	07°04'26.079" W	400	1335.75	4457.91